

Abstract

All-electron partitioning of wave functions into products $\Psi_{core}\Psi_{val}$ of core and valence parts in orbital space results in the loss of core-valence antisymmetry, uncorrelation of motion of core and valence electrons, and core-valence overlap. These effects are studied with the variational Monte Carlo method using appropriately designed wave functions for the first-row atoms and positive ions.

It is shown that the loss of antisymmetry with respect to interchange of core and valence electrons is a dominant effect which increases rapidly through the row, while the effect of core-valence uncorrelation is generally smaller. Orthogonality of the core and valence parts partially substitutes the exclusion principle and is absolutely necessary for meaningful calculations with partitioned wave functions. Core-valence overlap may lead to nonsensical values of the total energy.

It has been found that even relatively crude core-valence partitioned wave functions generally can estimate ionization potentials with better accuracy than that of the traditional, non-partitioned ones, provided that they achieve maximum separation (independence) of core and valence shells accompanied by high internal flexibility of Ψ_{core} and Ψ_{val} . Our best core-valence partitioned wave function of that kind estimates the IP's with an accuracy comparable to the most accurate theoretical determinations in the literature.

Table of Contents

Abstract	ii
Acknowledgement	viii
Note on units	ix
1 Introduction	1
1.1 Core-Valence Partitioning	1
1.1.1 Partitioning in orbital space and physical space	2
1.1.2 Treatment of core electrons	5
1.2 Review of Methods Based on Core-Valence Separation	6
1.2.1 Pseudopotential methods	6
1.2.2 Damped-core quantum Monte Carlo method	10
1.2.3 Valence-electron-only calculations with core projection operators .	12
1.3 Problems of Core-Valence Partitioning	14
1.4 The Scope of the Present Study	16
2 Model Wave Functions	17
2.1 Construction of the Trial Wave Functions	17
2.1.1 General considerations for construction of trial wave functions . .	17
2.1.2 The complete wave function	19
2.1.3 Full-atomic implementation of the core-valence partitioning	22
2.2 Study of the Core-Valence Separation Effects	24

Table 10

Year	Value
1990	1.00
1991	1.00
1992	1.00
1993	1.00
1994	1.00
1995	1.00
1996	1.00
1997	1.00
1998	1.00
1999	1.00
2000	1.00
2001	1.00
2002	1.00
2003	1.00
2004	1.00
2005	1.00
2006	1.00
2007	1.00
2008	1.00
2009	1.00
2010	1.00
2011	1.00
2012	1.00
2013	1.00
2014	1.00
2015	1.00
2016	1.00
2017	1.00
2018	1.00
2019	1.00
2020	1.00

2.2.1	The loss of core-valence antisymmetry	24
2.2.2	The core-valence overlap effect	25
2.2.3	The core-valence correlation effect	26
2.2.4	Further study of electron correlation	27
3	Variational Monte Carlo Method	29
3.1	Variational Method	29
3.2	Monte Carlo Integration	30
3.3	Estimation of the Variational Integral	32
3.4	Metropolis Sampling	33
3.4.1	Description of the algorithm	33
3.4.2	Generalized Metropolis algorithm	37
3.5	Optimization of the Wave Functions	37
4	Running Simulations	39
4.1	Implementation of the Metropolis Algorithm	39
4.1.1	Estimation of the variance	39
4.1.2	Variance reduction: Improved sampling technique	41
4.1.3	Simulation algorithm	43
4.2	The 'Core' and 'Valence' Energy	45
5	Results	47
5.1	Optimized Wave Functions for Atoms and Ions	47
5.2	Calculations on Atoms and Ions	51
5.3	Ionization Potentials	57
6	Discussion and Conclusions	59
6.1	Atomic Calculations with the Complete wave Function	59

10	Introduction	10
11	1.1. The problem	11
12	1.2. The model	12
13	1.3. The algorithm	13
14	1.4. The results	14
15	2. The algorithm	15
16	2.1. The algorithm	16
17	2.2. The algorithm	17
18	2.3. The algorithm	18
19	2.4. The algorithm	19
20	2.5. The algorithm	20
21	2.6. The algorithm	21
22	2.7. The algorithm	22
23	2.8. The algorithm	23
24	2.9. The algorithm	24
25	2.10. The algorithm	25
26	2.11. The algorithm	26
27	2.12. The algorithm	27
28	2.13. The algorithm	28
29	2.14. The algorithm	29
30	2.15. The algorithm	30
31	2.16. The algorithm	31
32	2.17. The algorithm	32
33	2.18. The algorithm	33
34	2.19. The algorithm	34
35	2.20. The algorithm	35
36	2.21. The algorithm	36
37	2.22. The algorithm	37
38	2.23. The algorithm	38
39	2.24. The algorithm	39
40	2.25. The algorithm	40
41	2.26. The algorithm	41
42	2.27. The algorithm	42
43	2.28. The algorithm	43
44	2.29. The algorithm	44
45	2.30. The algorithm	45
46	2.31. The algorithm	46
47	2.32. The algorithm	47
48	2.33. The algorithm	48
49	2.34. The algorithm	49
50	2.35. The algorithm	50
51	2.36. The algorithm	51
52	2.37. The algorithm	52
53	2.38. The algorithm	53
54	2.39. The algorithm	54
55	2.40. The algorithm	55
56	2.41. The algorithm	56
57	2.42. The algorithm	57
58	2.43. The algorithm	58
59	2.44. The algorithm	59
60	2.45. The algorithm	60
61	2.46. The algorithm	61
62	2.47. The algorithm	62
63	2.48. The algorithm	63
64	2.49. The algorithm	64
65	2.50. The algorithm	65
66	2.51. The algorithm	66
67	2.52. The algorithm	67
68	2.53. The algorithm	68
69	2.54. The algorithm	69
70	2.55. The algorithm	70
71	2.56. The algorithm	71
72	2.57. The algorithm	72
73	2.58. The algorithm	73
74	2.59. The algorithm	74
75	2.60. The algorithm	75
76	2.61. The algorithm	76
77	2.62. The algorithm	77
78	2.63. The algorithm	78
79	2.64. The algorithm	79
80	2.65. The algorithm	80
81	2.66. The algorithm	81
82	2.67. The algorithm	82
83	2.68. The algorithm	83
84	2.69. The algorithm	84
85	2.70. The algorithm	85
86	2.71. The algorithm	86
87	2.72. The algorithm	87
88	2.73. The algorithm	88
89	2.74. The algorithm	89
90	2.75. The algorithm	90
91	2.76. The algorithm	91
92	2.77. The algorithm	92
93	2.78. The algorithm	93
94	2.79. The algorithm	94
95	2.80. The algorithm	95
96	2.81. The algorithm	96
97	2.82. The algorithm	97
98	2.83. The algorithm	98
99	2.84. The algorithm	99
100	2.85. The algorithm	100

6.2	Calculations with the Partitioned Functions	61
6.2.1	Wave function Ψ_2 : The loss of core-valence antisymmetry	61
6.2.2	Wave function Ψ_2 : The core-valence overlap	61
6.2.3	Wave function Ψ_3 : The effect of core-valence correlation	62
6.2.4	Wave functions Ψ_4 and Ψ_5 : Improving electron correlation	63
6.3	Comparative Performance of the Wave Functions	63
6.4	Comments, Suggestions	68
6.5	Conclusions	69
Appendices		70
A The Wave Function as a Product of Slater Determinants		70
B Cusp Conditions		74
B.1	Electron-nuclear cusp conditions	74
B.1.1	General electron-nuclear cusp conditions	74
B.1.2	Specific cusp conditions imposed on the atomic orbitals	77
B.2	Electron-electron cusp conditions	77
C Simplex Optimization		80
D Compendium of Formulas		83
D.1	Numerical evaluation of the integral $\langle \phi_{1s} \phi_{2s} \rangle$	83
D.2	Derivatives of the atomic orbitals and correlation functions	84
D.3	The local energy	85
Bibliography		88

List of Tables

2.1	Parametrization of wave functions Ψ_1 – Ψ_5	28
5.1	Optimized wave functions Ψ_1 for atoms and ions	48
5.2	Optimized wave functions Ψ_2 for atoms and ions	49
5.3	Optimized wave functions Ψ_3 for atoms and ions	49
5.4	Optimized wave functions Ψ_4 for atoms and ions	50
5.5	Optimized wave functions Ψ_5 for atoms and ions	50
5.6	Properties estimated with optimized wave function Ψ_1	52
5.7	Properties estimated with optimized wave function Ψ_2	53
5.8	Properties estimated with optimized wave function Ψ_3	53
5.9	Properties estimated with optimized wave function Ψ_4	54
5.10	Properties estimated with optimized wave function Ψ_5	54
5.11	Ionization potentials based on the total energies	57
5.12	Ionization potentials based on the valence energies	57
6.1	Selected atomic properties estimated using the optimized wave functions of Schmidt and Moskowitz	60
6.2	Accuracy of the ionization potentials	65
6.3	Ionization potentials by various methods	66

List of Figures

5.1	Effects of the partial loss of antisymmetry and core-valence correlation on the first row atoms	55
5.2	Effects of the partial loss of antisymmetry and core-valence correlation on the first row positive ions	55
5.3	The core-valence overlap effect	56
5.4	Deviations of the computed ionization potentials from the exact values .	58
6.1	Comparison of the accuracy of Ψ_4 -ionization potentials with literature . .	67

Acknowledgement

I gratefully acknowledge many helpful discussions and support for carrying out this work from my professors Stuart M. Rothstein and Jan Vrbik.

I also wish to thank my fellow graduate physics student Peter Langfelder for valuable suggestions which always helped to resolve complications.

Finally, I am very grateful to G. R. Finlay family for a financial award in the form of the Gordon R. Finlay Scholarship, and to Mr. and Mrs. Penner who supported me with the Edgar and Irmgard Penner Scholarship.

Note on units

Atomic units are used throughout the thesis. Various trial wave functions are denoted with the capital Greek letter Ψ and a numeral subscript: Ψ_1 , Ψ_2 , and so on.

The following repetitive symbols may appear in the text without explanation.

n	the total number of electrons
n_c	the number of core electrons (in this study equal to 2)
n_v	the number of valence electrons
n^\uparrow (n^\downarrow)	the number of spin-up (spin-down) electrons
n_c^\uparrow (n_c^\downarrow)	the number of core spin-up (spin-down) electrons
n_v^\uparrow (n_v^\downarrow)	the number of valence spin-up (spin-down) electrons
\mathbf{r}_i	three-dimensional position vector of electron i
$r_i = \mathbf{r}_i $	distance of electron i from the nucleus
\mathbf{R}_i	$3n$ -dimensional vector of the i -th electron configuration
ϕ_i, φ_i	spatial atomic orbitals
ψ_D^\uparrow (ψ_D^\downarrow)	Slater determinant of spatial atomic orbitals for spin-up (spin-down) electrons
ψ_D	Slater determinant of spatial atomic orbitals without reference to spin
N_C	the number of configurations in the ensemble
N_B	the number of blocks of iterations
N_I	the number of iterations per block

CONTENTS

THESE THESISES CONTIENENT DES RECHERCHES QUI SONT LE FRUIT D'UN TRAVAIL INDIVIDUEL. LES RECHERCHES SONT LE FRUIT D'UN TRAVAIL INDIVIDUEL. LES RECHERCHES SONT LE FRUIT D'UN TRAVAIL INDIVIDUEL.

INTRODUCTION	1
CHAPITRE I. - GÉNÉRALITÉS	1
CHAPITRE II. - MÉTHODES	2
CHAPITRE III. - RÉSULTATS	3
CHAPITRE IV. - CONCLUSIONS	4
CHAPITRE V. - BIBLIOGRAPHIE	5
CHAPITRE VI. - ANNEXES	6
CHAPITRE VII. - RÉFÉRENCES	7
CHAPITRE VIII. - INDEX	8
CHAPITRE IX. - TABLE DES MATIÈRES	9
CHAPITRE X. - LISTE DES AUTEURS	10
CHAPITRE XI. - LISTE DES TITRES	11
CHAPITRE XII. - LISTE DES ANNÉES	12
CHAPITRE XIII. - LISTE DES PAGES	13
CHAPITRE XIV. - LISTE DES COLONNES	14
CHAPITRE XV. - LISTE DES LIGNES	15
CHAPITRE XVI. - LISTE DES CARACTÈRES	16
CHAPITRE XVII. - LISTE DES SYMBOLES	17
CHAPITRE XVIII. - LISTE DES UNITÉS	18
CHAPITRE XIX. - LISTE DES FORMES	19
CHAPITRE XX. - LISTE DES COULEURS	20
CHAPITRE XXI. - LISTE DES TONALITÉS	21
CHAPITRE XXII. - LISTE DES RYTHMES	22
CHAPITRE XXIII. - LISTE DES MÉTRIQUES	23
CHAPITRE XXIV. - LISTE DES SCHEMES	24
CHAPITRE XXV. - LISTE DES FIGURES	25
CHAPITRE XXVI. - LISTE DES TABLEAUX	26
CHAPITRE XXVII. - LISTE DES CARTES	27
CHAPITRE XXVIII. - LISTE DES DIAGRAMMES	28
CHAPITRE XXIX. - LISTE DES SCHEMES	29
CHAPITRE XXX. - LISTE DES FIGURES	30
CHAPITRE XXXI. - LISTE DES TABLEAUX	31
CHAPITRE XXXII. - LISTE DES CARTES	32
CHAPITRE XXXIII. - LISTE DES DIAGRAMMES	33
CHAPITRE XXXIV. - LISTE DES SCHEMES	34
CHAPITRE XXXV. - LISTE DES FIGURES	35
CHAPITRE XXXVI. - LISTE DES TABLEAUX	36
CHAPITRE XXXVII. - LISTE DES CARTES	37
CHAPITRE XXXVIII. - LISTE DES DIAGRAMMES	38
CHAPITRE XXXIX. - LISTE DES SCHEMES	39
CHAPITRE XL. - LISTE DES FIGURES	40
CHAPITRE XLI. - LISTE DES TABLEAUX	41
CHAPITRE XLII. - LISTE DES CARTES	42
CHAPITRE XLIII. - LISTE DES DIAGRAMMES	43
CHAPITRE XLIV. - LISTE DES SCHEMES	44
CHAPITRE XLV. - LISTE DES FIGURES	45
CHAPITRE XLVI. - LISTE DES TABLEAUX	46
CHAPITRE XLVII. - LISTE DES CARTES	47
CHAPITRE XLVIII. - LISTE DES DIAGRAMMES	48
CHAPITRE XLIX. - LISTE DES SCHEMES	49
CHAPITRE L. - LISTE DES FIGURES	50
CHAPITRE LI. - LISTE DES TABLEAUX	51
CHAPITRE LII. - LISTE DES CARTES	52
CHAPITRE LIII. - LISTE DES DIAGRAMMES	53
CHAPITRE LIV. - LISTE DES SCHEMES	54
CHAPITRE LV. - LISTE DES FIGURES	55
CHAPITRE LVI. - LISTE DES TABLEAUX	56
CHAPITRE LVII. - LISTE DES CARTES	57
CHAPITRE LVIII. - LISTE DES DIAGRAMMES	58
CHAPITRE LIX. - LISTE DES SCHEMES	59
CHAPITRE LX. - LISTE DES FIGURES	60
CHAPITRE LXI. - LISTE DES TABLEAUX	61
CHAPITRE LXII. - LISTE DES CARTES	62
CHAPITRE LXIII. - LISTE DES DIAGRAMMES	63
CHAPITRE LXIV. - LISTE DES SCHEMES	64
CHAPITRE LXV. - LISTE DES FIGURES	65
CHAPITRE LXVI. - LISTE DES TABLEAUX	66
CHAPITRE LXVII. - LISTE DES CARTES	67
CHAPITRE LXVIII. - LISTE DES DIAGRAMMES	68
CHAPITRE LXIX. - LISTE DES SCHEMES	69
CHAPITRE LXX. - LISTE DES FIGURES	70
CHAPITRE LXXI. - LISTE DES TABLEAUX	71
CHAPITRE LXXII. - LISTE DES CARTES	72
CHAPITRE LXXIII. - LISTE DES DIAGRAMMES	73
CHAPITRE LXXIV. - LISTE DES SCHEMES	74
CHAPITRE LXXV. - LISTE DES FIGURES	75
CHAPITRE LXXVI. - LISTE DES TABLEAUX	76
CHAPITRE LXXVII. - LISTE DES CARTES	77
CHAPITRE LXXVIII. - LISTE DES DIAGRAMMES	78
CHAPITRE LXXIX. - LISTE DES SCHEMES	79
CHAPITRE LXXX. - LISTE DES FIGURES	80
CHAPITRE LXXXI. - LISTE DES TABLEAUX	81
CHAPITRE LXXXII. - LISTE DES CARTES	82
CHAPITRE LXXXIII. - LISTE DES DIAGRAMMES	83
CHAPITRE LXXXIV. - LISTE DES SCHEMES	84
CHAPITRE LXXXV. - LISTE DES FIGURES	85
CHAPITRE LXXXVI. - LISTE DES TABLEAUX	86
CHAPITRE LXXXVII. - LISTE DES CARTES	87
CHAPITRE LXXXVIII. - LISTE DES DIAGRAMMES	88
CHAPITRE LXXXIX. - LISTE DES SCHEMES	89
CHAPITRE LXXXX. - LISTE DES FIGURES	90
CHAPITRE LXXXXI. - LISTE DES TABLEAUX	91
CHAPITRE LXXXXII. - LISTE DES CARTES	92
CHAPITRE LXXXXIII. - LISTE DES DIAGRAMMES	93
CHAPITRE LXXXXIV. - LISTE DES SCHEMES	94
CHAPITRE LXXXXV. - LISTE DES FIGURES	95
CHAPITRE LXXXXVI. - LISTE DES TABLEAUX	96
CHAPITRE LXXXXVII. - LISTE DES CARTES	97
CHAPITRE LXXXXVIII. - LISTE DES DIAGRAMMES	98
CHAPITRE LXXXXIX. - LISTE DES SCHEMES	99
CHAPITRE LXXXXX. - LISTE DES FIGURES	100

Chapter 1

Introduction

1.1 Core-Valence Partitioning

Ever since the emergence of computational quantum chemistry, calculations on atoms and molecules of heavy elements have been regarded as a distinct problem, deserving special treatment. The reason is that conventional all-electron *ab initio* methods, which perform very well for light atoms and molecules, become impractical if the number of electrons treated explicitly is large. Primarily, this is due to a tremendous increase in computation time. For example, in Hartree-Fock calculations, computational times are approximately proportional to the fourth power of the number of basis functions, and the problem of storage of immense number of integrals is no less severe. In quantum Monte Carlo methods, the CPU time for a fixed statistical precision is estimated to increase with atomic number Z as $Z^{5.5-6.5}$ [1]. Given the large number of electrons together with complications due to relativistic effects and the electron correlation problem, even the fastest modern computers are still not adequate for highly accurate all-electron treatment of heavy elements and their compounds. This urges one to identify and utilize the most significant contributions from their electronic structure to the particular properties of interest.

Much of what is understood on a qualitative level about chemical reactivity in terms of atomic and molecular orbitals occupied by electrons ('hooks-and-arrows' in mechanisms, for example) rests on the assumption that only the outermost (valence) electrons

constituting the valence region determine reactivity and other properties of large systems, while the innermost (**core**) electrons provide merely a setting for the valence ones.

A natural idea is then to treat the core and valence electrons separately or even to treat the valence electrons only, thus reducing the all-electron problem to the valence-only one. Design of such **core-valence partitioning** schemes is a complicated and extremely relevant problem challenging theorists. As any other approximation, it is not perfect, and the sources of error must be well understood. This thesis is an endeavor to provide such understanding. It is necessary to point out that in the present work we limit our scope to atomic systems so the magnitude of core-valence separation errors can be quantified with good accuracy.

1.1.1 Partitioning in orbital space and physical space

The foremost incongruity of the idea of partitioning the electrons comprising a system into core and valence is that in reality (and quantum mechanics demands that) the electrons are indistinguishable. Not being found within formal theory, it can be introduced in one or another manner suitable for the particular purposes.

An allusion to core-valence partitioning is already present in a widely used concept of electronic shells. By definition, an electronic shell is a collection of all electrons with the same principal quantum number. Usually the valence shell is defined as the last occupied electronic shell, while the core as consisting of all the inner ones. This approach is justified by the order of successive ionization potentials of the atoms.

Partitioning in *orbital space* implies that the orbitals can be divided in two groups, so that instead of a complete wave function one deals with a product of the core and valence functions, which is written in obvious notation as

$$\Psi(1, 2, \dots, n) = \hat{\mathcal{A}} \Psi_{core}(1, 2, \dots, n_c) \Psi_{val}(n_c+1, \dots, n), \quad (1.1)$$

where \hat{A} is the operator completing antisymmetrization of the product Ψ_{core} and Ψ_{val} , each of which should be already antisymmetric.

In practice, antisymmetry with respect to interchange of core and valence electrons is not rigorously built into the partitioned wave function, so that effectively one *approximates* Ψ with a non-antisymmetrized product

$$\Psi(1, 2, \dots, n) \approx \Psi_{core}(1, 2, \dots, n_c) \Psi_{val}(n_c + 1, \dots, n). \quad (1.2)$$

Such a formulation gives rise to a concern about imminent collapse of valence electrons into the core orbitals. This undesired effect can be prevented by using *orthogonal* orbitals for constructing functions Ψ_{core} and Ψ_{val} . Elaboration on this issue is a part of the present work.

The objective of any partitioning is to allow one to work with the ‘valence Schrödinger equation’

$$\hat{H}_{val} \Psi_{val} = E_{val} \Psi_{val}, \quad (1.3)$$

where \hat{H}_{val} is the ‘valence Hamiltonian’, and E_{val} the ‘valence energy’. There is no universal definition of any of the quantities appearing in Eq. (1.3), so their interpretation varies from one method to another.

An example of *exact* partitioning in orbital space is one in the framework of the Hartree–Fock method, where electrons occupy ‘distinct’ Hartree–Fock orbitals, the complete wave function is antisymmetrized, and the total energy includes the sum of orbital energies, $\epsilon_i = \epsilon_{1s}, \epsilon_{2s}$, etc. It is therefore always possible to find the total energy of a many-electron subshell from the appropriate sum of the orbital energies, remembering, however, that one must also correct for the interelectronic repulsions which are double counted in any sum of Hartree–Fock eigenvalues.

There exist other conceptions of core–valence separation. A description of the system based on the stationary ground-state electron density $\rho(\mathbf{r})$ can be used to introduce

The following information is for informational purposes only and should not be used for medical advice. The information is not intended to be a substitute for professional medical advice, diagnosis, or treatment. Always seek the advice of your physician or other qualified health provider with any questions you may have regarding a medical condition. Never disregard professional medical advice or delay in seeking it because of something you have read in this article. If you are experiencing a medical emergency, please call 911 or your local emergency number.

The following information is for informational purposes only and should not be used for medical advice. The information is not intended to be a substitute for professional medical advice, diagnosis, or treatment. Always seek the advice of your physician or other qualified health provider with any questions you may have regarding a medical condition. Never disregard professional medical advice or delay in seeking it because of something you have read in this article. If you are experiencing a medical emergency, please call 911 or your local emergency number.

The following information is for informational purposes only and should not be used for medical advice. The information is not intended to be a substitute for professional medical advice, diagnosis, or treatment. Always seek the advice of your physician or other qualified health provider with any questions you may have regarding a medical condition. Never disregard professional medical advice or delay in seeking it because of something you have read in this article. If you are experiencing a medical emergency, please call 911 or your local emergency number.

The following information is for informational purposes only and should not be used for medical advice. The information is not intended to be a substitute for professional medical advice, diagnosis, or treatment. Always seek the advice of your physician or other qualified health provider with any questions you may have regarding a medical condition. Never disregard professional medical advice or delay in seeking it because of something you have read in this article. If you are experiencing a medical emergency, please call 911 or your local emergency number.

partitioning in physical space. Analyzing the radial density function

$$R(r) = 4\pi r^2 \rho(r), \quad (1.4)$$

where $\rho(r)$ is the total electron density¹ at a distance r from the nucleus with charge Z , Politzer and Parr [2] showed that its outermost minimum defines a physically meaningful boundary surface separating core and valence regions. Later Politzer [3] proposed that this boundary surface can also be defined as the global minimum in the ‘average local electrostatic potential’, $V(r)/\rho(r)$, and found that any maximum in the local potential corresponds to a minimum in the radial density function $\rho(r)$.

The point r_b at which the outermost minimum in the radial density function occurs falls within the interval in which the linear $\ln \rho(r)$ vs r plot of first row atoms changes slope. On that account one can imagine that there exists an inner spherical core with radius r_b centered at the nucleus and an outer valence region extending from r_b to infinity. The number of core electrons, n_c , is then given by [4]

$$n_c = 4\pi \int_0^{r_b} r^2 \rho(r) dr. \quad (1.5)$$

The value of n_c is now determined by the definition of r_b .

When the core and valence regions are defined in the above manner, an estimate of the valence region electronic energy can be obtained with the formula [2]

$$E_{val} = -\frac{12\pi}{7} (Z - n_c) \int_{r_b}^{\infty} r \rho(r) dr. \quad (1.6)$$

Using this expression Desmarais and Fliszár [4] showed with CI calculations that $n_c = 2$ for the first row atoms and $n_c = 2$ or $n_c = 10$ for the larger atoms indeed define physically meaningful cores.

¹ $\rho(\mathbf{r}) = \rho(r)$ because of the spherical symmetry of the electron density.

1.1.2 Treatment of core electrons

Whether in orbital or physical space, one can imagine two fashions of core-valence partitioning based on the manner of treating the core electrons. In the first approach, which can be termed as the *core-retained* method, core electrons are kept while their treatment is substantially reduced. A representative example of this method — the damped-core technique — is discussed below. Alternatively, one can use the so-called *frozen-core approximation* — the assumption that the core does not change with chemical (valence) environment, — in order to treat explicitly the core mean potential, as well as some of core-valence exchange, correlation, and relaxation effects on the valence electrons' properties only once, and thereafter transfer the core orbitals to another system without re-computation.

The second fashion, in which the core orbitals and electrons are removed altogether, is also based on the frozen-core approximation. Here the effects of the core electrons on the atom's properties are determined from an accurate calculation and incorporated into a certain potential function, called an *effective pseudopotential*, which replaces the full-atomic potential, and serves to bind the valence electrons to the nucleus and at the same time prevents their collapse. Such strategy is less accurate, but more convenient.

Thus, in the valence-only approach, the end of core-valence partitioning is to quantify the effects of core electrons incorporated in pseudopotential functions so that one can perform subsequently only calculations on valence electrons. The objective of the core-retained methods is to devise a scheme which would permit one to decrease the efforts of treating the core and focus attention on the valence electrons. Qualitative justification for either procedure — that the core electrons are so strongly bound to the nucleus that they are relatively inert — has been supported by successful applications of these approximations.

1.2 Review of Methods Based on Core-Valence Separation

Several diverse methods have been proposed for calculations on heavier atoms, notably the valence-electron-only techniques with pseudopotentials and pseudo-hamiltonians and all-electron ones such as the damped core method and various accelerated sampling algorithms (in Monte Carlo methods). Here we discuss those relevant to our work.

1.2.1 Pseudopotential methods

As mentioned above, the pseudopotential approach is an approximation based on the idea that the core electrons can be replaced by a suitably chosen potential function.

Two types of pseudopotentials are distinguished. One is usually called *effective core potential* (ECP), and the other is referred to as ‘*ab initio* model potential’ (MP). The term ‘pseudopotential’ is sometimes used as a more general name for the valence-electron-only techniques. All pseudopotential methods have in common the replacement of the core electrons by a linear combination of Gaussian functions which contain terms arising from core-valence repulsion and orthogonality condition. The most straightforward application of pseudopotential calculations produces valence orbital energies, although other properties can be computed as well.

Effective core potentials. Consider a wave function taken as a non-antisymmetrized product (1.2). If core electrons are removed, the valence Schrödinger equation (1.3) can be formulated as

$$\hat{H}_{val}\chi_v = \sum_{i=1}^{n_v} \left[-\frac{1}{2}\nabla_i^2 - \frac{Z_{eff}}{r_i} + \sum_{i<j}^{n_v} \frac{1}{r_{ij}} + \hat{U}(r_i) \right] \chi_v = \epsilon_v \chi_v, \quad (1.7)$$

where $Z_{eff} = Z - n_c$ is the ‘effective charge’, χ_v is the so-called valence *pseudo-orbital*, and the *nonlocal* potential function \hat{U} , the pseudopotential, replaces the core-valence repulsion and the core-valence orthogonality condition.

The pseudo-orbital χ_v is given a smoothed nodeless shape under condition that it match exactly the Hartree–Fock valence orbital outside the core region (*shape-consistent* ECP’s) or reproduce atomic excitation and ionization energies (*energy-consistent* ECP’s).

The pseudopotential $\hat{U}(r_i)$ is usually cast in the form

$$\hat{U}(r_i) = U_{l_{\max}+1}(r_i) + \sum_{l=0}^{l_{\max}} \sum_{m=-l}^l |Y_{ml}(\Omega_i)\rangle U_l(r_i) \langle Y_{ml}(\Omega_i)|, \quad (1.8)$$

where Ω_i is the solid angle of electron i from the nucleus, l_{\max} is the largest angular momentum quantum number among the core electrons, $U_l(r_i)$ is a radial pseudopotential which depends only on the distance r_i between electron i and the nucleus, and the quantum number of angular momentum l . The role of spherical harmonics Y_{ml} is to ensure correct orthogonality between the missing core and the valence wave functions.

The functions $U_l(r_i)$ are commonly generated on a grid from all-electron atomic Hartree–Fock calculations, and then fit to the analytical form

$$U_l(r) = \frac{1}{r^2} \sum_k A_{l,k} r^{n_{l,k}} e^{-B_{l,k} r^2}, \quad (1.9)$$

where $A_{l,k}$, $B_{l,k}$, and $n_{l,k}$ are the fit parameters.

The most reliable formulation of effective core potentials (both relativistic and non-relativistic) is based on the definition of pseudo-orbitals originally proposed by Christiansen *et al.* [6], who argued that the pseudo-orbital must accurately represent the valence electron density in the valence region.

The first step in the derivation procedure is a highly accurate Hartree–Fock calculation on a generator state of an atom or atomic ion. The corresponding Fock equation for a valence atomic orbital is

$$\hat{F}\phi_v = \left[-\frac{1}{2}\nabla^2 - \frac{Z}{r} + \hat{V}_{core} + \hat{V}_{val} \right] \phi_v = \epsilon_v \phi_v, \quad (1.10)$$

where operators \hat{V}_{core} and \hat{V}_{val} are the sums of Coulomb and exchange potentials of the

core and valence electrons, respectively, related to the $1/r_{ij}$ operators in \hat{H} ,

$$\begin{aligned}\hat{V}_{core} &= \sum_{i=1}^{n_c} (2\hat{J}_i - \hat{K}_i), \\ \hat{V}_{val} &= \sum_{i=n_c+1}^n (2\hat{J}_i - \hat{K}_i).\end{aligned}\quad (1.11)$$

In order to eliminate the core electrons, the all-electron H.-F. valence orbitals ϕ_v are converted into pseudo-orbitals χ_v which contain no radial nodes in the core region, while \hat{V}_{val} and \hat{V}_{core} are replaced by \hat{W}_{val} (where the Coulomb and exchange operators are defined for χ_v rather than for ϕ_v) and the pseudopotential \hat{U}^{ECP} , respectively,

$$\left[-\frac{1}{2}\nabla^2 - \frac{Z_{\text{eff}}}{r} + \hat{W}_{val} + \hat{U}^{ECP} \right] \chi_v = \epsilon_v \chi_v. \quad (1.12)$$

The pseudo-orbital and its eigenvalue are now used to generate a numerical potential, by ‘inversion’ of the modified Hartree–Fock equations (1.12). ‘Inversion’ means finding a \hat{U}^{ECP} which, when used in the Hartree–Fock Hamiltonian, reproduces a previously determined wave function and energy of an atom to a satisfactory degree. Formally, the result is given by

$$\hat{U}^{ECP} = \epsilon_v + \frac{Z_{\text{eff}}}{r} + \frac{[\frac{1}{2}\nabla^2 - \hat{W}_{val}]\chi_v}{\chi_v}. \quad (1.13)$$

Using numerical ECP’s and a large Gaussian basis set, one can generate analytical functions for the pseudo-orbital and for the numerical potential (1.13). Most commonly ECP’s are fit to the form of Eq. (1.8). The functions $U_l(r)$ appearing in \hat{U}^{ECP} , fit to a linear combination of Gaussians (1.9), determine the actual form of the potential.

Although there are no explicit orthogonality conditions imposed on the pseudo-orbitals, one assumes that the orthogonality requirements are enforced by the shape of the potential in the core region [6].

Within the variational Monte Carlo framework, the effective core potentials have been applied to a range of systems up to solid diamond, graphite, and silicon [8].

The use of pseudopotentials leads to inaccuracies when the core significantly influences the valence electrons. Contributions come from several sources [7, 9]:

- (1) nonconstancy of the atomic core with the increasing number of valence electrons and changes in the molecular environment — the break-up of the frozen-core approximation;
- (2) core-valence overlap due to the absence of explicit core-valence orthogonality conditions;
- (3) core-polarization effects — distortion of the spherical symmetry of the atomic core by the valence electrons which has repercussions on the motion of valence electrons themselves;
- (4) inability to take into account intra-core and core-valence correlation effects;
- (5) errors originating in the fit procedure and those due to defects in the basis sets;
- (6) possible overestimation of valence correlation effects due to the inner nodeless behavior of the valence orbitals.

Core polarization and core-valence correlation effects can be treated by introducing additional terms to the pseudopotential, such as semiempirical polarization potentials [10].

Model potentials. The difference between the model potentials and the effective core potentials is that the valence orbitals of the MP approximation retain the correct nodal structure. This is achieved by using the so-called energy level shift operator

$$\Delta_{nl}\hat{\Omega}_{nl} \equiv \Delta_{nl}|\phi_{nl}^c\rangle\langle\phi_{nl}^c|, \quad (1.14)$$

which raises the energy of a core orbital $|\phi_{nl}^c\rangle$ by the amount Δ_{nl} . If the energy shift is chosen properly, this operator places the core orbitals above the valence in energy, so that the electrons first occupy the lowest valence orbital.

For example, in the case of Li-Ne atoms ($1s^2$ -core) the explicit form of the valence Hamiltonian is [11]

$$\hat{H}_{val} = \sum_{i=1}^{n_v} \left[-\frac{1}{2} \nabla_i^2 + \sum_{i<j}^{n_v} \frac{1}{r_{ij}} + \hat{U}^{MP}(r_i) \right], \quad (1.15)$$

where

$$\hat{U}^{MP}(r_i) = V^{MP}(r_i) + \Delta_{1s} \hat{\Omega}_{1s} \quad (1.16)$$

is the *model potential*, and

$$V^{MP}(r_i) = -\frac{Z_{eff}}{r_i} \left[1 + \sum_{k=1}^{n_c} A_k \exp(-B_k r^2) \right], \quad (1.17)$$

with $\Delta_{1s} = -2\epsilon_{1s}$ and $n_c = 2$.

Core and valence orbitals can be obtained from SCF calculations. This allows one to construct Ψ_{core} such that the core orbitals ϕ_{nl}^c are exactly orthogonal to Ψ_{val} . In this case, the projection operators (1.14) yield zero, and only the $V^{MP}(r)$ terms in (1.16) need to be evaluated. The disadvantage of MP's is that they require much larger basis sets than those used for construction of nodeless pseudo-orbitals of the ECP method.

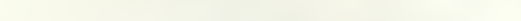
1.2.2 Damped-core quantum Monte Carlo method

The damped-core method was proposed by Hammond *et al.* [12] as an approach to heavy atoms that avoids the use of pseudopotentials. The authors used a non-antisymmetrized product wave function (1.2). In quantum Monte Carlo simulations, Ψ_{core} and Ψ_{val} can be chosen as accurately as desired, including explicit interelectronic distance terms.

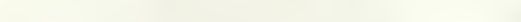
The distribution of the core electrons is simulated variationally with probability density $|\Psi_{core}|^2$ by the Metropolis algorithm (see below). The valence electrons, which are distinguishable from the core as a result of the factorization of the wave function, are sampled using quantum Monte Carlo (QMC) method which yields a more accurate electron distribution than the variational one. Moving the valence electrons in the potential created by the core electrons, one finds the valence energy of the system.

The first two steps of the synthesis are shown in Scheme 1.

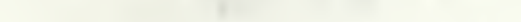


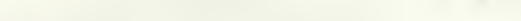
(2) 

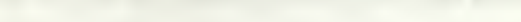
(3) 

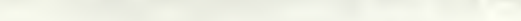
(4) 

(5) 

(6) 

(7) 

(8) 

(9) 

(10) 

(11) 

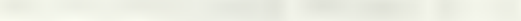
(12) 

(13) 

(14) 

(15) 

(16) 

(17) 

(18) 

(19) 

(20) 

(21) 

(22) 

(23) 

(24) 

Core and valence trial functions are obtained from the all-electron SCF determinant by partitioning it into core and valence orbital groups,

$$\Psi_{core} = |\chi_1(1) \cdots \chi_{n_c}(n_c)|, \quad (1.18)$$

$$\Psi_{val} = |\chi_{n_c+1}(n_c+1) \cdots \chi_n(n)|, \quad (1.19)$$

and the product $\Psi_{core}\Psi_{val}$ is multiplied by an electron-electron and electron-nuclear correlation functions.

The two Hamiltonians are as follows

$$\hat{H}_{core} = \sum_{k=1}^{n_c} \left[-\frac{1}{2} \nabla_k^2 - \frac{Z}{r_k} + \sum_{k < j}^{n_c} \frac{1}{r_{kj}} \right] \quad (1.20)$$

and

$$\hat{H}_{val} = \sum_{i=1}^{n_v} \left[-\frac{1}{2} \nabla_i^2 - \frac{Z}{r_i} + \sum_{i < j}^{n_v} \frac{1}{r_{ij}} + \sum_{k=1}^{n_c} \frac{1}{r_{ik}} \right]. \quad (1.21)$$

The advantage of this scheme is that the valence electrons, unrestricted by the much faster core time scale, can make significantly larger steps than possible with standard QMC method, and thus rapidly reach equilibrium in the core potential. The core itself also evolves, enabling one to sample a representative distribution of core electrons.

Although wave functions Ψ_{cor} and Ψ_{val} are orthogonal to each other by construction, QMC sampling changes the valence electron distribution from $|\Psi_{val}|^2$ to $|\Psi_{val}\Phi_{val}|$, so the simulated exact valence wave function Φ_{val} is no longer strictly orthogonal to the core function Ψ_{core} . In order to prevent the valence electrons from occupying the core orbitals, the branching of configurations of valence electrons in the core region within a certain cutoff radius is damped out by an r -dependent branching factor.

Since the core electrons appear explicitly, the damped-core method can incorporate the core polarization and most of the correlation effect, without introducing semiempirical polarization potentials. There remains, however, an open problem of inexact core-valence orthogonality.

Ionization potentials and electron affinities of carbon, silicon, and germanium calculated using this method with the cores consisting of 2, 10, and 28 electrons, respectively, were found to be in excellent agreement with experiment.

1.2.3 Valence-electron-only calculations with core projection operators

Standing somewhat off the mainstream is another method, proposed by Leasure *et al.* [13, 14], aiming at a direct calculation using the valence-electron-only wave function Ψ_{val} with no explicit reference to the core electrons.

This technique is based on analysis of the energy expression arising from a Hartree–Fock-type wave function for a closed-shell atom and assignment of the various contributions to the energy as originating from either core or valence electrons. The all-electron closed-shell Hartree–Fock wave function has the form

$$\Psi = |\phi_1 \bar{\phi}_1 \cdots \phi_{n_c/2} \bar{\phi}_{n_c/2} \phi_{n_c/2+1} \bar{\phi}_{n_c/2+1} \cdots \phi_{n/2} \bar{\phi}_{n/2}|, \quad (1.22)$$

where there are n_c electrons occupying the core orbitals ϕ_1 to $\phi_{n_c/2}$, and the remaining $n_v = n - n_c$ electrons are in the valence orbitals $\phi_{n_c/2+1}$ to $\phi_{n/2}$.

Provided that the orbitals in the wave function are mutually orthogonal, the total energy corresponding to this wave function can be written as

$$\begin{aligned} E &= \langle \Psi | \hat{H} | \Psi \rangle \\ &= \left[2 \sum_{k=1}^{n_c/2} h_{kk} + \sum_{k=1}^{n_c/2} \sum_{k'=1}^{n_c/2} (2J_{kk'} - K_{kk'}) \right] + \left[\sum_{i=1}^{n_v/2} \sum_{k=1}^{n_c/2} (4J_{ki} - 2K_{ki}) \right] \\ &\quad + \left[2 \sum_{i=1}^{n_v/2} h_{ii} + \sum_{i=1}^{n_v/2} \sum_{i'=1}^{n_v/2} (2J_{ii'} - K_{ii'}) \right], \end{aligned} \quad (1.23)$$

where h_{kk} and h_{ii} are matrix elements of the one-electron energy operators and $J_{kk'}$ and $K_{ii'}$ are the Coulomb and exchange integrals arising from the electron-electron repulsion. The energy expression (1.23) is partitioned into the following terms: intra-core

energy, core-valence interaction energy, and intra-valence energy. The intra-core energy remains unchanged in different chemical environments and is totally absent from a valence-electron-only calculation. The two other terms constitute the valence energy. The theory aims to reproduce this energy in a valence-electron-only atomic SCF calculation.

The valence wave function is given the form

$$\Psi_{val} = |\chi_{n_c/2+1} \bar{\chi}_{n_c/2+1} \cdots \chi_{n/2} \bar{\chi}_{n/2}|. \quad (1.24)$$

Since the core orbitals are entirely absent from the valence-electron-only wave function, there is nothing to maintain the orthogonality of the pseudo-valence orbital χ_i to the core orbitals. The method must therefore give the correct energy expression when used with pseudo-valence orbitals contaminated with an arbitrary amount of core orbitals, i.e. imagined as being of the form

$$\chi_i = \phi_i + \sum_k^{n_c/2} a_k \phi_k. \quad (1.25)$$

The improper normalization of χ_i is necessary because it is only in this way that the pseudo-orbital can become identical to the true valence orbital ϕ_i of the all-electron calculations in the valence region.

For the pseudo-orbital χ_i to yield the correct valence energy, the core orbital contributions to the matrix elements in (1.23) must be explicitly projected out. This is achieved by the use of effective Coulomb, exchange and Hamiltonian operators which contain the core projection operators

$$\hat{P}_{core} = \sum_{k=1}^{n_c/2} |\phi_k\rangle\langle\phi_k|. \quad (1.26)$$

where the summation is over all core spin-orbitals.

The energy calculated with this method is guaranteed to converge, as the size of orbital basis increases, to the limit of valence energy which would be obtained from all-electron calculation using a frozen SCF description of the core electrons. It is suggested

that the theory may be extended to make allowances for the core-valence correlation effect and core polarization.

The technique differs from the pseudopotential methods in several respects. Firstly, unlike the ECP's, based on the average field approximation, every term which occurs in the all-electron frozen-core energy expression is exactly reproduced. Secondly, in pseudopotential methods the collapse of the valence orbitals into the core subspace is prevented by introduction of a repulsive potential, while in this method it is accomplished by the explicit use of core projection operators.

1.3 Problems of Core-Valence Partitioning

From the preceding discussion it becomes clear that the benefits of core-valence partitioning are at the same time associated with a major problem — it is very difficult to incorporate completely into a partitioning scheme rather complex interrelations between core and valence electrons. Principal effects contributing to this problem can be summarized as follows.

The loss of antisymmetry. A many-electron wave function (1.2), which has 'core' and 'valence' parts, does not satisfy the Pauli exclusion principle with respect to interchange of core and valence electrons. Some authors call this effect 'the Pauli exclusion holes' [15], referring to the fact that in a system described with the incompletely antisymmetrized wave function, the valence electrons can occupy core orbitals as if the core electrons did not exist, 'falling through' onto the core. It is an open question of to what extent the loss of core-valence antisymmetry of the product wave function (1.2) is recovered by the orthogonality condition of the damped-core technique, by the repulsive potential of the ECP approximation, or by the projection operators of the MP method.

Core-valence orthogonality If the partitioned wave function is not an antisymmetrized product, it is necessary that Ψ_{core} and Ψ_{val} be exactly orthogonal to each other. Any non-zero *core-valence overlap* will result in a certain error. It is therefore desirable to know the magnitude of this error as a function of the overlap.

Static core-relaxation effects. This refers to mean-field ‘breathing’ of core orbitals which minimizes the potential energy during a change in the valence configuration or chemical environment. It manifests itself in the Hartree–Fock formulations of core-valence partitioning based on the frozen-core approximation.

Static core-polarization effects. In the Hartree–Fock treatment, which is a basis for several valence-electron methods, the charge distribution of the atomic core is spherically symmetric and not affected by the motion of valence electrons. In fact, the core *does* deviate from the spherical symmetry (‘polarizes’) depending on the instantaneous positions of the valence electrons, and the potential, in which the valence electrons move, is different from the potential in the independent electron approximation. Peculiar to the valence-electron-only techniques, this effect can be treated by introducing additional terms in the expression for the potential experienced by valence electrons.

Dynamical core-valence correlation effects. If the core electrons do not appear explicitly, correct treatment of electron correlation in the valence-electron-only methods presents a problem. Since the true correlation energy is non-linear with respect to contributions from different electrons, separating contributions of the core and valence electrons to the appropriate effective Hamiltonians cannot be clearly defined. The question is how the failure to allow for the core-valence correlation in calculations with a partitioned wave function affects the results.

1.4 The Scope of the Present Study

The objective of this work is to study various model *all-electron* core-valence partitioning schemes *in orbital space* represented by the non-antisymmetrized product wave function of type (1.2). This will be done by constructing suitable trial wave functions and employing them in calculations of selected atomic properties. Conclusions will be drawn by comparing performance of a non-partitioned ('complete') wave function and that of wave functions representing different levels of separation to the extent that their flexibility, specifically, the number and type of variational parameters, is comparable.

Using all-electron partitioned non-antisymmetrized wave functions we can study significance of the following effects occurring in atomic systems:

- core-valence antisymmetry,
- core-valence orthogonality,
- dynamical core-valence correlation.

Because we intend to treat the core electrons explicitly, we will be unable within this approach to study the static core-polarization and core relaxation effects, peculiar to the partitioning schemes where the core electrons are removed.

We are interested in the errors induced by omission of the above effects and their trends as we go through a series of atomic systems. Furthermore, since in chemical applications one usually deals with properties which are differences between certain quantities in two states, calculation and comparison of such property as ionization potential will be used to determine to which the extent these errors cancel. As will be shown, variational Monte Carlo (VMC) method is an excellent tool to achieve this goal.

THE JOURNAL OF THE

THE JOURNAL OF THE

THE JOURNAL OF THE

THE JOURNAL OF THE

THE JOURNAL OF THE

THE JOURNAL OF THE

THE JOURNAL OF THE

THE JOURNAL OF THE

THE JOURNAL OF THE

THE JOURNAL OF THE

THE JOURNAL OF THE

THE JOURNAL OF THE

THE JOURNAL OF THE

THE JOURNAL OF THE

Chapter 2

Model Wave Functions

2.1 Construction of the Trial Wave Functions

In the preceding chapter we described the nature of the effects which ideally should be preserved in partitioned wave functions. In this chapter we develop models to estimate the errors resulting from omission of these effects quantitatively.

Although the variational Monte Carlo (VMC) method, which we use in the present study, is described in detail only in the Chapter 3, the following discussion is not restricted to this particular technique.

2.1.1 General considerations for construction of trial wave functions

All averages in VMC are evaluated with respect to a certain trial function Ψ_T , so that its choice determines the accuracy of the results. Of course, a simple Ψ_T is easy to implement, but a more elaborate wave function gives better estimates of the properties and with a lower variance.

Any acceptable trial wave function must be: *continuous*, *single-valued*, and *square integrable*. A function meeting these requirements is said to be *well-behaved*. In addition to these properties, a wave function must exhibit a proper behavior near the points of configuration space where charged particles meet. For this, it must have a discontinuity in its first derivative at such points. This discontinuity is called a *cusp*. Cusp conditions may impose specific requirements on variational parameters (see Appendix B).

CHAPTER 10

10.1. THE BASIC DEFINITIONS AND NOTATION

Let X be a set. A *relation* on X is a subset R of the Cartesian product $X \times X$. If $(x, y) \in R$, we say that x is related to y , and write $x R y$. If R is a relation on X , we define the *domain* of R to be the set of all $x \in X$ such that $x R y$ for some $y \in X$. We also define the *range* of R to be the set of all $y \in X$ such that $x R y$ for some $x \in X$. If R is a relation on X , we say that R is *reflexive* if $x R x$ for all $x \in X$. We say that R is *symmetric* if $x R y$ implies $y R x$ for all $x, y \in X$. We say that R is *transitive* if $x R y$ and $y R z$ implies $x R z$ for all $x, y, z \in X$. A relation R on X which is reflexive, symmetric, and transitive is called an *equivalence relation*. If R is an equivalence relation on X , we define the *equivalence class* of $x \in X$ to be the set of all $y \in X$ such that $x R y$. We denote the equivalence class of x by $[x]$.

10.2. PARTIAL ORDERINGS AND LATTICES

Let X be a set. A *partial ordering* on X is a relation R on X which is reflexive, antisymmetric, and transitive. We say that R is a *total ordering* if $x R y$ or $y R x$ for all $x, y \in X$. If R is a partial ordering on X , we say that x is *less than* y , and write $x < y$, if $x R y$ and $x \neq y$. We say that x and y are *comparable* if $x < y$ or $y < x$. A partial ordering R on X is called a *lattice ordering* if for any two elements $x, y \in X$, there is a unique element $z \in X$ such that $x < z$ and $y < z$, and $z < w$ for any $w \in X$ such that $x < w$ and $y < w$. We denote this element z by $x \vee y$, and call it the *join* of x and y . We also denote the unique element $w \in X$ such that $x < w$ and $y < w$ by $x \wedge y$, and call it the *meet* of x and y .

Let X be a set. A *lattice* is a set X with a partial ordering R which is a lattice ordering, and with two distinguished elements 0 and 1 such that $0 < x < 1$ for all $x \in X$. We say that X is a *bounded lattice*. If X is a bounded lattice, we say that x is *less than* y , and write $x < y$, if $x R y$ and $x \neq y$. We say that x and y are *comparable* if $x < y$ or $y < x$. A bounded lattice X is called a *distributive lattice* if for any three elements $x, y, z \in X$, we have $x \wedge (y \vee z) = (x \wedge y) \vee (x \wedge z)$ and $x \vee (y \wedge z) = (x \vee y) \wedge (x \vee z)$. A bounded distributive lattice X is called a *Boolean algebra* if for every element $x \in X$, there is a unique element $y \in X$ such that $x \wedge y = 0$ and $x \vee y = 1$. We denote this element y by x' , and call it the *complement* of x .

If X is a Boolean algebra, we say that x is *less than* y , and write $x < y$, if $x R y$ and $x \neq y$.

Finally, for fermion systems, a many-electron valid wave function must satisfy the **antisymmetry (exclusion) principle**: it must be antisymmetric with respect to the interchange of the coordinates of any two electrons. Partitioned wave functions do not satisfy this requirement.

The exact ground-state eigenvalue and eigenfunction of the non-relativistic, stationary nucleus Hamiltonian are called the *exact* energy E_{exact} and the *exact* wave function, respectively. Except for certain trivial cases the exact wave function is unknown. Approximate wave functions are usually expressed using expansions of one-electron functions, known as orbitals. The expectation value associated with a *valid* approximate non-relativistic wave function Ψ_T is always above E_{exact} . The larger and more complete is the set of basis orbitals used to construct the approximate wave function, the greater is the degree of flexibility in the expansion and the lower is the variational energy \bar{E} .

In the Hartree-Fock method, enlargement of the basis set lowers the energy until a certain limit is reached, known as the *Hartree-Fock limit*. The Hartree-Fock limit is never equal to the exact energy because the exact wave function cannot be expressed as a single determinant, and the motion of electrons with opposite spins is not correlated within the Hartree-Fock approximation. The difference between the exact energy of the system E_{exact} and the Hartree-Fock limit E_{HF} is called the **correlation energy**

$$E_{\text{corr}} \stackrel{\text{def}}{=} E_{\text{exact}} - E_{\text{HF}}. \quad (2.1)$$

A wave function performing better than the best uncorrelated single determinant of spin-orbitals is referred to as a 'post-Hartree-Fock' function. Normally, instead of the absolute value of the correlation energy recovered by a certain post-Hartree-Fock wave function, one uses the percent expression defined as

$$\%E_{\text{corr}} \stackrel{\text{def}}{=} \frac{E_{\text{exact}} - \bar{E}}{E_{\text{exact}} - E_{\text{HF}}} 100\%. \quad (2.2)$$

The first part of the book is a general introduction to the subject of the book. It discusses the importance of the subject and the scope of the book. It also discusses the organization of the book and the author's objectives.

The second part of the book is a detailed discussion of the subject. It covers the basic concepts and principles of the subject. It also discusses the various methods and techniques used in the study of the subject. The third part of the book is a discussion of the applications of the subject. It shows how the concepts and principles of the subject can be applied to various fields of study.

The fourth part of the book is a discussion of the future of the subject. It discusses the current trends and developments in the field and predicts the future direction of the subject. The fifth part of the book is a conclusion and a summary of the main points of the book.

Chapter 2: Basic Concepts

This chapter discusses the basic concepts and principles of the subject. It covers the definitions of the terms used in the subject and the relationships between them. It also discusses the basic laws and principles of the subject.

Chapter 3: Methods and Techniques

This chapter discusses the various methods and techniques used in the study of the subject. It covers the experimental methods, the theoretical methods, and the computational methods.

This is a customary measure of the quality of a post-Hartree–Fock wave function.

The treatment of electron correlation is a difficult problem. It can be approached directly by introduction of an *electron correlation function* which contains explicitly interelectronic distances r_{ij} . However, in conventional methods this leads to molecular integrals that are inconvenient for analytical integration or not analytically integrable at all. The other approach — *full configuration interaction* — is based on the idea that the exact wave function can be expanded as a linear combination of all possible n -electron Slater determinants formed from a complete set of spin-orbitals. The resulting wave function may include a tremendous number of Slater determinants, but as long as r_{ij} -terms never appear in the expansion, all the integrals can be evaluated analytically.

One of the advantages of Monte Carlo methods is the flexibility they afford in the choice of trial wave functions. In contrast to other *ab initio* methods, VMC can use wave functions of arbitrary forms — notably with explicit interelectronic distance dependencies — which, even if they are relatively compact, allow one to go beyond the Hartree–Fock limit to recover a considerable part of the correlation energy and ultimately to approach the exact non-relativistic solution.

2.1.2 The complete wave function

The complete wave function, which we will call Ψ_1 and its expectation value E_1 , is a bench mark for subsequent modifications. Understandably, it should incorporate as many qualities of the exact wave function as possible.

As shown in Appendix A, instead of the complete $n \times n$ Slater determinant of spin-orbitals, in variational calculations one can use a wave function in the form of the product of Slater determinants of *spatial* orbitals for spin-up and spin-down electrons, without explicit inclusion of spin-functions. All spin-independent properties estimated with such

a wave function within variational method are unchanged with respect to the single determinant of spin-orbitals, whereas breaking one determinant into two of smaller dimensions is computationally advantageous.

Following a common practice, we chose the wave function Ψ_1 to be of this pair-product form

$$\begin{aligned}\Psi_1 &= \begin{vmatrix} \phi_1(1) & \phi_1(2) & \dots & \phi_1(n^\uparrow) \\ \phi_2(1) & \phi_2(2) & \dots & \phi_2(n^\uparrow) \\ \vdots & \vdots & \ddots & \vdots \\ \phi_{n^\uparrow}(1) & \phi_{n^\uparrow}(2) & \dots & \phi_{n^\uparrow}(n^\uparrow) \end{vmatrix} \begin{vmatrix} \phi_1(n^\uparrow+1) & \phi_1(n^\uparrow+2) & \dots & \phi_1(n) \\ \phi_2(n^\uparrow+1) & \phi_2(n^\uparrow+2) & \dots & \phi_2(n) \\ \vdots & \vdots & \ddots & \vdots \\ \phi_{n^\downarrow}(n^\uparrow+1) & \phi_{n^\downarrow}(n^\uparrow+2) & \dots & \phi_{n^\downarrow}(n) \end{vmatrix} J \\ &= \psi_D^\uparrow \psi_D^\downarrow J,\end{aligned}\quad (2.3)$$

where ψ_D^\uparrow and ψ_D^\downarrow denote Slater determinants of atomic orbitals for spin-up and spin-down electrons, respectively. As shown in Chapter 3, in the VMC method one needs not know the normalization factor in (2.3).

To allow explicitly for electron correlation the simple product of the determinants is multiplied by a Padé–Jastrow pair-correlation function

$$J = J(r_{ij}) = \exp \left(\sum_{i=1}^{n-1} \sum_{j=i+1}^n \frac{ar_{ij}}{1 + br_{ij}} \right). \quad (2.4)$$

The value of a is determined from the electron-electron cusp conditions (Appendix B),

$$a = \begin{cases} \frac{1}{4} & \text{if } i \text{ and } j \text{ are of like spin,} \\ \frac{1}{2} & \text{if } i \text{ and } j \text{ are of unlike spin,} \end{cases} \quad (2.5)$$

while b is an optimized variational parameter.

The functional form of atomic orbitals used to construct determinants ψ_D^\uparrow and ψ_D^\downarrow was developed by Langfelder [16]. These resemble hydrogen-type orbitals¹, and because of

¹It is essential since a simple STO 2s-orbital does not have the proper cusp behavior.

inclusion of the electron-nuclear correlation factors the set can be viewed as ‘double-zeta’ quality. In the explicit form,

$$\begin{aligned}\phi_{1s} &= e^{-\zeta_{1s}r} e^{-\frac{w_{1s}r}{1+v_{1s}r}}, \\ \phi_{2s} &= (1+cr) e^{-\zeta_{2s}r} e^{-\frac{w_{2s}r}{1+v_{2s}r}}, \\ \phi_{2p_q} &= q e^{-\zeta_{2p}r} e^{-\frac{w_{2p}r}{1+v_{2p}r}},\end{aligned}\tag{2.6}$$

where $q = x, y, z$.

As shown in Appendix B, the electron-nuclear cusp conditions produce the following relationships between the parameters

$$\begin{aligned}w_{1s} &= Z - \zeta_{1s} \\ w_{2s} &= Z - \zeta_{2s} + c \\ w_{2p} &= \frac{Z}{2} - \zeta_{2p}\end{aligned}\tag{2.7}$$

where Z is the charge of the nucleus.

No distinction is made between ζ_{2s} and ζ_{2p} , w_{1s} and w_{2s} , v_{1s} and v_{2s} , so that by grouping we obtain

$$\begin{aligned}\zeta_{2s} = \zeta_{2p} &\equiv \zeta_2 \\ w_{1s} = w_{2s} &\equiv w_s \\ v_{1s} = v_{2s} &\equiv v_s.\end{aligned}\tag{2.8}$$

Eq. (2.7) and (2.8) determine the value of parameter c . For consistency, we also introduce

$$\begin{aligned}w_p &\equiv w_{2p} \\ v_p &\equiv v_{2p}.\end{aligned}\tag{2.9}$$

Since w_s , w_p , and c are not independent, the total number of optimization parameters for wave function Ψ_1 varies from 3 to 5 (see Table 2.1 below).

assessing the impact of the intervention on the outcome variable. The results of the analysis are presented in Table 1.

$$\begin{aligned} (1) \quad & \text{Outcome}_{it} = \alpha_0 + \alpha_1 \text{Time}_{it} + \alpha_2 \text{Group}_{it} + \alpha_3 \text{Time}_{it} \times \text{Group}_{it} + \epsilon_{it} \\ (2) \quad & \text{Outcome}_{it} = \alpha_0 + \alpha_1 \text{Time}_{it} + \alpha_2 \text{Group}_{it} + \alpha_3 \text{Time}_{it} \times \text{Group}_{it} + \alpha_4 \text{Covariates}_{it} + \epsilon_{it} \\ (3) \quad & \text{Outcome}_{it} = \alpha_0 + \alpha_1 \text{Time}_{it} + \alpha_2 \text{Group}_{it} + \alpha_3 \text{Time}_{it} \times \text{Group}_{it} + \alpha_4 \text{Covariates}_{it} + \alpha_5 \text{Covariates}_{it}^2 + \epsilon_{it} \end{aligned}$$

where Outcome_{it} is the outcome variable, Time_{it} is the time variable, Group_{it} is the group variable, Covariates_{it} are the covariates, and ϵ_{it} is the error term.

$$\begin{aligned} (4) \quad & \text{Outcome}_{it} = \alpha_0 + \alpha_1 \text{Time}_{it} + \alpha_2 \text{Group}_{it} + \alpha_3 \text{Time}_{it} \times \text{Group}_{it} + \alpha_4 \text{Covariates}_{it} + \alpha_5 \text{Covariates}_{it}^2 + \alpha_6 \text{Covariates}_{it}^3 + \epsilon_{it} \\ (5) \quad & \text{Outcome}_{it} = \alpha_0 + \alpha_1 \text{Time}_{it} + \alpha_2 \text{Group}_{it} + \alpha_3 \text{Time}_{it} \times \text{Group}_{it} + \alpha_4 \text{Covariates}_{it} + \alpha_5 \text{Covariates}_{it}^2 + \alpha_6 \text{Covariates}_{it}^3 + \alpha_7 \text{Covariates}_{it}^4 + \epsilon_{it} \end{aligned}$$

where Covariates_{it}^2 is the squared covariates, Covariates_{it}^3 is the cubed covariates, and Covariates_{it}^4 is the fourth power of the covariates.

$$\begin{aligned} (6) \quad & \text{Outcome}_{it} = \alpha_0 + \alpha_1 \text{Time}_{it} + \alpha_2 \text{Group}_{it} + \alpha_3 \text{Time}_{it} \times \text{Group}_{it} + \alpha_4 \text{Covariates}_{it} + \alpha_5 \text{Covariates}_{it}^2 + \alpha_6 \text{Covariates}_{it}^3 + \alpha_7 \text{Covariates}_{it}^4 + \alpha_8 \text{Covariates}_{it}^5 + \epsilon_{it} \\ (7) \quad & \text{Outcome}_{it} = \alpha_0 + \alpha_1 \text{Time}_{it} + \alpha_2 \text{Group}_{it} + \alpha_3 \text{Time}_{it} \times \text{Group}_{it} + \alpha_4 \text{Covariates}_{it} + \alpha_5 \text{Covariates}_{it}^2 + \alpha_6 \text{Covariates}_{it}^3 + \alpha_7 \text{Covariates}_{it}^4 + \alpha_8 \text{Covariates}_{it}^5 + \alpha_9 \text{Covariates}_{it}^6 + \epsilon_{it} \end{aligned}$$

where Covariates_{it}^5 is the fifth power of the covariates, and Covariates_{it}^6 is the sixth power of the covariates.

$$\begin{aligned} (8) \quad & \text{Outcome}_{it} = \alpha_0 + \alpha_1 \text{Time}_{it} + \alpha_2 \text{Group}_{it} + \alpha_3 \text{Time}_{it} \times \text{Group}_{it} + \alpha_4 \text{Covariates}_{it} + \alpha_5 \text{Covariates}_{it}^2 + \alpha_6 \text{Covariates}_{it}^3 + \alpha_7 \text{Covariates}_{it}^4 + \alpha_8 \text{Covariates}_{it}^5 + \alpha_9 \text{Covariates}_{it}^6 + \alpha_{10} \text{Covariates}_{it}^7 + \epsilon_{it} \\ (9) \quad & \text{Outcome}_{it} = \alpha_0 + \alpha_1 \text{Time}_{it} + \alpha_2 \text{Group}_{it} + \alpha_3 \text{Time}_{it} \times \text{Group}_{it} + \alpha_4 \text{Covariates}_{it} + \alpha_5 \text{Covariates}_{it}^2 + \alpha_6 \text{Covariates}_{it}^3 + \alpha_7 \text{Covariates}_{it}^4 + \alpha_8 \text{Covariates}_{it}^5 + \alpha_9 \text{Covariates}_{it}^6 + \alpha_{10} \text{Covariates}_{it}^7 + \alpha_{11} \text{Covariates}_{it}^8 + \epsilon_{it} \end{aligned}$$

where Covariates_{it}^7 is the seventh power of the covariates, and Covariates_{it}^8 is the eighth power of the covariates.

The wave function Ψ_1 is continuous, single-valued, and square integrable. It has correct discontinuities of its first derivatives, and is antisymmetric with respect to interchange of electrons with like spins. Although this wave function is relatively simple, it is good enough to recover consistently 60–62% of the correlation energy for the Be – Ne atoms, and up to 91% for the Li atom (see Chapter 5).

2.1.3 Full-atomic implementation of the core-valence partitioning

We partition the complete wave function Ψ_1 into core and valence parts such that the electrons of the K-shell (1s orbitals) constitute the core, while the remaining electrons belong to the valence group.

In Ψ_1 each of the Slater determinants incorporates all electrons with like spins. This means that we do distinguish two types of electrons — those with spin ‘up’ and those with spin ‘down’. This seeming violation of the indistinguishability principle notwithstanding, the use of wave function Ψ_1 does not lead to any troubles, because Ψ_1 still satisfies a modified formulation of the exclusion principle: each *spatial* orbital can be occupied by no more than *two* electrons *with opposite spins*. When two or more electrons with the same spin occupy the same spatial orbital, one of the determinants of Ψ_1 vanishes. In other words, the n -electron identity requirement has been partially substituted by an appropriate form of the wave function.

Now consider a partitioned wave function with a $1s^2$ -core. The partitioning is achieved by splitting each of the determinants of Ψ_1 into core and valence parts. If there is no antisymmetrizer (which enforces unit occupation numbers) and if the valence orbitals are not orthogonal to the $1s$ -core orbital, there is nothing that can prevent the valence electrons from occupying the core orbitals and thereby admixing bosonic states to the ground state wave function of supposed fermions! Since this model bears no relationship to reality, the total energy of such a system may drop below the experimental value.

Once electrons become distinguishable as either core or valence, the antisymmetry is broken, and to prevent the collapse one must re-introduce the orthogonality explicitly by constructing a partitioned wave function $\Psi = \Psi_{core}\Psi_{val}$ such that $\langle \Psi_{core} | \Psi_{val} \rangle = 0$.

Function Ψ_{core} will be orthogonal to Ψ_{val} if each atomic orbital used to construct Slater determinant(s) Ψ_{val} is orthogonal to every atomic orbital in Ψ_{core} . In the basis set used in this work, the core orbital is ϕ_{1s} and the valence ones are ϕ_{2s} and ϕ_{2p} , given by Eq. (2.6). Orbitals ϕ_{2p} are orthogonal to ϕ_{1s} by virtue of their angular parts, but the ϕ_{2s} orbital is not. To obtain the (un-normalized) orthogonal orbital ϕ_{2s}^\perp , we use Gram-Schmidt orthogonalization

$$\phi_{2s}^\perp = N_{2s}\phi_{2s} - S_{12}N_{1s}\phi_{1s}, \quad (2.10)$$

where N_1 and N_2 are normalization factors, and

$$S_{12} = N_{1s}N_{2s} \int \phi_{1s}\phi_{2s} dV. \quad (2.11)$$

This method accomplishes exactly what is desired: removal of the core component from a valence orbital².

Finally, the values of parameter a appearing in Eq. (2.4), determined by the electron-electron cusp conditions (Appendix B), are slightly different from those for the complete wave function, namely

$$a = \begin{cases} \frac{1}{4} & \text{if electrons } i \text{ and } j \text{ belong to the same determinant,} \\ \frac{1}{2} & \text{if electrons } i \text{ and } j \text{ belong to different determinants.} \end{cases} \quad (2.12)$$

Thus a can be 1/2 even if the electrons have the like spins but belong to different shells.

²Other orthogonalization procedures exist. Recently Banerjee [17] proposed an orthogonalization method which allows construction of valence orbitals that are orthogonal to the core orbitals and yet involve *no* component of the core, unlike Gram-Schmidt and symmetric orthogonalizations. A very useful application of this procedure has been suggested for the effective core potential method.

the following: (1) the patient is not a resident of the United States; (2) the patient is not a citizen of the United States; (3) the patient is not a permanent resident of the United States; (4) the patient is not a member of the American Medical Association.

The following are the conditions of the American Medical Association's policy on the use of the word "physician" in the title of a medical professional: (1) the patient must be a resident of the United States; (2) the patient must be a citizen of the United States; (3) the patient must be a permanent resident of the United States; (4) the patient must be a member of the American Medical Association. The American Medical Association's policy on the use of the word "physician" in the title of a medical professional is based on the following: (1) the patient is not a resident of the United States; (2) the patient is not a citizen of the United States; (3) the patient is not a permanent resident of the United States; (4) the patient is not a member of the American Medical Association.

1914

AMERICAN MEDICAL ASSOCIATION

THE AMERICAN MEDICAL ASSOCIATION'S POLICY ON THE USE OF THE WORD "PHYSICIAN" IN THE TITLE OF A MEDICAL PROFESSIONAL

1915

AMERICAN MEDICAL ASSOCIATION

The American Medical Association's policy on the use of the word "physician" in the title of a medical professional is based on the following: (1) the patient is not a resident of the United States; (2) the patient is not a citizen of the United States; (3) the patient is not a permanent resident of the United States; (4) the patient is not a member of the American Medical Association.

The American Medical Association's policy on the use of the word "physician" in the title of a medical professional is based on the following: (1) the patient is not a resident of the United States; (2) the patient is not a citizen of the United States; (3) the patient is not a permanent resident of the United States; (4) the patient is not a member of the American Medical Association.

1916

AMERICAN MEDICAL ASSOCIATION

1917

AMERICAN MEDICAL ASSOCIATION

The American Medical Association's policy on the use of the word "physician" in the title of a medical professional is based on the following: (1) the patient is not a resident of the United States; (2) the patient is not a citizen of the United States; (3) the patient is not a permanent resident of the United States; (4) the patient is not a member of the American Medical Association.

2.2 Study of the Core-Valence Separation Effects

The next step in our plan is the design of model partitioned wave functions imitating the absence of effects occurring in Ψ_1 . Explicit treatment of all electrons is necessary to avoid any effects other than the one being studied.

2.2.1 The loss of core-valence antisymmetry

We have seen that although the wave function Ψ_1 is *neither* symmetric *nor* antisymmetric with respect to interchange of electrons with opposite spins, this fact has no effect on the variational estimates. This is a consequence of Ψ_1 's not being an eigenfunction of spin-operators. However, any further loss of antisymmetry, in particular, resulting in distinguishing 'core' and 'valence' electrons is expected to lead to a change in variational estimates, since the wave function is no longer strictly valid. In order to study this effect, we split both the spin-up and spin-down determinants of Ψ_1 into core and valence parts, while at the same time keeping the Jastrow correlation function unchanged. We call the resulting wave function Ψ_2

$$\begin{aligned}\Psi_2 &= |\phi_1^c(1)| |\phi_1^c(2)| |\phi_1^v(n_c+1) \cdots \phi_{n_v}^v(n_c+n_v^\uparrow)| |\phi_1^v(n_c+n_v^\uparrow+1) \cdots \phi_{n_v}^v(n)| J \\ &= \psi_{D_c}^\uparrow \psi_{D_c}^\downarrow \psi_{D_v}^\uparrow \psi_{D_v}^\downarrow J.\end{aligned}\tag{2.13}$$

Peculiarly, the antisymmetry principle is satisfied within a group of electrons of the same spin only if the determinant accommodates two or more such electrons. It follows that Ψ_{core} , with two 1s-electrons representing the core, is in fact *not* even partially antisymmetric. This is also true for the valence shells of Li, Be, Be⁺, B, B⁺, and C⁺.

In any case, the wave function Ψ_2 as a whole is neither symmetric nor antisymmetric with respect to interchange of one core and one valence electron of the same spin. The core and valence parts of Ψ_2 must therefore be orthogonal to each other.

THE PHILOSOPHY OF LANGUAGE SOCIETY

...the philosophy of language is a branch of philosophy which is concerned with the study of the nature and structure of language, and the relationship between language and the world. It is a branch of philosophy which is concerned with the study of the nature and structure of language, and the relationship between language and the world.

THE PHILOSOPHY OF LANGUAGE SOCIETY

...the philosophy of language is a branch of philosophy which is concerned with the study of the nature and structure of language, and the relationship between language and the world. It is a branch of philosophy which is concerned with the study of the nature and structure of language, and the relationship between language and the world.

THE PHILOSOPHY OF LANGUAGE SOCIETY

...the philosophy of language is a branch of philosophy which is concerned with the study of the nature and structure of language, and the relationship between language and the world. It is a branch of philosophy which is concerned with the study of the nature and structure of language, and the relationship between language and the world.

Orbitals (2.6) are used to construct the determinants $\psi_{D_c}^\uparrow$, $\psi_{D_c}^\downarrow$, $\psi_{D_v}^\uparrow$, and $\psi_{D_v}^\downarrow$. Orthogonality is maintained using ϕ_{2s}^\perp as given by (2.10).

Variational parameters of Ψ_2 are the same type as those of Ψ_1 . The optimized expectation value of total energy is denoted E_2 . The difference between E_2 and E_1 characterizes the partial loss of antisymmetry, assuming that Ψ_1 and Ψ_2 match in terms of number of variational parameters and the basis set. Other interesting properties to calculate using Ψ_2 include electron-nuclear distances for the core and valence electrons, 'core' and 'valence' energies, and first ionization potentials.

2.2.2 The core-valence overlap effect

The extent to which the total energy of a partitioned system is affected by inexact orthogonality of core and valence parts of the wave function (*core-valence overlap*) can be assessed by computing the total energy of a system described with a partitioned wave function Ψ_2 , in which the strict orthogonality condition of ϕ_{1s} core and ϕ_{2s} valence orbitals is released.

For this purpose we introduce a Schmidt-modified ϕ_{2s} -type orbital

$$\phi'_{2s} = \frac{1}{\sqrt{1 + k^2 - 2kS_{12}}} [N_{2s}\phi_{2s} - kN_{1s}\phi_{1s}], \quad (2.14)$$

where S_{12} is given by (2.11) and k can be changed so as to allow various values of the overlap integral

$$Q = N_{1s}N'_{2s} \int \phi_{1s} \phi'_{2s} dV = (S_{12} - k) \frac{1}{\sqrt{1 + k^2 - 2kS_{12}}}. \quad (2.15)$$

Of course, Q can be both positive and negative. Solution of Eq. (2.15) for k gives

$$k = S_{12} - Q \sqrt{\frac{1 - S_{12}^2}{1 - Q^2}}. \quad (2.16)$$

In the particular case of $Q = 0$, which corresponds to $\phi'_{2s} = \phi_{2s}^\perp$, $k = S_{12}$.

Varying the overlap Q we can explore how sensitive the total energy is to the exactness of the core-valence orthogonality condition.

2.2.3 The core-valence correlation effect

In wave function Ψ_1 (2.3), motion of core and valence electrons is correlated by virtue of the factor J which includes all possible electron pairs *via* r_{ij} . To estimate the magnitude of the core-valence correlation effect, we will construct a wave function where the motion of the core and valence electrons is correlated within the shells but not between them. This is achieved when *both* determinantal and correlation parts of the complete wave function Ψ_1 are separated into core and valence parts. We call this wave function Ψ_3

$$\begin{aligned}
 \Psi_3 &= |\phi_1^c(1)| |\phi_1^c(2)| \\
 &\times |\phi_1^v(n_c+1) \cdots \phi_{n_v}^v(n_c+n_v^{\uparrow})| |\phi_1^v(n_c+n_v^{\uparrow}+1) \cdots \phi_{n_v}^v(n)| \\
 &\times \exp \left(\sum_{i=1}^{n_c-1} \sum_{j=i+1}^{n_c} \frac{ar_{ij}}{1+br_{ij}} \right) \exp \left(\sum_{i=n_c+1}^{n-1} \sum_{j=i+1}^n \frac{ar_{ij}}{1+br_{ij}} \right) \\
 &= \psi_{D_c}^{\uparrow} \psi_{D_c}^{\downarrow} \psi_{D_v}^{\uparrow} \psi_{D_v}^{\downarrow} J_c J_v.
 \end{aligned} \tag{2.17}$$

Alternatively, the product $J_c J_v$ can be viewed as a complete correlation function J from which all core-valence interaction terms are excluded.

Atomic orbitals used to construct Ψ_3 are the same as those for Ψ_1 and Ψ_2 . It is necessary for a valid comparison with Ψ_1 and Ψ_2 that a *single* electron-electron Jastrow parameter b be used for both the core and valence electrons, because Ψ_3 should have no advantage over Ψ_1 or Ψ_2 in terms of flexibility.

The differences $\Delta E_{31} \equiv E_3 - E_1$ of the total energies computed with wave functions Ψ_3 and Ψ_1 , respectively, give the combined effect of losing antisymmetry and neglecting core-valence correlation. Other properties mentioned above are also computed.

Let \mathcal{C} be a collection of subsets of \mathbb{R}^n . We say that \mathcal{C} is a *chain* if for any two sets $A, B \in \mathcal{C}$, either $A \subseteq B$ or $B \subseteq A$.

LEMMA 2.1. Let \mathcal{C} be a chain of subsets of \mathbb{R}^n .

Then the union of all sets in \mathcal{C} is also in \mathcal{C} . Moreover, if \mathcal{C} is a chain of closed sets, then the intersection of all sets in \mathcal{C} is also in \mathcal{C} . Finally, if \mathcal{C} is a chain of compact sets, then the intersection of all sets in \mathcal{C} is also compact.

PROOF. Let \mathcal{C} be a chain of subsets of \mathbb{R}^n .

$$(1) \text{ Let } A = \bigcup_{C \in \mathcal{C}} C. \text{ Then } A \in \mathcal{C}. \\ (2) \text{ Let } \mathcal{C} \text{ be a chain of closed sets. Then } \bigcap_{C \in \mathcal{C}} C \in \mathcal{C}. \\ (3) \text{ Let } \mathcal{C} \text{ be a chain of compact sets. Then } \bigcap_{C \in \mathcal{C}} C \text{ is compact.}$$

PROOF. (1) Let $A = \bigcup_{C \in \mathcal{C}} C$. Then A is the union of a chain of sets, so it is also in the chain.

(2) Let \mathcal{C} be a chain of closed sets. Then $\bigcap_{C \in \mathcal{C}} C$ is the intersection of a chain of closed sets, so it is also closed.

(3) Let \mathcal{C} be a chain of compact sets. Then $\bigcap_{C \in \mathcal{C}} C$ is the intersection of a chain of compact sets, so it is also compact.

2.2.4 Further study of electron correlation

Much of chemistry is the science of energy differences rather than of absolute energies. Specifically, ionization potentials based on Ψ_1 – Ψ_3 provide a more useful and realistic indication of the validity of a core-valence partitioning scheme.

The findings presented in Chapter 5 indicate that the wave function Ψ_3 consistently outperforms the two others in terms of ionization potentials. We assume that the unexpected good performance of Ψ_3 is accounted for by a better treatment of *intra-shell* electron correlation than in Ψ_2 and even Ψ_1 . If this is true, then a more flexible correlation function $J = J_c J_v$ should provide even better estimates of the ionization potentials. In such a wave function, denoted as Ψ_4 , there are two *distinct* parameters b_c and b_v , one for the core and the other for valence electrons,

$$\begin{aligned}
 \Psi_4 &= |\phi_1^c(1)| |\phi_1^c(2)| \\
 &\times |\phi_1^v(n_c+1) \cdots \phi_{n_v}^v(n_c+n_v^\dagger)| |\phi_1^v(n_c+n_v^\dagger+1) \cdots \phi_{n_v}^v(n)| \\
 &\times \exp\left(\sum_{i=1}^{n_c-1} \sum_{j=i+1}^{n_c} \frac{ar_{ij}}{1+b_c r_{ij}}\right) \exp\left(\sum_{i=n_c+1}^{n-1} \sum_{j=i+1}^n \frac{ar_{ij}}{1+b_v r_{ij}}\right) \\
 &= \psi_{D_c}^\dagger \psi_{D_c}^\dagger \psi_{D_v}^\dagger \psi_{D_v}^\dagger J_c J'_v.
 \end{aligned} \tag{2.18}$$

When Ψ_4 indeed proved to be superior to Ψ_3 in terms of accuracy of ionization potentials, we decided to make the next step — to re-introduce the core-valence correlation terms into Ψ_4 , this time, however, associated with an independent variational parameter b_{cv} . This new wave function is denoted as Ψ_5 ,

$$\begin{aligned}
 \Psi_5 &= |\phi_1^c(1)| |\phi_1^c(2)| \\
 &\times |\phi_1^v(n_c+1) \cdots \phi_{n_v}^v(n_c+n_v^\dagger)| |\phi_1^v(n_c+n_v^\dagger+1) \cdots \phi_{n_v}^v(n)| \\
 &\times \exp\left(\sum_{i=1}^{n_c-1} \sum_{j=i+1}^{n_c} \frac{ar_{ij}}{1+b_c r_{ij}}\right) \exp\left(\sum_{i=n_c+1}^{n-1} \sum_{j=i+1}^n \frac{ar_{ij}}{1+b_v r_{ij}}\right) \exp\left(\sum_{i=1}^{n_c} \sum_{j=n_c+1}^n \frac{ar_{ij}}{1+b_{cv} r_{ij}}\right) \\
 &= \psi_{D_c}^\dagger \psi_{D_c}^\dagger \psi_{D_v}^\dagger \psi_{D_v}^\dagger J_c J'_v J_{cv}.
 \end{aligned} \tag{2.19}$$

... (faint text) ...

... (faint text) ...

$$H^1(X, \mathbb{Z}) \cong \mathbb{Z}^2$$

(1.1)
$$\left(\frac{x}{y}, \frac{z}{y} \right) \in \left(\frac{x}{y}, \frac{z}{y} \right) \iff \left(\frac{x}{y}, \frac{z}{y} \right) \in \left(\frac{x}{y}, \frac{z}{y} \right)$$

... (faint text) ...

$$H^1(X, \mathbb{Z}) \cong \mathbb{Z}^2$$

(1.2)
$$\left(\frac{x}{y}, \frac{z}{y} \right) \in \left(\frac{x}{y}, \frac{z}{y} \right) \iff \left(\frac{x}{y}, \frac{z}{y} \right) \in \left(\frac{x}{y}, \frac{z}{y} \right)$$

Thus, $J_c J'_v J_{cv}$ can be viewed as our most flexible analog of J . In the former, parameter b depends on the nature of electrons involved in the correlated pair, whereas in J it has a single value for all possible pairs.

Table 2.1 summarizes the parametrization of the trial wave functions.

Table 2.1: Parametrization of wave functions Ψ_1 – Ψ_5 .

System	Parameters		
	Ψ_1, Ψ_2, Ψ_3	Ψ_4	Ψ_5
Li^+	ζ_1, v_s, b		
Li, Be^+	ζ_1, ζ_2, v_s, b	$\zeta_1, \zeta_2, v_s, b_c$	$\zeta_1, \zeta_2, v_s, b_c, b_{cv}$
Be, B^+		$\zeta_1, \zeta_2, v_s, b_c, b_v$	$\zeta_1, \zeta_2, v_s, b_c, b_v, b_{cv}$
$\text{B – Ne, C}^+ \text{ – Ne}^+$	$\zeta_1, \zeta_2, v_s, v_p, b$	$\zeta_1, \zeta_2, v_s, v_p, b_c, b_v$	$\zeta_1, \zeta_2, v_s, v_p, b_c, b_v, b_{cv}$

Chapter 3

Variational Monte Carlo Method

In this chapter, we give a detailed description of the methods employed in our work: variational method, the Monte Carlo procedure for evaluating definite integrals, its important particular case — variational Monte Carlo method, and the Metropolis algorithm — an effective sampling technique necessary to perform the integration.

3.1 Variational Method

The variational method is based on the **variation principle** [18]: given a system with Hamiltonian operator \hat{H} and any well-behaved function Ψ , it is true that

$$E[\Psi] = \frac{\int \Psi^* \hat{H} \Psi d\tau}{\int \Psi^* \Psi d\tau} \geq E_{\text{exact}}, \quad (3.1)$$

where $E[\Psi]$ is the *variational energy*, which can be treated as a functional, and E_{exact} is the true lowest energy eigenvalue of \hat{H} .

The variation principle for the ground state guarantees that the energy associated with an approximate wave function Ψ is always higher than the ground-state exact energy. Thus the quality of a trial wave function can be measured by its variational energy: the lower the energy, the better the wave function¹. The idea of the variational method, is to take a trial wave function, which depends on certain parameters, and vary these parameters to get the lowest possible expectation value $E[\Psi]$. The expectation value depends, of course, on the functional form of Ψ and the variational parameters.

¹A more universal criterion is the constancy of the quantity $\hat{H}\Psi/\Psi$, which has the exact zero variance only for the exact wave function Φ .

Chapter 2

2.1. The Laplace Transform

Let $f(t)$ be a function defined for $t \geq 0$. The Laplace transform of $f(t)$ is the function $F(s)$ defined by the integral

$$F(s) = \int_0^{\infty} e^{-st} f(t) dt$$

provided the integral exists. The Laplace transform is a linear transformation, and it has many useful properties. For example, the Laplace transform of a constant function $f(t) = 1$ is $F(s) = 1/s$.

2.2. The Inverse Laplace Transform

The inverse Laplace transform of $F(s)$ is the function $f(t)$ defined by the integral

$$f(t) = \frac{1}{2\pi i} \int_{\gamma - i\infty}^{\gamma + i\infty} e^{st} F(s) ds$$

provided the integral exists. The inverse Laplace transform is a linear transformation, and it has many useful properties. For example, the inverse Laplace transform of $1/s$ is the constant function $f(t) = 1$.

$$F(s) = \frac{1}{s^2 + 1}$$

Find $f(t)$. The function $F(s)$ is the Laplace transform of $f(t)$. The inverse Laplace transform of $F(s)$ is $f(t)$.

The function $f(t)$ is the inverse Laplace transform of $F(s)$. The Laplace transform of $f(t)$ is $F(s)$. The inverse Laplace transform of $F(s)$ is $f(t)$. The Laplace transform is a linear transformation, and it has many useful properties. For example, the Laplace transform of a constant function $f(t) = 1$ is $F(s) = 1/s$.

The function $f(t)$ is the inverse Laplace transform of $F(s)$. The Laplace transform of $f(t)$ is $F(s)$. The inverse Laplace transform of $F(s)$ is $f(t)$. The Laplace transform is a linear transformation, and it has many useful properties. For example, the Laplace transform of a constant function $f(t) = 1$ is $F(s) = 1/s$.

$E[\Psi]$ can be estimated numerically or analytically, whichever method is more adequate. We discuss here a numerical procedure known as Monte Carlo integration which is particularly suitable for evaluation of the integral (3.1).

3.2 Monte Carlo Integration

The generic name ‘Monte Carlo’ refers to a whole group of numerical methods which use random numbers similar to those coming out in roulette games, to simulate behavior of a physical system. These methods are therefore *stochastic*, in contrast to *deterministic* simulation methods such as molecular dynamics. Monte Carlo simulations are frequently applied in the study of systems with a large number of degrees of freedom. Over the past years these methods have proved to be remarkably successful tools of quantum chemistry [19, 20], where they are used for evaluation of definite integrals, particularly multidimensional integrals with complicated boundary conditions, and for solving the partial differential Schrödinger equation [21].

How are random numbers utilized for integration? Let us consider [19] first the case of a one-dimensional definite integral

$$I = \int_a^b f(x) dx. \quad (3.2)$$

One can approximate I in terms of the finite sum S_N :

$$I = \lim_{N \rightarrow \infty} S_N = \lim_{N \rightarrow \infty} \frac{b-a}{N} \sum_{i=1}^N f(x_i) = \langle f(x) \rangle. \quad (3.3)$$

The sample points $\{x_i\}$, at which the function $f(x)$ is evaluated, should completely cover the domain from a to b . If N is finite, the sum will fluctuate depending on the choice of $\{x_i\}$. Thus one confronts the problem of generating the proper set of sample points. The simplest choice is a uniform one-dimensional grid, and in very simple cases this approach is indeed satisfactory. However, for complex forms of $f(x)$ and for higher

dimensions, this procedure is computationally extremely inefficient. In fact, it proves to be advantageous to choose the points $\{x_i\}$ randomly. From the mathematical standpoint, one will have a certain probability density distribution function $f(x)$, from which the random variables x_1, x_2, \dots, x_N are drawn.

The stochastic analog of the grid is the uniform sampling of $\{x_i\}$ with direct application of formula (3.3). However, the principal contributions to the integral come from the regions where the integrand $f(x)$ is large, so that the uniform sampling does not produce enough points in these important regions to provide an accurate estimate of the integral, while much effort is wasted at the tails of the integrand whose contributions are negligible. It is therefore desirable to have the majority of sample points clustered in the regions where the integrand is large, rather than having all the points distributed uniformly. This can be achieved by drawing the sample points from a probability distribution $p(x)$ such that $p(x) \sim f(x)$, which allows one to generate more variables in the important regions. Such methods are called **importance sampling**.

To illustrate how the importance sampling works, we choose a normalized probability density distribution function $p(x)$, approximately proportional to $f(x)$, and introduce a new function $\eta(x)$ defined as

$$\eta(x) \stackrel{\text{def}}{=} f(x)/p(x), \quad (3.4)$$

so that the integral is now obtained as

$$I = \int_a^b f(x) dx = \int_a^b \frac{f(x)}{p(x)} p(x) dx = \int_a^b \eta(x) p(x) dx \equiv \langle \eta(x) \rangle_{p(x)}. \quad (3.5)$$

Since $p(x) \sim f(x)$, the integrand $\eta(x)$ does not vary sizeably over the integration range, so the estimate is more reliable.

Thus, with a sufficiently large number of points $\{x_i\}$ sampled from distribution $p(x)$,

$$I = \int_a^b \eta(x) p(x) dx \approx \frac{b-a}{N} \sum_{i=1}^N \eta(x_i) = \frac{b-a}{N} \sum_{i=1}^N \frac{f(x_i)}{p(x_i)}. \quad (3.6)$$

A method using these principles to evaluate the variational integral for an arbitrary form of the trial wave function Ψ is the so-called *variational Monte Carlo* method. With this background, we can understand how it works.

3.3 Estimation of the Variational Integral

In VMC, the expectation value \bar{A} of operator \hat{A} is obtained by evaluation of the multi-dimensional integral

$$\bar{A} = \frac{\int \Psi_T^* \hat{A} \Psi_T d\mathbf{R}}{\int \Psi_T^* \Psi_T d\mathbf{R}}, \quad (3.7)$$

where $\Psi_T = \Psi_T(\mathbf{R})$ is the trial wave function (not necessarily normalized) defined in $3n$ -dimensional space of electron configurations $\{\mathbf{R}\}$.

To implement the importance sampling technique, this integral is transformed as follows

$$\bar{A} = \int \frac{\hat{A} \Psi_T}{\Psi_T} \frac{|\Psi_T|^2}{\int |\Psi_T|^2 d\mathbf{R}} d\mathbf{R} = \int A_L \frac{|\Psi_T|^2}{\int |\Psi_T|^2 d\mathbf{R}} d\mathbf{R}. \quad (3.8)$$

In the case of $\hat{A} = \hat{H}$ (the Hamiltonian of the system), the quantity

$$E_L = \frac{\hat{H} \Psi_T}{\Psi_T} \quad (3.9)$$

is called the *local energy*. The variational estimate is therefore the expectation value of the *local* property, sampled from probability distribution

$$p(\mathbf{R}) = \frac{|\Psi_T|^2}{\int |\Psi_T|^2 d\mathbf{R}} \geq 0. \quad (3.10)$$

One averages the local energies E_L and other properties computed at sample points \mathbf{R}_i drawn from the distribution (3.10). Thus the estimate of the variational energy amounts to finding the sum

$$\bar{E} = \int E_L \frac{|\Psi_T|^2}{\int |\Psi_T|^2 d\mathbf{R}} d\mathbf{R} = \langle E_L \rangle_{\Psi_T^2} \approx \frac{1}{N} \sum_{i=1}^N E_L(\mathbf{R}_i). \quad (3.11)$$

where \mathcal{L} is the Laplace transform of \mathcal{F} and \mathcal{L}^{-1} is the inverse Laplace transform. The function $\mathcal{L}^{-1}(\mathcal{L}(\mathcal{F}))$ is the function \mathcal{F} and the function $\mathcal{L}(\mathcal{L}^{-1}(\mathcal{F}))$ is the function \mathcal{F} . The function $\mathcal{L}(\mathcal{L}^{-1}(\mathcal{F}))$ is the function \mathcal{F} and the function $\mathcal{L}^{-1}(\mathcal{L}(\mathcal{F}))$ is the function \mathcal{F} .

where \mathcal{L} is the Laplace transform of \mathcal{F} and \mathcal{L}^{-1} is the inverse Laplace transform.

where \mathcal{L} is the Laplace transform of \mathcal{F} and \mathcal{L}^{-1} is the inverse Laplace transform.

$$(1.4) \quad \frac{\partial}{\partial t} \left(\frac{\partial \mathcal{F}}{\partial t} \right) = \mathcal{F}$$

where \mathcal{L} is the Laplace transform of \mathcal{F} and \mathcal{L}^{-1} is the inverse Laplace transform.

where \mathcal{L} is the Laplace transform of \mathcal{F} and \mathcal{L}^{-1} is the inverse Laplace transform.

$$(1.5) \quad \frac{\partial}{\partial t} \left(\frac{\partial \mathcal{F}}{\partial t} \right) = \mathcal{F}$$

where \mathcal{L} is the Laplace transform of \mathcal{F} and \mathcal{L}^{-1} is the inverse Laplace transform.

$$(1.6) \quad \frac{\partial}{\partial t} \left(\frac{\partial \mathcal{F}}{\partial t} \right) = \mathcal{F}$$

where \mathcal{L} is the Laplace transform of \mathcal{F} and \mathcal{L}^{-1} is the inverse Laplace transform.

$$(1.7) \quad \frac{\partial}{\partial t} \left(\frac{\partial \mathcal{F}}{\partial t} \right) = \mathcal{F}$$

where \mathcal{L} is the Laplace transform of \mathcal{F} and \mathcal{L}^{-1} is the inverse Laplace transform.

$$(1.8) \quad \frac{\partial}{\partial t} \left(\frac{\partial \mathcal{F}}{\partial t} \right) = \mathcal{F}$$

Provided that all sample points are independent, this value is associated with the variance

$$\sigma^2(\overline{E}) = \frac{1}{N-1} \left(\langle E_L^2 \rangle_{\Psi_T^2} - \langle E_L \rangle_{\Psi_T^2}^2 \right). \quad (3.12)$$

In an important special case, when Ψ_T is an eigenfunction of \hat{H} , the local energy E_L is constant, and the variance is therefore zero.

So far we have not discussed an important question: How does one generate in VMC the sample points from probability distribution $p(\mathbf{R}) \propto |\Psi_T|^2$? This is achieved by the Metropolis algorithm.

3.4 Metropolis Sampling

The Metropolis sampling technique was first described by Metropolis *et al.* [22]. This method belongs to the group of rejection techniques, so named because a trial value for a random variable is *selected* and *proposed*. Subjected to a test, the proposed move may be accepted or rejected. If it is rejected, the cycle of choosing and testing a trial value is repeated until an acceptance takes place. The Metropolis algorithm can be used to sample essentially any probability density function regardless of analytic complexity and the number of dimensions.

3.4.1 Description of the algorithm

In the following discussion based on the description due to Kalos [23], we will specify a state of the system by a point \mathbf{R} in multidimensional space $\{\mathbf{R}\}$. The evolution of the system can be described with a probability density function $P(\mathbf{R}' \leftarrow \mathbf{R})$ which gives the probability of a stochastic transition of a system known to be at \mathbf{R} to \mathbf{R}' .

A necessary condition that a system evolve toward equilibrium and stay there is that the system be, on the average, as likely to move from a neighborhood of \mathbf{R} into a specific neighborhood of \mathbf{R}' as to move exactly in the reverse direction. If the probability density

of observing the system in equilibrium near \mathbf{R} is $p(\mathbf{R})$, and $p(\mathbf{R}')$ near \mathbf{R}' , then the kinetics must satisfy the **detailed balance** condition

$$P(\mathbf{R}' \leftarrow \mathbf{R}) p(\mathbf{R}) = P(\mathbf{R} \leftarrow \mathbf{R}') p(\mathbf{R}'). \quad (3.13)$$

Here $P(\mathbf{R}' \leftarrow \mathbf{R}) p(\mathbf{R})$ is the probability of moving from \mathbf{R} to \mathbf{R}' is expressed as the *a priori* chance of finding the system near \mathbf{R} times the conditional probability $P(\mathbf{R}' \leftarrow \mathbf{R})$ that it will move from \mathbf{R} to \mathbf{R}' .

In the Metropolis algorithm, transitions from, say, \mathbf{R} to \mathbf{R}' can be proposed using essentially *any* distribution $T(\mathbf{R}' \leftarrow \mathbf{R})$. On comparing $p(\mathbf{R}')$ with $p(\mathbf{R})$ and taking into account $T(\mathbf{R}' \leftarrow \mathbf{R})$, the system is either moved to \mathbf{R}' (the move is said to be 'accepted') or returned to \mathbf{R} (the move is 'rejected').

The moves are accepted with probability $A(\mathbf{R}' \leftarrow \mathbf{R})$, which must be calculated so as to satisfy the detailed balance condition. Thus $A(\mathbf{R}' \leftarrow \mathbf{R})$ is determined by

$$P(\mathbf{R}' \leftarrow \mathbf{R}) = A(\mathbf{R}' \leftarrow \mathbf{R}) T(\mathbf{R}' \leftarrow \mathbf{R}). \quad (3.14)$$

Detailed balance requires

$$A(\mathbf{R}' \leftarrow \mathbf{R}) T(\mathbf{R}' \leftarrow \mathbf{R}) p(\mathbf{R}) = A(\mathbf{R} \leftarrow \mathbf{R}') T(\mathbf{R} \leftarrow \mathbf{R}') p(\mathbf{R}'). \quad (3.15)$$

Then

$$A(\mathbf{R}' \leftarrow \mathbf{R}) = A(\mathbf{R} \leftarrow \mathbf{R}') \frac{T(\mathbf{R} \leftarrow \mathbf{R}') p(\mathbf{R}')}{T(\mathbf{R}' \leftarrow \mathbf{R}) p(\mathbf{R})}. \quad (3.16)$$

We introduce a quantity $q(\mathbf{R}' \leftarrow \mathbf{R})$ defined as

$$q(\mathbf{R}' \leftarrow \mathbf{R}) \stackrel{\text{def}}{=} \frac{T(\mathbf{R} \leftarrow \mathbf{R}') p(\mathbf{R}')}{T(\mathbf{R}' \leftarrow \mathbf{R}) p(\mathbf{R})}. \quad (3.17)$$

From $q(\mathbf{R}' \leftarrow \mathbf{R})$ the probability of accepting a move can be calculated. A frequently used possibility is

$$A(\mathbf{R}' \leftarrow \mathbf{R}) = \min [1, q(\mathbf{R}' \leftarrow \mathbf{R})]. \quad (3.18)$$

It is important to note that the above results are only valid for the case of a single input. In the case of multiple inputs, the results are more complicated and will be discussed in Chapter 2.

1.1.1. The case of a single input. In this section, we will consider the case of a single input. The results are as follows:

Proposition 1.1.1. Let $f: \mathbb{R} \rightarrow \mathbb{R}$ be a function. Then the following conditions are equivalent: (i) f is linear; (ii) f satisfies the Cauchy functional equation; (iii) f is additive and homogeneous.

Proof. (i) \Rightarrow (ii) is obvious. (ii) \Rightarrow (i) follows from the fact that $f(x+y) = f(x) + f(y)$ and $f(ax) = af(x)$ for all $x, y \in \mathbb{R}$ and $a \in \mathbb{R}$. (iii) \Rightarrow (i) follows from the fact that $f(x+y) = f(x) + f(y)$ and $f(ax) = af(x)$ for all $x, y \in \mathbb{R}$ and $a \in \mathbb{R}$.

The above proposition shows that the Cauchy functional equation is equivalent to the condition that f is linear. This is a very important result in the theory of linear functions.

1.1.2. The case of multiple inputs. In this section, we will consider the case of multiple inputs. The results are as follows:

Proposition 1.1.2. Let $f: \mathbb{R}^n \rightarrow \mathbb{R}$ be a function. Then the following conditions are equivalent: (i) f is linear; (ii) f satisfies the multivariate Cauchy functional equation; (iii) f is additive and homogeneous.

Proof. (i) \Rightarrow (ii) is obvious. (ii) \Rightarrow (i) follows from the fact that $f(x+y) = f(x) + f(y)$ and $f(ax) = af(x)$ for all $x, y \in \mathbb{R}^n$ and $a \in \mathbb{R}$.

The above proposition shows that the multivariate Cauchy functional equation is equivalent to the condition that f is linear. This is a very important result in the theory of linear functions.

1.1.3. The case of a single input. In this section, we will consider the case of a single input. The results are as follows:

Proposition 1.1.3. Let $f: \mathbb{R} \rightarrow \mathbb{R}$ be a function. Then the following conditions are equivalent: (i) f is linear; (ii) f satisfies the Cauchy functional equation; (iii) f is additive and homogeneous.

Proof. (i) \Rightarrow (ii) is obvious. (ii) \Rightarrow (i) follows from the fact that $f(x+y) = f(x) + f(y)$ and $f(ax) = af(x)$ for all $x, y \in \mathbb{R}$ and $a \in \mathbb{R}$.

The above proposition shows that the Cauchy functional equation is equivalent to the condition that f is linear. This is a very important result in the theory of linear functions.

Consider the case when the transition probability $T(\mathbf{R}' \leftarrow \mathbf{R})$ is assumed to be constant over a domain $\Delta\mathbf{R}$ in space $\{\mathbf{R}\}$. That is to say that

$$T(\mathbf{R}' \leftarrow \mathbf{R}) = \begin{cases} 1/\Delta\mathbf{R} & \text{if } \mathbf{R}' \in \Delta\mathbf{R} \\ 0 & \text{otherwise.} \end{cases} \quad (3.19)$$

This corresponds to a uniform random sampling of \mathbf{R} in $\Delta\mathbf{R}$:

$$\mathbf{R}' = \mathbf{R} + \alpha\mathbf{N}, \quad (3.20)$$

where \mathbf{N} is the unit uniform $3n$ -dimensional random variate and α is a scaling coefficient.

This choice yields

$$T(\mathbf{R}' \leftarrow \mathbf{R}) = T(\mathbf{R} \leftarrow \mathbf{R}'),$$

so that $q(\mathbf{R}' \leftarrow \mathbf{R})$ becomes

$$q(\mathbf{R}' \leftarrow \mathbf{R}) = \frac{p(\mathbf{R}')}{p(\mathbf{R})}. \quad (3.21)$$

In improved techniques, by making $T(\mathbf{R}' \leftarrow \mathbf{R})$ approximate $p(\mathbf{R}')$, rapid convergence and small correlation are obtained, since $q(\mathbf{R}' \leftarrow \mathbf{R})$ approaches unity, as can be seen from Eq. (3.17). Were it possible to sample $T(\mathbf{R}' \leftarrow \mathbf{R}) = p(\mathbf{R}')$ exactly, then all moves would be accepted and the samples would be independent².

Since we need to compute only the ratio $p(\mathbf{R}')/p(\mathbf{R})$, *knowledge of the normalization factor for the probability density distribution function is not required*. This is an extremely attractive feature of the method because determination of this factor would require evaluation of another multidimensional integral.

Normally, at the very first step, the distribution of walkers \mathbf{R} is far from $p(\mathbf{R})$. How does the simulation produce the equilibrium distribution $p(\mathbf{R})$?

If $\xi_k(\mathbf{R})$ is the probability density distribution of \mathbf{R} at step k , then the distribution $\xi_{k+1}(\mathbf{R}')$ of walkers \mathbf{R}' at step $(k+1)$ is determined by two contributions: the probability

²However, if it were possible to generate random variables from $p(\mathbf{R})$ distribution, there would be no need to use the Metropolis algorithm.

we obtain $g'(t) = 0$. We conclude that the function g has a local maximum at $t = 0$. Since $g(0) = 1$, we have $g(t) \leq 1$ for all t in the interval $[-1, 1]$.

$$\text{20. } \frac{d}{dt} \left(\frac{1}{2} \pi r^2 h \right) = \frac{1}{2} \pi \left(2r \frac{dr}{dt} h + r^2 \frac{dh}{dt} \right) = \frac{1}{2} \pi \left(2(1) \frac{dr}{dt} (1) + (1)^2 \frac{dh}{dt} \right) = \frac{1}{2} \pi \left(2 \frac{dr}{dt} + \frac{dh}{dt} \right)$$

Since $g(t) = 1$ for all t in the interval $[-1, 1]$, we have $g'(t) = 0$ for all t in the interval $[-1, 1]$.

$$\text{21. } \frac{d}{dt} \left(\frac{1}{2} \pi r^2 h \right) = \frac{1}{2} \pi \left(2r \frac{dr}{dt} h + r^2 \frac{dh}{dt} \right) = \frac{1}{2} \pi \left(2(1) \frac{dr}{dt} (1) + (1)^2 \frac{dh}{dt} \right) = \frac{1}{2} \pi \left(2 \frac{dr}{dt} + \frac{dh}{dt} \right)$$

Since $g(t) = 1$ for all t in the interval $[-1, 1]$, we have $g'(t) = 0$ for all t in the interval $[-1, 1]$.

$$\text{22. } \frac{d}{dt} \left(\frac{1}{2} \pi r^2 h \right) = \frac{1}{2} \pi \left(2r \frac{dr}{dt} h + r^2 \frac{dh}{dt} \right) = \frac{1}{2} \pi \left(2(1) \frac{dr}{dt} (1) + (1)^2 \frac{dh}{dt} \right) = \frac{1}{2} \pi \left(2 \frac{dr}{dt} + \frac{dh}{dt} \right)$$

Since $g(t) = 1$ for all t in the interval $[-1, 1]$, we have $g'(t) = 0$ for all t in the interval $[-1, 1]$.

$$\text{23. } \frac{d}{dt} \left(\frac{1}{2} \pi r^2 h \right) = \frac{1}{2} \pi \left(2r \frac{dr}{dt} h + r^2 \frac{dh}{dt} \right) = \frac{1}{2} \pi \left(2(1) \frac{dr}{dt} (1) + (1)^2 \frac{dh}{dt} \right) = \frac{1}{2} \pi \left(2 \frac{dr}{dt} + \frac{dh}{dt} \right)$$

Since $g(t) = 1$ for all t in the interval $[-1, 1]$, we have $g'(t) = 0$ for all t in the interval $[-1, 1]$.

Since $g(t) = 1$ for all t in the interval $[-1, 1]$, we have $g'(t) = 0$ for all t in the interval $[-1, 1]$.

Since $g(t) = 1$ for all t in the interval $[-1, 1]$, we have $g'(t) = 0$ for all t in the interval $[-1, 1]$.

Since $g(t) = 1$ for all t in the interval $[-1, 1]$, we have $g'(t) = 0$ for all t in the interval $[-1, 1]$.

Since $g(t) = 1$ for all t in the interval $[-1, 1]$, we have $g'(t) = 0$ for all t in the interval $[-1, 1]$.

Since $g(t) = 1$ for all t in the interval $[-1, 1]$, we have $g'(t) = 0$ for all t in the interval $[-1, 1]$.

Since $g(t) = 1$ for all t in the interval $[-1, 1]$, we have $g'(t) = 0$ for all t in the interval $[-1, 1]$.

Since $g(t) = 1$ for all t in the interval $[-1, 1]$, we have $g'(t) = 0$ for all t in the interval $[-1, 1]$.

Since $g(t) = 1$ for all t in the interval $[-1, 1]$, we have $g'(t) = 0$ for all t in the interval $[-1, 1]$.

Since $g(t) = 1$ for all t in the interval $[-1, 1]$, we have $g'(t) = 0$ for all t in the interval $[-1, 1]$.

Since $g(t) = 1$ for all t in the interval $[-1, 1]$, we have $g'(t) = 0$ for all t in the interval $[-1, 1]$.

Since $g(t) = 1$ for all t in the interval $[-1, 1]$, we have $g'(t) = 0$ for all t in the interval $[-1, 1]$.

Since $g(t) = 1$ for all t in the interval $[-1, 1]$, we have $g'(t) = 0$ for all t in the interval $[-1, 1]$.

of entering into the vicinity of \mathbf{R}'

$$\int A(\mathbf{R}' \leftarrow \mathbf{R}) T(\mathbf{R}' \leftarrow \mathbf{R}) \xi_k(\mathbf{R}) d\mathbf{R}, \quad (3.22)$$

and the probability that once the system is at \mathbf{R}' , it will stay there, i.e. the probability that a move away from \mathbf{R}' is not accepted

$$\int [1 - A(\mathbf{R} \leftarrow \mathbf{R}')] T(\mathbf{R} \leftarrow \mathbf{R}') d\mathbf{R}. \quad (3.23)$$

Since the probability that the system is at \mathbf{R}' in step k is $\xi_k(\mathbf{R}')$, the probability that it will stay at \mathbf{R}' will be

$$\xi_k(\mathbf{R}') \int [1 - A(\mathbf{R} \leftarrow \mathbf{R}')] T(\mathbf{R} \leftarrow \mathbf{R}') d\mathbf{R}. \quad (3.24)$$

This gives the following relationship for $\xi_{k+1}(\mathbf{R}')$

$$\begin{aligned} \xi_{k+1}(\mathbf{R}') &= \int A(\mathbf{R}' \leftarrow \mathbf{R}) T(\mathbf{R}' \leftarrow \mathbf{R}) \xi_k(\mathbf{R}) d\mathbf{R} \\ &+ \xi_k(\mathbf{R}') \int [1 - A(\mathbf{R} \leftarrow \mathbf{R}')] T(\mathbf{R} \leftarrow \mathbf{R}') d\mathbf{R}. \end{aligned} \quad (3.25)$$

The random walk thus generates a recursion relationship for the density functions.

Setting $\xi_k(\mathbf{R}) = p(\mathbf{R})$ in Eq. (3.25) we obtain

$$\begin{aligned} \xi_{k+1}(\mathbf{R}') &= \int A(\mathbf{R}' \leftarrow \mathbf{R}) T(\mathbf{R}' \leftarrow \mathbf{R}) p(\mathbf{R}) d\mathbf{R} \\ &+ \int [1 - A(\mathbf{R} \leftarrow \mathbf{R}')] T(\mathbf{R} \leftarrow \mathbf{R}') p(\mathbf{R}') d\mathbf{R} \\ &= \int T(\mathbf{R} \leftarrow \mathbf{R}') p(\mathbf{R}') d\mathbf{R} = p(\mathbf{R}'), \end{aligned} \quad (3.26)$$

since $\int T(\mathbf{R} \leftarrow \mathbf{R}') d\mathbf{R} = 1$. If the move is accepted, \mathbf{R}' and $p(\mathbf{R}')$ become \mathbf{R} and $p(\mathbf{R})$ in our notation. Therefore, $p(\mathbf{R})$ is guaranteed to be the asymptotic distribution of the random walk.

Unfortunately, because of the asymptotic behavior, we must throw away a certain number of first steps N_{eq} of the random walk until the steps are being sampled from

the following two cases:

$$(1) \quad \frac{\partial \log L(\theta)}{\partial \theta} = 0 \quad \text{and} \quad \frac{\partial^2 \log L(\theta)}{\partial \theta^2} < 0$$

then the maximum likelihood estimate of θ is the value of θ that satisfies the first condition and the second condition is satisfied.

$$(2) \quad \frac{\partial \log L(\theta)}{\partial \theta} = 0 \quad \text{and} \quad \frac{\partial^2 \log L(\theta)}{\partial \theta^2} = 0$$

then the maximum likelihood estimate of θ is the value of θ that satisfies the first condition and the second condition is not satisfied.

$$(3) \quad \frac{\partial \log L(\theta)}{\partial \theta} = 0 \quad \text{and} \quad \frac{\partial^2 \log L(\theta)}{\partial \theta^2} = 0$$

then the maximum likelihood estimate of θ is the value of θ that satisfies the first condition and the second condition is not satisfied.

$$\frac{\partial \log L(\theta)}{\partial \theta} = 0 \quad \text{and} \quad \frac{\partial^2 \log L(\theta)}{\partial \theta^2} = 0$$

$$(4) \quad \frac{\partial \log L(\theta)}{\partial \theta} = 0 \quad \text{and} \quad \frac{\partial^2 \log L(\theta)}{\partial \theta^2} = 0$$

then the maximum likelihood estimate of θ is the value of θ that satisfies the first condition and the second condition is not satisfied.

then the maximum likelihood estimate of θ is the value of θ that satisfies the first condition and the second condition is not satisfied.

$$\frac{\partial \log L(\theta)}{\partial \theta} = 0 \quad \text{and} \quad \frac{\partial^2 \log L(\theta)}{\partial \theta^2} = 0$$

$$\frac{\partial \log L(\theta)}{\partial \theta} = 0 \quad \text{and} \quad \frac{\partial^2 \log L(\theta)}{\partial \theta^2} = 0$$

$$(5) \quad \frac{\partial \log L(\theta)}{\partial \theta} = 0 \quad \text{and} \quad \frac{\partial^2 \log L(\theta)}{\partial \theta^2} = 0$$

then the maximum likelihood estimate of θ is the value of θ that satisfies the first condition and the second condition is not satisfied.

then the maximum likelihood estimate of θ is the value of θ that satisfies the first condition and the second condition is not satisfied.

then the maximum likelihood estimate of θ is the value of θ that satisfies the first condition and the second condition is not satisfied.

$p(\mathbf{R})$. In addition, N_{eq} is very difficult to estimate in advance by a method other than trial and error.

In VMC, the probability density $p(\mathbf{R})$ of Eq. (3.5) is the probability of observing the system near \mathbf{R} given by Eq. (3.10), whereas the sampled quantity $\eta(x)$ is the local energy (3.9).

3.4.2 Generalized Metropolis algorithm

The above description of the Metropolis algorithm can be summarized in its generalized form as a recipe for one walker:

- (1) pick an arbitrary initial state \mathbf{R} ;
- (2) being in state \mathbf{R} , propose a possible next state \mathbf{R}' with probability $T(\mathbf{R}' \leftarrow \mathbf{R})$;
- (3) accept the move to \mathbf{R}' with the probability $A(\mathbf{R} \leftarrow \mathbf{R}')$ calculated using Eq. (3.18);
- (4) if the move is accepted, the new state is \mathbf{R}' , otherwise it is \mathbf{R} ;
- (5) repeat steps 2 through 4;

After a sufficiently long run, states \mathbf{R} become drawn from the distribution $p(\mathbf{R})$.

3.5 Optimization of the Wave Functions

The search for the set of variational parameters corresponding to the best possible ground state trial wave function is a typical optimization problem. Optimization methods may differ from one another by the search technique and by the quantity being optimized. Ordinarily, wave functions are optimized with respect to variational parameters by

- (i) minimization of the total energy,
- (ii) minimization of the variance of the local energy.

Minimization of the variance of the local energy has the advantage that the true minimum of the variance is always known to be zero. The disadvantage of the variance optimization is that it is less sensitive to the valence region than to the nuclear where the local energy is a more strongly varying function. Energy optimization is more sensitive to the nuclear region too, but to a lesser degree.

In either case, the principal problem is that the energy (or the variance) associated with a parameter set cannot be *precisely* known: one always obtains it with a certain statistical error. For that reason it is sometimes difficult to find that unique set of parameters that correspond to the true minimum. Obvious strategies to deal with this problem include increasing of the ensemble size and improving the efficiency of the sampling algorithm, both of which lower the variance and are used in the present work.

Chapter 4

Running Simulations

This chapter deals with practical issues and specific problems of the variational Monte Carlo simulations.

4.1 Implementation of the Metropolis Algorithm

Terminology. Simulations are performed on an ensemble of n -electron configurations ('walkers') $\{\mathbf{R}_i\}$, $i = 1, 2, \dots, N_C$, where N_C is the number of configurations and \mathbf{R}_i is the $3n$ -dimensional vector representing the coordinates of n electrons in the i -th configuration. Each step in the development of a walker is called *iteration*. A series of consecutive iterations constitutes a *block*.

4.1.1 Estimation of the variance

One of the disadvantages of the Metropolis technique is that successively produced sample points are correlated, sometimes very strongly. In this case, there is a positive correlation in the successive values of the integrand, too. As a result, one cannot use separate iterations as independent sources of the local energy E_L (3.9) because the resulting variance (and, consequently, standard error) will be *underestimated*.

Quantitatively, if successive values of the random quantity x are statistically independent, the variance of the mean is estimated as

$$\text{var}(\bar{x}) = \sigma_0^2 = \frac{1}{N-1} \sum_{i=1}^N (x_i - \bar{x})^2. \quad (4.1)$$

Introduction

1.1. Statement of the problem

Let Ω be a bounded domain in \mathbb{R}^n with smooth boundary $\partial\Omega$. Consider the problem

$$-\Delta u = f \quad \text{in } \Omega, \quad u = 0 \quad \text{on } \partial\Omega. \quad (1.1)$$

Assume that $f \in L^2(\Omega)$. Then there exists a unique solution $u \in H_0^1(\Omega)$ to (1.1). The solution u can be represented as a series in terms of the eigenfunctions of the Laplacian. Let $\{\phi_k\}_{k=1}^\infty$ be an orthonormal basis of $L^2(\Omega)$ consisting of eigenfunctions of the Laplacian. Then we can write f and u as

$$f = \sum_{k=1}^\infty f_k \phi_k, \quad u = \sum_{k=1}^\infty u_k \phi_k, \quad (1.2)$$

where $f_k = \int_\Omega f \phi_k$ and $u_k = \int_\Omega u \phi_k$. Substituting (1.2) into (1.1), we obtain the following system of ordinary differential equations for the coefficients u_k :

$$-\lambda_k u_k = f_k, \quad u_k = 0, \quad \text{for } k = 1, 2, \dots, \quad (1.3)$$

where λ_k are the eigenvalues of the Laplacian. The solution of (1.3) is given by

$$u_k = -\frac{f_k}{\lambda_k}, \quad \text{for } k = 1, 2, \dots$$

However, if the values of x are correlated, then the correct expression is

$$\sigma^2 = \sigma_0^2 + 2 \operatorname{cov}\{x_i, x_j\} = \sigma_0^2 + \frac{2}{N-1} \sum_{i < j}^N (x_i - \bar{x})(x_j - \bar{x}). \quad (4.2)$$

Alternatively, this relationship can be expressed in terms of (auto)correlation (serial correlation) coefficients [24],

$$\rho_k \stackrel{\text{def}}{=} \frac{1}{\sigma_0^2 (N-1)} \sum_{i=1}^{N-k} (x_i - \bar{x})(x_{i+k} - \bar{x}), \quad k = 1, \dots, N-1 \quad (4.3)$$

Autocorrelation coefficients can be regarded as a measure of correlation between sample points in a random walk separated by k steps. Rewritten in terms of ρ_k , Eq. (4.2) assumes the following form

$$\sigma^2 = \sigma_0^2 \left(1 + 2 \sum_k^N \rho_k \right). \quad (4.4)$$

It follows from the definition of ρ_k that $0 \leq \rho_k \leq 1$. Normally, ρ_k decreases rapidly with k , so there exists k_0 such that $\rho_k \approx 0$ for all $k \geq k_0$. This k_0 is called the *correlation length*. It is therefore sufficient to sum only the first k_0 correlation coefficients to estimate the true variance (4.4).

In practice, taking into account even a finite number of correlation coefficients to estimate σ^2 is computationally expensive. A common alternative is to divide all iterations into ‘blocks’ of N_I iterations, which, if large enough, to a good approximation can be treated as independent. The i -th block average \bar{x}_i^B is defined as

$$\bar{x}_i^B = \frac{1}{N_I} \sum_{j=(i-1)N_I+1}^{iN_I} x_j, \quad i = 1, \dots, N_B. \quad (4.5)$$

It is not clear, however, what N_I should be chosen to make the blocks independent, since the block size is subject to variations depending on time steps, acceptance rate, variational parameters, etc. It is more reliable to adopt the extreme case: to count *all* iterations for each configuration as a single block. The number of blocks therefore will be $N_B = N_C$. Since the configurations are mutually independent, all block averages \bar{E}_i

Let \mathcal{A} be a subalgebra of \mathcal{B} . Then \mathcal{A} is a subalgebra of \mathcal{B} if and only if

$$(1.1) \quad \mathcal{A} \cap \mathcal{B} = \mathcal{A} \text{ and } \mathcal{A} \cap \mathcal{B} = \mathcal{A} \text{ for all } \mathcal{A} \in \mathcal{B}.$$

Let \mathcal{A} be a subalgebra of \mathcal{B} . Then \mathcal{A} is a subalgebra of \mathcal{B} if and only if

$$(1.2) \quad \mathcal{A} \cap \mathcal{B} = \mathcal{A} \text{ and } \mathcal{A} \cap \mathcal{B} = \mathcal{A} \text{ for all } \mathcal{A} \in \mathcal{B}.$$

Let \mathcal{A} be a subalgebra of \mathcal{B} . Then \mathcal{A} is a subalgebra of \mathcal{B} if and only if

$$(1.3) \quad \mathcal{A} \cap \mathcal{B} = \mathcal{A} \text{ and } \mathcal{A} \cap \mathcal{B} = \mathcal{A} \text{ for all } \mathcal{A} \in \mathcal{B}.$$

Let \mathcal{A} be a subalgebra of \mathcal{B} . Then \mathcal{A} is a subalgebra of \mathcal{B} if and only if

Let \mathcal{A} be a subalgebra of \mathcal{B} . Then \mathcal{A} is a subalgebra of \mathcal{B} if and only if

$$(1.4) \quad \mathcal{A} \cap \mathcal{B} = \mathcal{A} \text{ and } \mathcal{A} \cap \mathcal{B} = \mathcal{A} \text{ for all } \mathcal{A} \in \mathcal{B}.$$

Let \mathcal{A} be a subalgebra of \mathcal{B} . Then \mathcal{A} is a subalgebra of \mathcal{B} if and only if

will be independent, too, so that one can exactly estimate the expectation value \bar{x} and variance $\sigma^2(\bar{x})$ as follows

$$\bar{x} = \frac{1}{N_B} \sum_i^{N_B} \bar{x}_i^B, \quad (4.6)$$

$$\sigma^2(\bar{x}) = \frac{\sum_i^{N_B} (\bar{x}_i^B)^2 - [\sum_i^{N_B} \bar{x}_i^B]^2 / N_B}{(N_B - 1)}. \quad (4.7)$$

The standard error is then given by the expression

$$s(\bar{x}) = \sqrt{\frac{\sigma^2(\bar{x})}{N_B}}. \quad (4.8)$$

Sampling efficiency can be characterized not only by the correlation length but also by the so-called *correlation time* defined as [16]

$$T_c = \lim_{N \rightarrow \infty} \frac{\sigma_{N_B}^2}{\sigma_N^2}, \quad (4.9)$$

where $\sigma_{N_B}^2$ is based on truly independent blocks, and σ_N^2 ($N = N_I \times N_B$) on blocks of single iterations only. In the case of zero correlation, all iterations are completely independent, so that $T_c = 1$.

4.1.2 Variance reduction: Improved sampling technique

Even if we have secured correct estimates of the standard error, we have done nothing to improve efficiency of the sampling. The reason why the Metropolis algorithm may have low efficiency is that many values may be rejected before one is accepted. As shown in Chapter 3, the use of a *non-uniform* transition probability $T(\mathbf{R}' \leftarrow \mathbf{R})$ instead of a uniform one can increase the acceptance rate and thereby weaken the autocorrelation. This is particularly advantageous in combination with a technique where moves are proposed in spherical polar coordinates with the coordinate system originating at the nucleus, as suggested by Umrigar [25].

In this approach, the initial position of an electron is given by $\mathbf{r} = (r, \varphi, \theta)$. The new position of the electron is described by an isotropic vector \mathbf{r}' (i.e. φ' and $\cos \theta$ are sampled uniformly from intervals $[0, 2\pi]$ and $[-1, 1]$, respectively). The length of the new position vector r' is drawn from the distribution proposed by Langfelter¹ [16]

$$f(r' \leftarrow r) = f(r') = \frac{1}{\rho^2} r' e^{-r'^2/2\rho^2}, \quad (4.10)$$

where $\rho = \rho(r)$ is a function of the the initial electron-nucleus distance r

$$\rho(r) = \frac{r}{[\max\{\alpha, 1 + \beta(r - \gamma)\}]^{1/2}}, \quad (4.11)$$

which has the maximum at ρ with parameters α , β , and γ chosen by trial and error to provide as short correlation time as possible. In the case of Ψ_2 - Ψ_5 there are distinct β and γ parameters for core and valence electrons.

For large r , $\rho < r$, so that the new position is likely to be closer to the nucleus. On the contrary, when r is small, $\rho > r$, so the electron is likely to be pushed to the outer region. A necessary condition for an unbiased sampling is a reasonable probability of the reverse move, i.e. the move from r' to r .

The transition probability density $T(\mathbf{R}' \leftarrow \mathbf{R})$ is given by

$$T(\mathbf{R}' \leftarrow \mathbf{R}) = \frac{1}{4\pi r'^2} f(r' \leftarrow r), \quad (4.12)$$

¹This is done by the inverse transform method [26]. The cumulative probability distribution of r' is

$$F(r') = \int_0^{r'} f(t) dt = \int_0^{r'} \frac{1}{\rho^2} t e^{-t^2/2\rho^2} dt = 1 - e^{-r'^2/2\rho^2}.$$

Since $F(r')$ is a non-decreasing function, the inverse function $F^{-1}(r')$ may be defined for any value of r' between 0 and 1. If variable u is uniformly distributed over the interval (0,1), then $r' = F^{-1}(u)$ is distributed according to $f(r')$. If $f(r')$ is given by (4.10), then by setting $u = F(r') = 1 - e^{-r'^2/2\rho^2}$, which is equivalent to $u = 1 - F(r') = e^{-r'^2/2\rho^2}$, one obtains

$$r' = F^{-1}(u) = \rho \sqrt{-2 \ln u}.$$

because the probability density of choosing a point on a sphere is inversely proportional to the sphere's surface area.

The acceptance probability assumes the form

$$q = \min \left(1, \frac{|\Psi_T(\mathbf{R}')|^2 T(\mathbf{R} \leftarrow \mathbf{R}')}{|\Psi_T(\mathbf{R})|^2 T(\mathbf{R}' \leftarrow \mathbf{R})} \right). \quad (4.13)$$

Implementation of this technique results in a decrease of the correlation time by a factor of 2 to 3 with respect to the uniform sampling technique using 'time step' parameters².

4.1.3 Simulation algorithm

The nature of the simulation is a Metropolis walk in configuration space with the position probability density proportional to Ψ_T^2 , where Ψ_T is the trial wave function. We chose to move electrons one at a time. Before accumulating the data, the ensemble always was

²A common technique, called 'importance sampled VMC' [19] attempts to enhance sampling efficiency by guiding walkers toward regions of large $|\Psi_T(\mathbf{R})|^2$. This is done by choosing the transition probability $T(\mathbf{R}' \leftarrow \mathbf{R})$ to be of the form

$$T(\mathbf{R}' \leftarrow \mathbf{R}) = G(\mathbf{R}' \leftarrow \mathbf{R}, \tau) = \frac{1}{(2\pi\tau)^{3N/2}} \exp \left(-\frac{[\mathbf{R}' - \mathbf{R} - \tau\mathbf{F}(\mathbf{R})]^2}{2\tau} \right), \quad (4.14)$$

where

$$\mathbf{F}(\mathbf{R}) = \frac{\nabla \Psi_T(\mathbf{R})}{\Psi_T(\mathbf{R})} \quad (4.15)$$

is the 'drift' vector. It arises from the Fokker-Planck equation describing isotropic diffusion process with a drift caused by an external potential.

A new configuration \mathbf{R}' is proposed as follows

$$\mathbf{R}' = \mathbf{R} + \tau\mathbf{F}(\mathbf{R}) + \sqrt{\tau}\mathbf{N}(0, 1), \quad (4.16)$$

where $\mathbf{N}(0, 1)$ is a $3n$ -dimensional Gaussian random variable with zero mean and unit variance. It is the drift that causes the move to be biased by $\Psi_T(\mathbf{R})$. The acceptance probability is given by

$$A(\mathbf{R}' \leftarrow \mathbf{R}) = \min \left(1, \frac{|\Psi_T(\mathbf{R}')|^2 G(\mathbf{R} \leftarrow \mathbf{R}')}{|\Psi_T(\mathbf{R})|^2 G(\mathbf{R}' \leftarrow \mathbf{R})} \right).$$

We do not use this technique because its implementation is seriously complicated by nodal problems. In particular, configurations which happen to be near a nodal surface tend to be locked in their positions. The problem may be so severe that the ensemble does not reach the proper distribution even after many moves [27].

allowed to develop for 150–200 iterations until equilibrium is reached.

Following is the algorithmic description of the actual procedure.

1. Generate an ensemble of N_C electron configurations with random positions

$$\{\mathbf{R}_1, \mathbf{R}_2, \dots, \mathbf{R}_i, \dots, \mathbf{R}_{N_C}\},$$

where \mathbf{R}_i is a set of n one-electron position vectors \mathbf{r}_{ik} (k is the electron label) using random numbers drawn from the Gaussian distribution³.

2. Propose a move of electron k in \mathbf{R}_i in spherical coordinates from position \mathbf{r}_{ik} to $\mathbf{r}'_{ik} = (r', \varphi', \theta')$, where φ' and θ' are obtained from uniform distributions

$$\varphi' = u(0, 2\pi),$$

$$\cos \theta' = u(-1, 1),$$

and r' is sampled from distribution (4.10). The new configuration \mathbf{R}'_i differs from \mathbf{R}_i by the position of electron k .

3. Calculate the acceptance probability of this move

$$q = \min \left(1, \frac{|\Psi_T(\mathbf{R}'_i)|^2 T(\mathbf{R} \leftarrow \mathbf{R}')}{|\Psi_T(\mathbf{R}_i)|^2 T(\mathbf{R}' \leftarrow \mathbf{R})} \right).$$

Accept the move from \mathbf{R} to \mathbf{R}' with probability q as follows.

Draw a random variable from uniform distribution $u(0, 1)$:

if $q > u$, the move is accepted, and new configuration i is \mathbf{R}' ;

if $q < u$, the move is rejected, and new configuration i is \mathbf{R} .

³A pair of random numbers (g_1, g_2) from the Gaussian (normal) distribution with the zero mean and unit variance can be efficiently generated using the equations

$$g_1 = \sqrt{-2 \ln u_1} \sin(2\pi u_2),$$

$$g_2 = \sqrt{-2 \ln u_1} \cos(2\pi u_2),$$

where u_1 and u_2 are uniform random numbers taken from the interval (0,1).

Let \mathbf{y} be a vector of n observations on a continuous variable y .

Let \mathbf{X} be a matrix of n observations on p explanatory variables.

Let \mathbf{y}^* be a vector of n observations on a continuous variable y^* .

$$\mathbf{y}^* = \mathbf{X}\boldsymbol{\beta} + \boldsymbol{\epsilon}$$

Let \mathbf{y}^* be a vector of n observations on a continuous variable y^* .

Let \mathbf{X} be a matrix of n observations on p explanatory variables.

Let \mathbf{y}^* be a vector of n observations on a continuous variable y^* .

Let \mathbf{X} be a matrix of n observations on p explanatory variables.

$$\mathbf{y}^* = \mathbf{X}\boldsymbol{\beta} + \boldsymbol{\epsilon}$$

$$\mathbf{y}^* = \mathbf{X}\boldsymbol{\beta} + \boldsymbol{\epsilon}$$

Let \mathbf{y}^* be a vector of n observations on a continuous variable y^* .

Let \mathbf{X} be a matrix of n observations on p explanatory variables.

Let \mathbf{y}^* be a vector of n observations on a continuous variable y^* .

$$\left(\frac{\partial \mathbf{y}^*}{\partial \boldsymbol{\beta}} - \frac{\partial \mathbf{y}^*}{\partial \boldsymbol{\beta}} \frac{\partial \boldsymbol{\beta}}{\partial \boldsymbol{\beta}} \right) \mathbf{X}$$

Let \mathbf{y}^* be a vector of n observations on a continuous variable y^* .

Let \mathbf{X} be a matrix of n observations on p explanatory variables.

Let \mathbf{y}^* be a vector of n observations on a continuous variable y^* .

Let \mathbf{X} be a matrix of n observations on p explanatory variables.

Let \mathbf{y}^* be a vector of n observations on a continuous variable y^* .

Let \mathbf{X} be a matrix of n observations on p explanatory variables.

$$\mathbf{y}^* = \mathbf{X}\boldsymbol{\beta} + \boldsymbol{\epsilon}$$

$$\mathbf{y}^* = \mathbf{X}\boldsymbol{\beta} + \boldsymbol{\epsilon}$$

Let \mathbf{y}^* be a vector of n observations on a continuous variable y^* .

4. If the move is accepted, recompute the values of the wave function and derivatives for the new electron configuration. Repeat steps 2–3 for all n electrons in configuration i .
5. Compute the local energy E_{ij} and other properties of configuration i in iteration j .
6. Repeat steps 2–5 for all other configurations; this completes iteration j .
7. Repeat steps 2–6 for N_I iterations; this completes the simulation.
8. Compute $N_B = N_C$ block averages \bar{E}_i , each over N_I iterations

$$\bar{E}_i = \frac{1}{N_I} \sum_{j=1}^{N_I} E_{ij}.$$

and block averages for the other properties.

9. Using formulas (4.6)–(4.8) calculate the grand averages \bar{E} , \bar{r} etc. and associated standard errors.

We employ a very efficient and convenient technique to compute derivatives of the determinantal parts of Ψ_T and the ratio of Slater determinants, based on the use of inverse matrices, as was suggested by Ceperley *et al.* [28]⁴.

4.2 The ‘Core’ and ‘Valence’ Energy

The fact that in wave functions Ψ_2 and Ψ_3 the core electrons are distinguishable from valence ones allows us to define and calculate the ‘core’ and ‘valence’ energies — the total energies of the core and valence electron shells.

This corresponds to representing the total Hamiltonian operator as the sum

$$\hat{H} = \hat{H}_{core} + \hat{H}_{val}. \quad (4.17)$$

The choice of \hat{H}_{core} and \hat{H}_{val} now depends on how the Coulombic repulsion between

⁴Working formula (12) in that paper has a typing error: instead of \bar{D}_{kj}^s it should read \bar{D}_{ki}^s .

The first of these is the fact that the majority of the cases of this disease are reported from the United States and Europe. It is not known whether this is due to a higher prevalence of the disease in these countries or to a higher incidence of reporting. The second is the fact that the disease is more common in the summer months. This may be due to a higher incidence of the disease in these months or to a higher incidence of reporting. The third is the fact that the disease is more common in the young. This may be due to a higher incidence of the disease in these groups or to a higher incidence of reporting.



The fourth is the fact that the disease is more common in the warm climates. This may be due to a higher incidence of the disease in these areas or to a higher incidence of reporting. The fifth is the fact that the disease is more common in the tropical and subtropical regions. This may be due to a higher incidence of the disease in these areas or to a higher incidence of reporting. The sixth is the fact that the disease is more common in the summer months. This may be due to a higher incidence of the disease in these months or to a higher incidence of reporting.

1. The Clinical Course of the Disease

The clinical course of the disease is characterized by a sudden onset of fever, headache, and malaise. The fever is usually high and is accompanied by a rapid pulse. The headache is usually severe and is located in the frontal region. The malaise is usually severe and is accompanied by a loss of appetite. The disease is usually self-limiting and resolves within a few days.

2. The Pathogenesis of the Disease

The pathogenesis of the disease is not known. It is thought that the disease is caused by a virus. The virus is thought to be transmitted by a mosquito. The disease is thought to be caused by a virus. The virus is thought to be transmitted by a mosquito.

the core and valence electrons is assigned to the core and valence shells. As in the core-valence partitioning scheme suggested by Rothstein [29] for estimation of the valence energies of Cu and CuH, we assign *all* core-valence repulsion energy to the valence shell. This is necessary for \hat{H}_{core} to be the same even if the number of valence electrons varies.

The Hamiltonians corresponding to the ‘local core’ and ‘local valence energies’ are given by equations (1.20) and (1.21), respectively. The explicit expressions for E_{core} and E_{val} are straightforward. Use the formulas (D.17), (D.19), and (D.22) (Appendix D) to obtain the kinetic energy terms pertaining to the core or valence electrons, respectively, and equations (1.20) and (1.21) for the potential energy terms⁵.

The use of the valence energies for neutral atoms and ions is that they provide an alternative way to estimate the ionization potentials.

⁵One should distinguish this valence energy from the so-called ‘experimental’ valence energy defined by Desmarais and Fliszár [4, 5] as the energy of the ion left behind after removal of n_v valence electrons,

$$E_{val} = E^{atom} - E^{ion}, \quad (4.18)$$

namely, the difference between the energy of the neutral atom A and the energy of the n_c -electron ion $A^{(n-n_c)+}$. The energies of $A^{(n-n_c)+}$ are taken as the appropriate sums of experimental ionization potentials. This E_{val} is *not*, however, simply the sum of kinetic and potential energies of the electrons in the valence region, because the definition of the former accounts for any relaxation that accompanies an actual removal of the n_v valence electrons. In our definition, the valence energy is precisely the sum of kinetic and potential energies of the valence electrons.

Chapter 5

Results

This chapter contains the results of optimizations of wave functions Ψ_1 through Ψ_5 and variational Monte Carlo estimates of selected atomic properties.

5.1 Optimized Wave Functions for Atoms and Ions

All calculations on atoms and ions were performed for the respective ground states. Wave functions were optimized using the simplex method (see Appendix C for details). For several atoms, slightly better results were obtained using the steepest descent method.

Improved sampling does not require the use of a time-step parameter. Parameters α , β , and γ appearing in Eq. (4.11) were chosen so as to decrease the correlation time. The actual correlation times ranged between ~ 1.6 and ~ 3.5 . We did not run into the problem of locked configurations. The limit of ‘staleness’, set to 6–9 iterations, was never exceeded in our simulations.

At the early stage of the optimization the ensemble had the size $N_C = 150$, $N_I = 1125$, and the ‘restart coefficient’ $k = 3.5$ (see Appendix C). Every time the ensemble was to be enlarged, N_C and N_I were multiplied by $\sqrt{2}$ and rounded to the nearest integer, thereby increasing the ensemble size by a factor of 2. In the end, when the simplex reached its maximum size, the ensemble parameters were $N_C = 600$, $N_I = 4500$, and $k = 1.2$.

Optimized values of the variational parameters are listed in Tables 5.1 – 5.5. Three decimal digits are given only for reproducibility, although not all of them are significant.

Generally, ζ_1 ’s for ions are larger than ζ_1 ’s for the respective atoms. A distinct increase

of ζ_1 's is observed from Ψ_1 to Ψ_3 , while ζ_1 's for Ψ_4 and Ψ_5 are not much different from those for Ψ_3 . Electron correlation parameter b tends to steadily increase through the row, whereas for v_s and v_p the overall trend is a decrease.

Attempts to optimize wave functions Ψ_1 for negative ions to estimate electron affinities failed to yield sensible results. With correlation energies only 69% for Li^- to 42% for F^- , EA's were sometimes wrong even in sign.

The values of the optimized variational parameters for both the neutral atoms and positive ions are summarized¹ in Tables 5.1–5.5.

System	ζ_1	ζ_2	v_s	v_p	b
Li (2S)	2.300	0.613	0.299	-	0.697
Li ⁺ (1S)	2.415	-	0.438	-	0.736
Be (1S)	2.809	0.693	0.196	-	0.695
Be ⁺ (2S)	3.097	1.031	0.340	-	0.941
B (2P)	3.783	1.072	0.235	0.656	0.826
B ⁺ (1S)	3.806	1.216	0.262	-	0.872
C (3P)	4.313	1.048	0.190	0.436	0.932
C ⁺ (2P)	4.383	1.204	0.202	0.406	1.028
N (4S)	4.808	1.031	0.175	0.387	1.058
N ⁺ (3P)	5.062	1.378	0.208	0.422	1.006
O (3P)	5.425	1.140	0.182	0.402	1.155
O ⁺ (4S)	5.332	1.323	0.234	0.397	1.253
F (2P)	5.860	1.122	0.201	0.405	1.387
F ⁺ (3P)	6.048	1.247	0.183	0.380	1.447
Ne (1S)	6.186	0.951	0.179	0.361	1.276
Ne ⁺ (2P)	6.667	1.403	0.199	0.394	1.394

Table 5.1: Optimized wave functions Ψ_1 for atoms and ions.

¹In Tables 5.2–5.5 and 5.7–5.10 calculations on Li^+ are not shown because wave functions Ψ_2 – Ψ_5 for Li^+ are identical to Ψ_1 .

Let $f(x)$ be a function defined on the interval $[a, b]$. The function $f(x)$ is said to be continuous on $[a, b]$ if it is continuous at every point x in $[a, b]$. The function $f(x)$ is said to be discontinuous on $[a, b]$ if it is not continuous at some point x in $[a, b]$.

The function $f(x)$ is said to be continuous from the right at a if $\lim_{x \rightarrow a^+} f(x) = f(a)$. The function $f(x)$ is said to be continuous from the left at b if $\lim_{x \rightarrow b^-} f(x) = f(b)$.

The function $f(x)$ is said to be continuous on $[a, b]$ if it is continuous from the right at a and from the left at b .

The function $f(x)$ is said to be continuous on (a, b) if it is continuous at every point x in (a, b) .

The function $f(x)$ is said to be continuous on $[a, b)$ if it is continuous on (a, b) and continuous from the right at a .

x	$f(x)$	$f(x)$	$f(x)$	$f(x)$
0	1	1	1	1
1	2	2	2	2
2	3	3	3	3
3	4	4	4	4
4	5	5	5	5
5	6	6	6	6
6	7	7	7	7
7	8	8	8	8
8	9	9	9	9
9	10	10	10	10
10	11	11	11	11
11	12	12	12	12
12	13	13	13	13
13	14	14	14	14
14	15	15	15	15
15	16	16	16	16
16	17	17	17	17
17	18	18	18	18
18	19	19	19	19
19	20	20	20	20
20	21	21	21	21
21	22	22	22	22
22	23	23	23	23
23	24	24	24	24
24	25	25	25	25
25	26	26	26	26
26	27	27	27	27
27	28	28	28	28
28	29	29	29	29
29	30	30	30	30
30	31	31	31	31
31	32	32	32	32
32	33	33	33	33
33	34	34	34	34
34	35	35	35	35
35	36	36	36	36
36	37	37	37	37
37	38	38	38	38
38	39	39	39	39
39	40	40	40	40
40	41	41	41	41
41	42	42	42	42
42	43	43	43	43
43	44	44	44	44
44	45	45	45	45
45	46	46	46	46
46	47	47	47	47
47	48	48	48	48
48	49	49	49	49
49	50	50	50	50
50	51	51	51	51
51	52	52	52	52
52	53	53	53	53
53	54	54	54	54
54	55	55	55	55
55	56	56	56	56
56	57	57	57	57
57	58	58	58	58
58	59	59	59	59
59	60	60	60	60
60	61	61	61	61
61	62	62	62	62
62	63	63	63	63
63	64	64	64	64
64	65	65	65	65
65	66	66	66	66
66	67	67	67	67
67	68	68	68	68
68	69	69	69	69
69	70	70	70	70
70	71	71	71	71
71	72	72	72	72
72	73	73	73	73
73	74	74	74	74
74	75	75	75	75
75	76	76	76	76
76	77	77	77	77
77	78	78	78	78
78	79	79	79	79
79	80	80	80	80
80	81	81	81	81
81	82	82	82	82
82	83	83	83	83
83	84	84	84	84
84	85	85	85	85
85	86	86	86	86
86	87	87	87	87
87	88	88	88	88
88	89	89	89	89
89	90	90	90	90
90	91	91	91	91
91	92	92	92	92
92	93	93	93	93
93	94	94	94	94
94	95	95	95	95
95	96	96	96	96
96	97	97	97	97
97	98	98	98	98
98	99	99	99	99
99	100	100	100	100

The function $f(x)$ is said to be continuous on $[a, b]$ if it is continuous on (a, b) and continuous from the right at a and from the left at b .

The function $f(x)$ is said to be continuous on (a, b) if it is continuous at every point x in (a, b) . The function $f(x)$ is said to be discontinuous on (a, b) if it is not continuous at some point x in (a, b) .

System	ζ_1	ζ_2	v_s	v_p	b
Li	2.302	0.609	0.250	-	0.671
Be	3.432	1.063	0.237	-	0.565
Be ⁺	3.227	1.086	0.307	-	0.787
B	3.941	1.094	0.156	0.511	0.704
B ⁺	4.083	1.302	0.142	-	0.668
C	4.542	1.210	0.108	0.385	0.678
C ⁺	4.703	1.394	0.138	0.451	0.792
N	4.992	1.004	0.131	0.390	1.126
N ⁺	5.063	1.127	0.102	0.319	0.964
O	6.015	1.305	0.078	0.430	1.064
O ⁺	5.744	1.267	0.107	0.344	1.026
F	6.213	1.151	0.124	0.403	1.311
F ⁺	6.300	1.225	0.093	0.336	1.156
Ne	6.831	1.114	0.102	0.383	1.352
Ne ⁺	7.244	1.522	0.085	0.394	1.233

Table 5.2: Optimized wave functions Ψ_2 for atoms and ions.

System	ζ_1	ζ_2	v_s	v_p	b
Li	2.590	0.638	0.654	-	0.574
Be	3.751	1.007	0.248	-	0.249
Be ⁺	3.575	1.061	0.885	-	0.935
B	4.423	1.197	0.124	1.118	0.261
B ⁺	4.706	1.506	0.254	-	0.328
C	4.918	1.214	0.087	0.611	0.309
C ⁺	5.117	1.409	0.097	0.634	0.351
N	5.955	1.722	0.118	0.938	0.420
N ⁺	5.901	1.732	0.109	0.699	0.314
O	6.164	1.357	0.094	0.468	0.537
O ⁺	6.518	1.843	0.193	0.717	0.565
F	6.572	1.315	0.106	0.437	0.714
F ⁺	7.168	1.821	0.117	0.598	0.822
Ne	7.460	1.891	0.158	0.558	0.642
Ne ⁺	7.802	1.947	0.130	0.567	0.816

Table 5.3: Optimized wave functions Ψ_3 for atoms and ions.

System	ζ_1	ζ_2	v_s	v_p	b_c	b_v
Li	Ψ_4 for Li is identical to Ψ_3					
Be	3.816	1.154	1.973	-	0.701	0.159
Be ⁺	3.361	0.967	0.422	-	0.825	-
B	4.304	1.258	0.346	1.735	0.954	0.376
B ⁺	4.175	1.265	0.272	-	0.829	0.198
C	4.812	1.404	0.215	0.786	1.001	0.321
C ⁺	5.176	1.602	0.213	1.282	0.663	0.397
N	5.791	1.547	0.086	0.660	0.578	0.378
N ⁺	5.796	1.720	0.121	0.653	0.819	0.344
O	6.372	1.653	0.136	0.598	1.016	0.512
O ⁺	6.154	1.537	0.111	0.500	1.079	0.519
F	6.503	1.321	0.120	0.431	1.526	0.649
F ⁺	6.667	1.700	0.158	0.485	1.742	0.628
Ne	7.156	1.517	0.115	0.423	0.831	0.603
Ne ⁺	7.347	1.613	0.093	0.408	1.460	0.619

Table 5.4: Optimized wave functions Ψ_4 for atoms and ions.

System	ζ_1	ζ_2	v_s	v_p	b_c	b_v	b_{cv}
Li	2.636	0.742	0.629	-	0.539	-	0.682
Be	3.332	1.121	0.308	-	0.695	0.173	0.875
Be ⁺	3.454	1.262	0.401	-	0.769	-	0.701
B	3.998	1.261	0.136	0.542	0.661	0.185	0.896
B ⁺	4.178	1.472	0.161	-	0.605	0.119	0.904
C	4.690	1.424	0.129	0.467	0.949	0.227	1.132
C ⁺	4.737	1.473	0.134	0.406	1.062	0.311	1.081
N	5.222	1.414	0.092	0.368	1.079	0.274	1.289
N ⁺	5.455	1.605	0.101	0.400	0.928	0.343	1.216
O	5.880	1.465	0.099	0.382	1.295	0.422	1.702
O ⁺	5.800	1.480	0.092	0.315	1.156	0.365	1.491
F	6.282	1.309	0.099	0.335	1.310	0.496	2.310
F ⁺	6.359	1.341	0.062	0.294	1.202	0.479	1.589
Ne	6.654	1.259	0.099	0.315	1.850	0.546	2.536
Ne ⁺	6.859	1.251	0.039	0.276	1.698	0.589	1.567

Table 5.5: Optimized wave functions Ψ_5 for atoms and ions.

5.2 Calculations on Atoms and Ions

Once the optimal set of parameters was found, a longer run was performed in order to decrease further the statistical errors and thus obtain more reliable estimates. In these verification runs, parameters specifying the ensemble size were chosen to be: $N_B(N_C) = 10^3$, $N_I = 5 \cdot 10^4$.

Simulation parameters of Eq. (4.10) for Ψ_1 were as follows: $\alpha = 0.04$, $\beta = \zeta_2$, $\gamma = 0.5$. For Ψ_2 – Ψ_5 : $\beta_c = 2.0$, $\beta_v = 1.0$, and $\gamma_c = 0.3$, $\gamma_v = 1.3$.

Selected properties of atoms and ions calculated with wave functions Ψ_1 – Ψ_5 are given in Tables 5.6–5.10. The energy differences $\Delta E_{21} \equiv E_2 - E_1$ and $\Delta E_{31} \equiv E_3 - E_1$ provide quantitative estimates of the effects of loss of core-valence antisymmetry and combined effect of the loss of antisymmetry and core-valence correlation, respectively. Correlation energies are reported only for Ψ_1 because the approximate non-antisymmetrized partitioned wave functions are not expected to reproduce the exact energy even in the limit of infinitely large basis set and sufficiently flexible electron-electron correlation function, hence the notion of E_{corr} is irrelevant to Ψ_2 – Ψ_5 .

Average distances of electrons from the nucleus \bar{r} are normalized to one electron. For Ψ_2 – Ψ_5 normalized distances from the nucleus are reported for both the core and valence electrons, denoted \bar{r}_c and \bar{r}_v , respectively. Virial ratios² \bar{V}/\bar{T} estimated for all wave

²It is well known that the virial theorem holds for the exact solution of the Schrödinger equation. For an approximate wave function, if a single nonlinear variational parameter multiplying all coordinates of the particles ('scale factor') is varied, the value of this parameter for which the energy is minimum is also the value for which the virial theorem is satisfied [30]. If a wave function contains a set of nonlinear variational parameters (k_1, k_2, \dots, k_m) , which can be viewed as a position vector \mathbf{k} in an m -dimensional Euclidean space, there exist a hyperplane in that space defined by the equation

$$\mathbf{k} \cdot \nabla E(\mathbf{k}) = 2\bar{T} + \bar{V} = 0,$$

whose points \mathbf{k} satisfy the virial theorem [31]. Since only one point \mathbf{k}^* corresponds to the minimum of the energy, fulfillment of the virial theorem for such wave functions is a necessary but not sufficient condition for the fulfillment of the variational principle.

functions³ indicate quality of optimization.

The effect of the core-valence overlap was studied using wave function Ψ_2 on several atoms. In all cases, a series of VMC runs was performed for the same set of optimized variational parameters and k allowing the overlap $Q = N_{1s}N'_{2s}\langle\phi_{1s}|\phi'_{2s}\rangle$ varying in the range $[-0.3, 0.4]$ with a step $\Delta Q = 0.01$ in the region $Q = [-0.1, 0.1]$ and $\Delta Q = 0.05$ outside that region. The typical result is presented in Fig. 5.3.

System	E_1	% E_{corr}	\bar{r}	V/T	E_{HF}^a	E_{exact}^b
Li	-7.47400(6)	91.0	1.6811(3)	-1.9992(7)	-7.43273	-7.47806
Li ⁺	-7.27587(6)	90.7	0.57124(8)	-2.0091(6)	-7.23642	-7.27991
Be	-14.63347(9)	64.1	1.5227(2)	-2.0073(5)	-14.57302	-14.66736
Be ⁺	-14.32062(8)	91.3	1.0475(1)	-2.0090(6)	-14.27739	-14.32476
B	-24.6039(1)	60.0	1.3307(1)	-2.0081(5)	-24.52906	-24.65391
B ⁺	-24.3031(1)	58.8	1.0555(1)	-2.0074(5)	-24.23758	-24.34892
C	-37.7852(2)	61.8	1.1807(1)	-2.0104(5)	-37.68862	-37.8450
C ⁺	-37.3757(2)	60.1	0.9892(1)	-2.0034(5)	-37.29222	-37.43103
N	-54.5194(2)	62.9	1.0417(1)	-2.0090(4)	-54.40093	-54.5892
N ⁺	-53.9918(2)	62.3	0.90897(9)	-2.0131(4)	-53.88800	-54.0546
O	-74.9697(3)	62.1	0.93758(8)	-2.0131(5)	-74.80940	-75.0673
O ⁺	-74.4929(4)	61.9	0.82833(7)	-2.0149(4)	-74.37261	-74.5668
F	-99.6092(4)	61.6	0.84966(7)	-2.0126(5)	-99.40935	-99.7339
F ⁺	-98.9999(4)	64.4	0.76398(6)	-2.0056(4)	-98.83172	-99.0928
Ne	-128.7924(6)	62.8	0.78267(6)	-2.0197(4)	-128.54710	-128.9376
Ne ⁺	-128.0290(5)	64.9	0.70406(5)	-2.0115(4)	-127.81781	-128.1431

^a Reference [33].

^b Reference [34].

Table 5.6: Properties estimated with optimized wave function Ψ_1 . Total energies E_1 (a.u.), average distances of electrons from the nucleus \bar{r} , virial ratios \bar{V}/\bar{T} .

³The standard error of the ratio

$$\xi = \frac{\bar{V}}{\bar{T}} = \frac{\sum_{i=1}^N V_i}{\sum_{i=1}^N T_i},$$

reported in Tables 5.1–5.1 is calculated according to [32] as

$$s(\xi) = \frac{1}{\bar{T}\sqrt{N}} \sqrt{\frac{\sum_{i=1}^N (V_i - \xi T_i)^2}{N-1}}.$$

System	E_2^c	E_2^v	E_2	\bar{r}_c	\bar{r}_v	\bar{r}	V/T
Li	-7.27211(6)	-0.20021(4)	-7.47231(6)	0.56477(8)	3.898(1)	1.6758(4)	-1.9941(5)
Be	-13.6290(1)	-0.99896(9)	-14.6280(1)	0.40983(6)	2.5700(2)	1.4899(1)	-2.0072(5)
Be ⁺	-13.64477(8)	-0.66869(8)	-14.3135(1)	0.41315(6)	2.3283(2)	1.05152(9)	-2.0123(5)
B	-21.9959(2)	-2.5885(2)	-24.5844(2)	0.32380(5)	1.9845(1)	1.32024(9)	-2.0152(5)
B ⁺	-21.9949(2)	-2.3013(2)	-24.2953(2)	0.32192(5)	1.7551(1)	1.03850(6)	-2.0108(5)
C	-32.3406(2)	-5.3883(2)	-37.7289(3)	0.26842(4)	1.5720(1)	1.13749(7)	-2.0185(4)
C ⁺	-32.3592(2)	-4.9774(2)	-37.3365(3)	0.26695(4)	1.4641(1)	0.98526(5)	-2.0214(5)
N	-44.7363(3)	-9.6782(3)	-54.4145(3)	0.22746(4)	1.39751(9)	1.06321(7)	-2.0245(5)
N ⁺	-44.7264(3)	-9.1810(3)	-53.9074(4)	0.22705(3)	1.25635(9)	0.91325(6)	-2.0217(4)
O	-59.0867(4)	-15.7217(4)	-74.8084(5)	0.19720(3)	1.18670(8)	0.93933(6)	-2.0217(5)
O ⁺	-59.0812(4)	-15.2752(4)	-74.3564(5)	0.19847(3)	1.08982(8)	0.83515(6)	-2.0287(4)
F	-75.4526(5)	-23.9247(6)	-99.3773(6)	0.17594(3)	1.05507(7)	0.85971(6)	-2.0282(4)
F ⁺	-75.4430(5)	-23.3500(6)	-98.7930(6)	0.17560(3)	0.96614(7)	0.76850(5)	-2.0263(4)
Ne	-93.8056(7)	-34.6676(7)	-128.4732(7)	0.15776(3)	0.93443(6)	0.77910(5)	-2.0274(4)
Ne ⁺	-93.7975(6)	-33.9345(7)	-127.7320(8)	0.15744(3)	0.86903(6)	0.71090(5)	-2.0289(4)

Table 5.7: Properties estimated with optimized wave function Ψ_2 . Core, valence, and total energies E_2^c , E_2^v , E_2 (a.u.), average distances of core and valence electrons from the nucleus \bar{r}_c and \bar{r}_v , average distances for all electrons \bar{r} , virial ratios \bar{V}/\bar{T} .

System	E_3^c	E_3^v	E_3	\bar{r}_c	\bar{r}_v	\bar{r}	V/T
Li	-7.27505(7)	-0.18800(6)	-7.46304(9)	0.57024(8)	4.0326(1)	1.7244(4)	-2.0119(5)
Be	-13.6374(1)	-0.9749(1)	-14.6123(2)	0.40802(6)	2.7078(3)	1.5579(1)	-1.9965(5)
Be ⁺	-13.65116(8)	-0.6400(1)	-14.2911(1)	0.41170(6)	2.5004(3)	1.1079(1)	-2.0104(5)
B	-22.0113(2)	-2.5548(2)	-24.5660(3)	0.32188(4)	2.0788(2)	1.3760(1)	-2.0067(5)
B ⁺	-22.0132(2)	-2.2444(3)	-24.2576(3)	0.32044(4)	1.8101(1)	1.06525(6)	-1.9970(5)
C	-32.3870(2)	-5.3246(3)	-37.7116(4)	0.26543(4)	1.7123(1)	1.23003(8)	-2.0115(5)
C ⁺	-32.3878(2)	-4.9095(4)	-37.2973(4)	0.26464(4)	1.5119(1)	1.01302(7)	-2.0043(5)
N	-44.7640(2)	-9.6357(5)	-54.3997(5)	0.22532(3)	1.36517(8)	1.03950(6)	-2.0050(4)
N ⁺	-44.7606(2)	-9.1082(5)	-53.8688(5)	0.22602(3)	1.29224(8)	0.93684(6)	-2.0162(5)
O	-59.1414(3)	-15.6538(6)	-74.7952(6)	0.19606(3)	1.22596(8)	0.96849(6)	-2.0082(4)
O ⁺	-59.1422(2)	-15.1582(6)	-74.3005(7)	0.19731(3)	1.12583(8)	0.86054(6)	-2.0232(4)
F	-75.5199(3)	-23.8458(8)	-99.3657(8)	0.17370(3)	1.06451(7)	0.86655(5)	-2.0014(4)
F ⁺	-75.5201(3)	-23.2184(8)	-98.7386(8)	0.17305(3)	0.98010(7)	0.77833(5)	-2.0028(4)
Ne	-93.8899(3)	-34.5818(9)	-128.472(1)	0.15668(3)	0.95228(6)	0.79316(5)	-2.0171(4)
Ne ⁺	-93.8954(3)	-33.8004(9)	-127.696(1)	0.15562(2)	0.88478(6)	0.72275(4)	-2.0090(4)

Table 5.8: Properties estimated with optimized wave function Ψ_3 . Core, valence, and total energies E_3^c , E_3^v , E_3 (a.u.), average distances of core and valence electrons from the nucleus \bar{r}_c and \bar{r}_v , average distances for all electrons \bar{r} , virial ratios \bar{V}/\bar{T} .

System	E_4^c	E_4^v	E_4	\bar{r}_c	\bar{r}_v	\bar{r}	V/T
Li	Ψ_4 for Li is identical to Ψ_3						
Be	-13.64671(9)	-0.9740(1)	-14.6207(2)	0.40575(5)	2.6617(2)	1.5337(1)	-1.9944(5)
Be ⁺	-13.65191(7)	-0.6377(1)	-14.2896(1)	0.41208(6)	2.4928(3)	1.1056(1)	-2.0046(5)
B	-22.0258(1)	-2.5332(2)	-24.5590(3)	0.32088(4)	2.0584(2)	1.3634(1)	-1.9991(5)
B ⁺	-22.0257(1)	-2.2277(3)	-24.2534(3)	0.32159(4)	1.9209(1)	1.12127(7)	-2.0061(5)
C	-32.4011(1)	-5.3111(4)	-37.7122(4)	0.26484(4)	1.6583(1)	1.19380(7)	-1.9983(5)
C ⁺	-32.3969(1)	-4.8974(4)	-37.2943(4)	0.26439(4)	1.5149(1)	1.01468(7)	-2.0018(5)
N	-44.7661(2)	-9.6405(5)	-54.4066(5)	0.22405(3)	1.38201(8)	1.05116(6)	-1.9977(4)
N ⁺	-44.7695(2)	-9.1008(5)	-53.8704(6)	0.22369(3)	1.26299(9)	0.91656(6)	-1.9926(5)
O	-59.1478(2)	-15.6518(6)	-74.7996(6)	0.19521(3)	1.21267(7)	0.95831(5)	-2.0033(4)
O ⁺	-59.1469(2)	-15.1555(6)	-74.3025(7)	0.19479(3)	1.11173(8)	0.84975(6)	-1.9949(4)
F	-75.5245(2)	-23.8450(7)	-99.3695(8)	0.17255(3)	1.07718(7)	0.87615(5)	-1.9973(4)
F ⁺	-75.5266(2)	-23.2100(9)	-98.7366(9)	0.17283(3)	0.97949(7)	0.77782(5)	-1.9938(4)
Ne	-93.8955(3)	-34.5905(9)	-128.486(1)	0.15586(3)	0.95416(6)	0.79450(4)	-2.0071(4)
Ne ⁺	-93.8967(3)	-33.8044(9)	-127.701(1)	0.15449(3)	0.88548(6)	0.72304(5)	-1.9969(4)

Table 5.9: Properties estimated with optimized wave function Ψ_4 . Core, valence, and total energies E_4^c , E_4^v , E_4 (a.u.), average distances of core and valence electrons from the nucleus \bar{r}_c and \bar{r}_v , average distances for all electrons \bar{r} , virial ratios \bar{V}/\bar{T} .

System	E_5^c	E_5^v	E_5	\bar{r}_c	\bar{r}_v	\bar{r}	V/T
Li	-7.27178(6)	-0.19932(4)	-7.47109(7)	0.56668(8)	3.8845(7)	1.6726(2)	-2.0065(4)
Be	-13.64296(9)	-1.0036(1)	-14.6466(1)	0.41186(6)	2.5465(2)	1.4792(1)	-2.0108(5)
Be ⁺	-13.64194(9)	-0.67230(7)	-14.3142(1)	0.41043(6)	2.2446(2)	1.02180(8)	-2.0008(5)
B	-22.0065(1)	-2.6086(2)	-24.6150(2)	0.32191(5)	1.9837(1)	1.31900(9)	-2.0068(5)
B ⁺	-22.0075(1)	-2.3103(2)	-24.3178(2)	0.32163(4)	1.7834(1)	1.05252(6)	-2.0124(5)
C	-32.3787(2)	-5.3941(2)	-37.7728(3)	0.26481(4)	1.6325(1)	1.17663(7)	-2.0089(5)
C ⁺	-32.3772(2)	-4.9874(3)	-37.3645(3)	0.26436(4)	1.4596(1)	0.98148(6)	-2.0059(5)
N	-44.7466(2)	-9.7314(3)	-54.4780(4)	0.22532(4)	1.36995(8)	1.04292(6)	-2.0110(4)
N ⁺	-44.7437(2)	-9.2079(4)	-53.9516(4)	0.22564(3)	1.25062(8)	0.90896(6)	-2.0161(4)
O	-59.1232(3)	-15.7592(4)	-74.8824(5)	0.19607(3)	1.19794(7)	0.94748(5)	-2.0126(4)
O ⁺	-59.1169(3)	-15.2979(4)	-74.4148(5)	0.19660(3)	1.08392(7)	0.83034(5)	-2.0146(4)
F	-75.5029(3)	-23.9692(6)	-99.4721(6)	0.17388(3)	1.06164(6)	0.86436(5)	-2.0144(4)
F ⁺	-75.4806(4)	-23.3773(6)	-98.8579(7)	0.17377(3)	0.98119(6)	0.77934(5)	-2.0202(4)
Ne	-93.8730(4)	-34.7140(8)	-128.5870(8)	0.15583(3)	0.93920(6)	0.78253(5)	-2.0108(4)
Ne ⁺	-93.8372(5)	-33.9770(8)	-127.8142(8)	0.15553(3)	0.86954(6)	0.71087(4)	-2.0134(4)

Table 5.10: Properties estimated with optimized wave function Ψ_5 . Core, valence, and total energies E_5^c , E_5^v , E_5 (a.u.), average distances of core and valence electrons from the nucleus \bar{r}_c and \bar{r}_v , average distances for all electrons \bar{r} , virial ratios \bar{V}/\bar{T} .

Year	Month	Day	Time	Location	Activity	Remarks
2010	Jan	1	10:00	Room 101	Meeting	Initial meeting with client.
2010	Jan	5	14:00	Room 101	Meeting	Follow-up meeting with client.
2010	Jan	10	10:00	Room 101	Meeting	Meeting with client and team.
2010	Jan	15	14:00	Room 101	Meeting	Meeting with client and team.
2010	Jan	20	10:00	Room 101	Meeting	Meeting with client and team.
2010	Jan	25	14:00	Room 101	Meeting	Meeting with client and team.
2010	Jan	30	10:00	Room 101	Meeting	Meeting with client and team.
2010	Feb	5	14:00	Room 101	Meeting	Meeting with client and team.
2010	Feb	10	10:00	Room 101	Meeting	Meeting with client and team.
2010	Feb	15	14:00	Room 101	Meeting	Meeting with client and team.
2010	Feb	20	10:00	Room 101	Meeting	Meeting with client and team.
2010	Feb	25	14:00	Room 101	Meeting	Meeting with client and team.
2010	Feb	30	10:00	Room 101	Meeting	Meeting with client and team.

Notes: All meetings were held in Room 101. The meetings were held on a regular basis, and the client was satisfied with the progress. The meetings were held on a regular basis, and the client was satisfied with the progress. The meetings were held on a regular basis, and the client was satisfied with the progress.

Year	Month	Day	Time	Location	Activity	Remarks
2010	Mar	1	10:00	Room 101	Meeting	Meeting with client and team.
2010	Mar	5	14:00	Room 101	Meeting	Meeting with client and team.
2010	Mar	10	10:00	Room 101	Meeting	Meeting with client and team.
2010	Mar	15	14:00	Room 101	Meeting	Meeting with client and team.
2010	Mar	20	10:00	Room 101	Meeting	Meeting with client and team.
2010	Mar	25	14:00	Room 101	Meeting	Meeting with client and team.
2010	Mar	30	10:00	Room 101	Meeting	Meeting with client and team.
2010	Apr	5	14:00	Room 101	Meeting	Meeting with client and team.
2010	Apr	10	10:00	Room 101	Meeting	Meeting with client and team.
2010	Apr	15	14:00	Room 101	Meeting	Meeting with client and team.
2010	Apr	20	10:00	Room 101	Meeting	Meeting with client and team.
2010	Apr	25	14:00	Room 101	Meeting	Meeting with client and team.
2010	Apr	30	10:00	Room 101	Meeting	Meeting with client and team.

Notes: All meetings were held in Room 101. The meetings were held on a regular basis, and the client was satisfied with the progress. The meetings were held on a regular basis, and the client was satisfied with the progress. The meetings were held on a regular basis, and the client was satisfied with the progress.

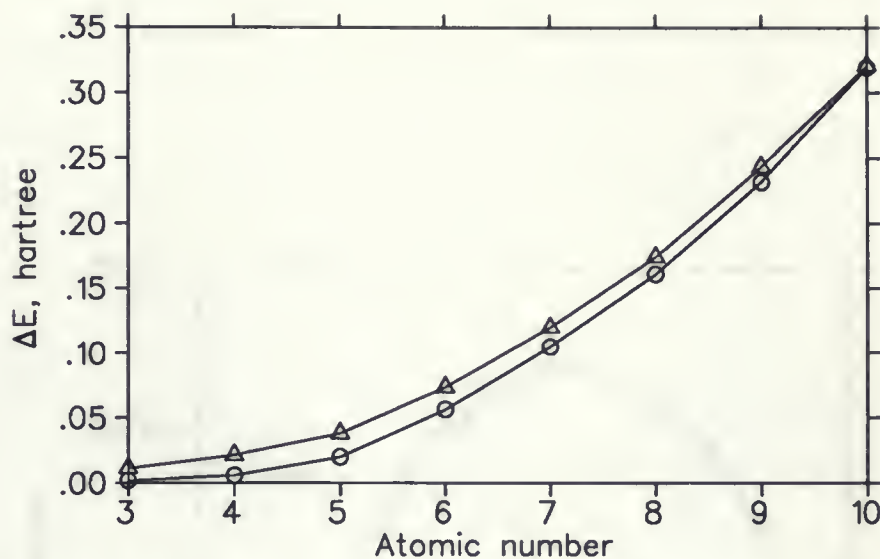


Figure 5.1: Increase in the total energy of the first-row *atoms* due to the loss of core-valence antisymmetry $\Delta E_{21} = E_2 - E_1$ (o), and combination of the losses of core-valence antisymmetry and core-valence correlation $\Delta E_{31} = E_3 - E_1$ (Δ).

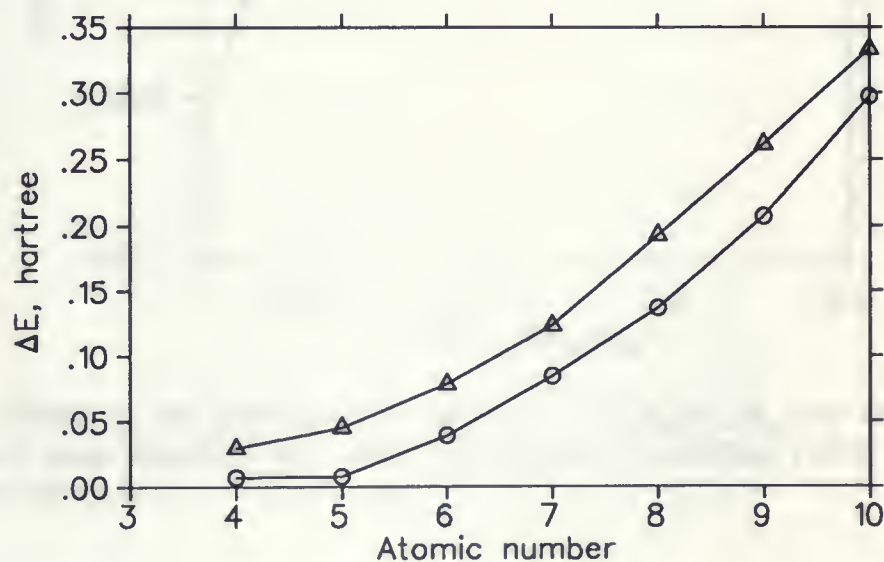


Figure 5.2: Increase in the total energy of the first-row positive *ions* due to the loss of core-valence antisymmetry $\Delta E_{21} = E_2 - E_1$ (o), and combination of the losses of core-valence antisymmetry and core-valence correlation $\Delta E_{31} = E_3 - E_1$ (Δ).



Figure 1. Relative error vs. number of points for a single curve. The relative error is defined as the absolute value of the difference between the exact and approximate values, divided by the exact value.



Figure 2. Relative error vs. number of points for two curves. The relative error is defined as the absolute value of the difference between the exact and approximate values, divided by the exact value.

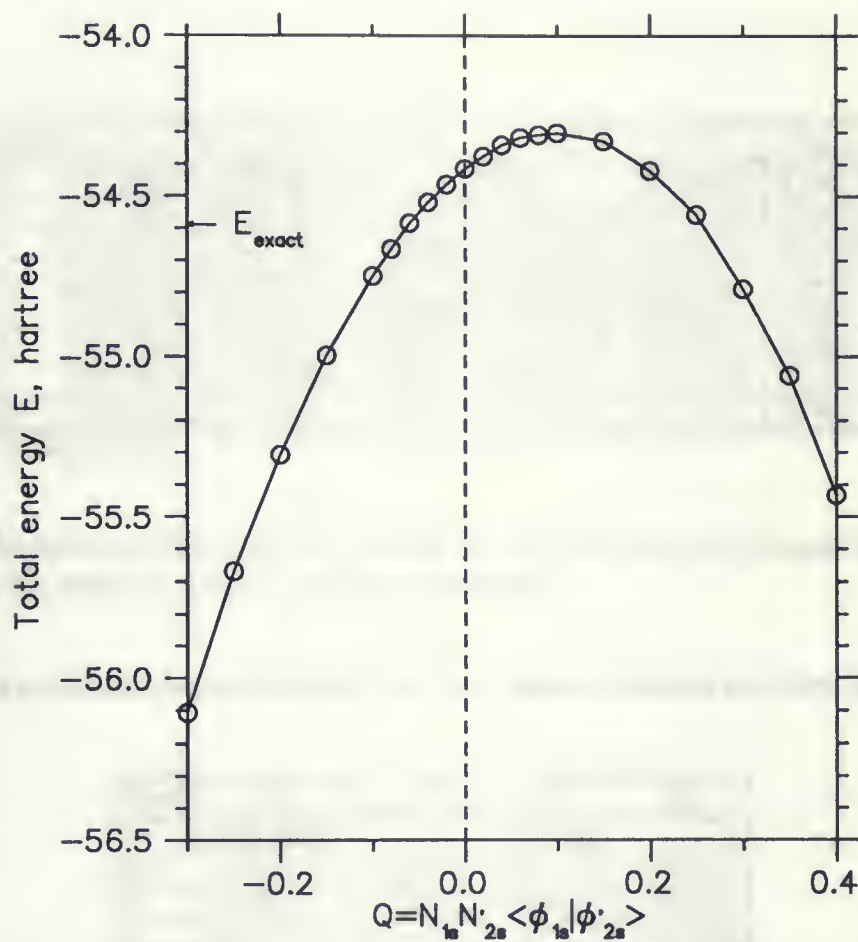


Figure 5.3: Effect of the core-valence overlap $Q = N_{1s} N_{2s} \langle \phi_{1s} | \phi'_{2s} \rangle$ on the total energy of the N atom computed with wave function Ψ_2 . See section (2.2.2) for details. $E_{\text{exact}} = -54.5892$ a.u.

5.3 Ionization Potentials

Table 5.11 summarizes the estimates of first ionization potentials (IP's) computed with wave functions Ψ_1 through Ψ_5 using the total energies, and cites exact values⁴ for comparison.

Atom	I_{Ψ_1}	$I_{\Psi_2}^{\text{tot}}$	$I_{\Psi_3}^{\text{tot}}$	$I_{\Psi_4}^{\text{tot}}$	$I_{\Psi_5}^{\text{tot}}$	I_{exact}^a
Li	0.19814(9)	0.19644(9)	0.1872(1)		0.1952(1)	0.19815
Be	0.3129(1)	0.3145(2)	0.3212(2)	0.3311(2)	0.3323(2)	0.34260
B	0.3009(2)	0.2891(3)	0.3084(4)	0.3056(4)	0.2972(3)	0.30499
C	0.4095(2)	0.3924(4)	0.4143(6)	0.4179(6)	0.4082(4)	0.4140
N	0.5275(3)	0.5071(5)	0.5309(8)	0.5362(8)	0.5264(5)	0.5346
O	0.4767(5)	0.4520(7)	0.4947(9)	0.4972(9)	0.4676(7)	0.5005
F	0.6093(6)	0.5843(9)	0.627(1)	0.633(1)	0.6141(9)	0.6411
Ne	0.7633(8)	0.741(1)	0.776(1)	0.785(1)	0.773(1)	0.7945

^a Reference [34]

Table 5.11: Ionization potentials (a.u.) based on the total energies computed with wave functions Ψ_1 – Ψ_5 and the ‘exact’ ionization potentials.

Ionization potentials found as difference of the valence energies are given in Table 5.12.

Atom	$I_{\Psi_2}^{\text{val}}$	$I_{\Psi_3}^{\text{val}}$	$I_{\Psi_4}^{\text{val}}$	$I_{\Psi_5}^{\text{val}}$
Li	0.20021(4)	0.18800(6)		
Be	0.3303(1)	0.3350(2)	0.3363(2)	0.3313(1)
B	0.2872(2)	0.3104(3)	0.3055(3)	0.2982(2)
C	0.4109(3)	0.4151(5)	0.4137(5)	0.4067(4)
N	0.4972(5)	0.5274(7)	0.5396(7)	0.5235(5)
O	0.4465(6)	0.4955(8)	0.4963(8)	0.4613(6)
F	0.5747(8)	0.627(1)	0.635(1)	0.5919(8)
Ne	0.733(1)	0.781(1)	0.786(1)	0.737(1)

Table 5.12: Ionization potentials (a.u.) based on the valence energies computed with wave functions Ψ_2 – Ψ_5 .

⁴Due to virtual cancellation of relativistic corrections to the total energies of systems A and A⁺, $I_{\text{exact}} \approx I_{\text{exptl}}$.

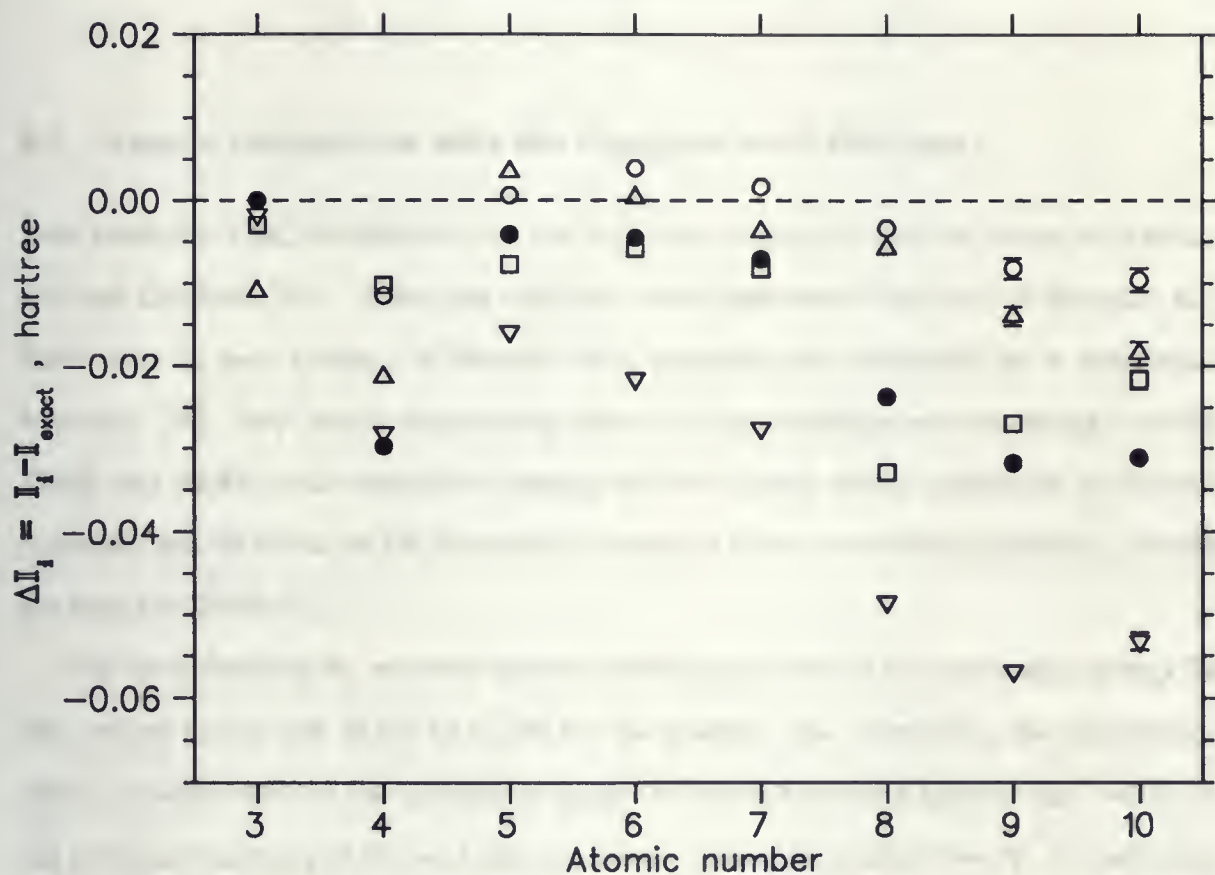


Figure 5.4: Deviations of the ionization potentials computed with wave functions Ψ_1 – Ψ_5 from the exact values (in hartrees). •: ΔI_1 (IP based on Ψ_1), ∇ : ΔI_2 (IP based on Ψ_2), \triangle : ΔI_3 (IP based on Ψ_3), ○: ΔI_4 (IP based on Ψ_4), □: ΔI_5 (IP based on Ψ_5).



FIG. 10. Difference in the time-averaged zonal wind (m s^{-1}) between the control and the perturbation. The contour interval is 10 m s^{-1} . The solid lines are positive and the dashed lines are negative. The shading is as in Fig. 9. The perturbation is the same as in Fig. 9.

Chapter 6

Discussion and Conclusions

6.1 Atomic Calculations with the Complete wave Function

Best available VMC calculations on the first row atoms and ions are those by Alexander and Coldwell [35]. Using the explicitly-correlated wave functions of Schmidt and Moskowitz (a pair product of Hartree–Fock determinants multiplied by a correlation function) [36], they found expectation values of the Hamiltonian containing between 70.0% and 99.8% of the correlation energy for the neutral atoms (nine-term correlation function) and 60.8% to 99.1% for selected cations (17-term correlation function). Details are found in Table 6.1.

Our wave function Ψ_1 recovers between 60.0% and 91.0% of the correlation energy for the neutral atoms and 58.8% to 91.3% for the positive ions. Generally, the expectation value contains $\sim 90\%$ of the correlation energy for the 2-3-electron systems and $\sim 61\%$ for the systems consisting of four and more electrons. From this perspective, Ψ_1 is reasonably good, especially considering its relative simplicity.

Not intending to reproduce ionization potentials, Alexander and Coldwell used wave functions with different flexibility for atoms and ions. For this reason, the estimates of ionization potentials based on their results are not as accurate as those computed by Moskowitz and Schmidt [37] who used wave functions of the same type with 9 parameters both for the ions and neutral atoms. To our knowledge Moskowitz and Schmidt's values are the best VMC estimates of ionization potential available at the present time (with

Introduction and Overview

1.1. *Abstract: This chapter provides an overview of the book's content and structure.*

This book is a comprehensive guide to the field of computer science. It covers the fundamentals of computer science, including the history of computing, the architecture of computers, and the principles of programming. The book is divided into several parts, each focusing on a different aspect of the field. The first part, "Introduction and Overview," provides a general introduction to the field and outlines the structure of the book. The second part, "Fundamentals of Computer Science," covers the basic concepts and principles of computer science. The third part, "Programming," discusses the various programming languages and paradigms used in computer science. The fourth part, "Computer Architecture," explores the internal structure of computers and the flow of data and instructions. The fifth part, "Computer Systems," examines the various components and subsystems of a computer system. The sixth part, "Computer Networks," discusses the principles of network communication and the various types of networks. The seventh part, "Computer Security," addresses the threats to computer systems and the measures taken to protect them. The eighth part, "Computer Applications," shows how computer science is applied in various fields, such as business, science, and education. The final part, "Conclusion," summarizes the key points of the book and provides a final overview of the field.

The book is written for students and professionals alike. It is suitable for use as a textbook in a computer science course, or as a reference for those working in the field. The book is written in a clear and concise style, with many examples and exercises to help readers understand the concepts. The book is also up-to-date, covering the latest developments in the field of computer science.

The book is organized into eight main parts, each with its own set of chapters. The first part, "Introduction and Overview," contains two chapters: "Introduction" and "Overview." The second part, "Fundamentals of Computer Science," contains three chapters: "History of Computing," "Computer Architecture," and "Computer Systems." The third part, "Programming," contains four chapters: "Programming Languages," "Paradigms," "Data Structures," and "Algorithms." The fourth part, "Computer Architecture," contains two chapters: "Internal Structure of Computers" and "Flow of Data and Instructions." The fifth part, "Computer Systems," contains three chapters: "Operating Systems," "File Systems," and "Database Systems." The sixth part, "Computer Networks," contains two chapters: "Network Communication" and "Types of Networks." The seventh part, "Computer Security," contains two chapters: "Threats to Computer Systems" and "Measures to Protect Them." The eighth part, "Computer Applications," contains three chapters: "Business Applications," "Science Applications," and "Education Applications." The final part, "Conclusion," contains one chapter: "Summary and Final Overview." The book is written in a clear and concise style, with many examples and exercises to help readers understand the concepts. The book is also up-to-date, covering the latest developments in the field of computer science.

System	E	$\%E_{corr}$	\bar{r}^a
Li (2S)	-7.4766(2)	97.6	1.721(2)
Li ⁺ (1S)	-7.2795(1)	99.1	0.5725(5)
Be (1S)	-14.639(2)	70.0	1.579(1)
Be ⁺ (2S)	-14.3189(4)	87.7	1.061(1)
B (2P)	-24.6174(5)	70.7	1.373(1)
C (3P)	-37.805(1)	74.4	1.200(1)
C ⁺ (2P)	-37.3850(9)	66.9	0.9976(8)
N (4S)	-54.552(3)	80.1	1.0577(9)
N ⁺ (3P)	-54.011(1)	73.7	0.9198(7)
O (3P)	-75.018(2)	80.9	0.9648(9)
O ⁺ (4S)	-74.527(2)	79.5	0.8359(7)
F (2P)	-99.689(3)	86.9	0.8737(7)
F ⁺ (3P)	-99.035(2)	78.6	0.7731(6)
Ne (1S)	-128.895(3)	89.2	0.7905(6)
Ne ⁺ (2P)	-128.095(3)	85.4	0.7157(6)

^a normalized to one electron

Table 6.1: Selected properties of the first-row atomic systems estimated by Alexander and Coldwell [35]. Total energies E_1 (a.u.), average electron-nuclear distance \bar{r} per electron.

the exception of Be comparable or better than IP's based on CI-SD [38]).

Performance of Ψ_1 on ionization potentials is of rather mediocre quality (see Tables 5.11 and 6.3). It is not surprising that the IP's of Schmidt and Moskowitz are better than those obtained with Ψ_1 , considering that electron-electron correlation factors and basis sets in their wave functions are much more complex than ours.

The conspicuous deviation of the IP for Be computed with Ψ_1 as compared to the exact value is observed because a single determinant cannot describe adequately non-dynamic correlation in the ground state of beryllium atom.

We consider the failure to obtain satisfactory estimates of the ground state energy levels of the negative ions and thereby the electron affinities to be another indication of insufficient flexibility of the electron correlation factor (2.4) and the small basis set.

6.2 Calculations with the Partitioned Functions

6.2.1 Wave function Ψ_2 : The loss of core-valence antisymmetry

The loss of core-valence antisymmetry represented by wave function Ψ_2 results in an increase of the total energy by amounts from nearly zero for Li to more than 0.3 hartree for Ne (see the lower plots in Figs. 5.1 and 5.2). In the valid wave function Ψ_1 , collapse of valence electrons does not occur because the determinants of Ψ_1 ensure antisymmetry. In Ψ_2 , which does not possess this property, the collapse is prevented by orthogonalization of the core and valence wave functions. However, the orthogonality does not substitute the antisymmetry: in fact it places the total energy E_2 above E_1 (see Tables 5.10 and 5.10).

The rapid increase of $\Delta E_{21} \equiv E_2 - E_1$ through the series Li–Ne is plausibly due to the fact that Ψ_2 is a ‘truncated expansion’ of Ψ_1 . The *proportion of missing terms increases rapidly as the number of electrons gets larger*, so that Ψ_2 becomes more and more deficient with the increase of n . The relative magnitude of the effect increases at a slower pace to reach $\sim 2.5\%$ of the total energy in the case of the Ne atom.

Performance of Ψ_2 is inferior with respect to that of Ψ_1 not only for the total energies. An obvious worsening is observed for the ionization potentials (see Fig. 5.4). Significantly, the core energies for atoms and respective ions differ by up to 0.02 hartree, which is a noticeable change.

6.2.2 Wave function Ψ_2 : The core-valence overlap

The approach to studying the core-valence overlap effect, as outlined above, was applied to several atomic systems, including boron, carbon, nitrogen and oxygen. We report only calculations on the nitrogen atom, because the results for the other systems are very similar except they are at a different level of the energy scale. The most remarkable features of the plot shown in Fig. 5.3 are the strong (quadratic) dependence of the total

1.1. Introduction and Overview

1.1.1. The Role of the Overview and Introduction

The role of the overview and introduction is to provide a high-level summary of the entire document. It is the first section that the reader encounters, and it sets the stage for the rest of the document. The overview and introduction should be written in a clear, concise, and engaging manner. It should provide a brief history of the project, the goals and objectives, and the scope of the work. It should also identify the key stakeholders and the roles of the team members. The overview and introduction should be written in a way that is easy to read and understand. It should be written in a way that is interesting and engaging. It should be written in a way that is informative and useful. The overview and introduction should be written in a way that is clear and concise. It should be written in a way that is easy to read and understand. It should be written in a way that is interesting and engaging. It should be written in a way that is informative and useful. The overview and introduction should be written in a way that is clear and concise. It should be written in a way that is easy to read and understand. It should be written in a way that is interesting and engaging. It should be written in a way that is informative and useful.

The overview and introduction should be written in a way that is clear and concise. It should be written in a way that is easy to read and understand. It should be written in a way that is interesting and engaging. It should be written in a way that is informative and useful.

The overview and introduction should be written in a way that is clear and concise. It should be written in a way that is easy to read and understand. It should be written in a way that is interesting and engaging. It should be written in a way that is informative and useful. The overview and introduction should be written in a way that is clear and concise. It should be written in a way that is easy to read and understand. It should be written in a way that is interesting and engaging. It should be written in a way that is informative and useful.

1.1.2. The Role of the Overview and Introduction

The role of the overview and introduction is to provide a high-level summary of the entire document. It is the first section that the reader encounters, and it sets the stage for the rest of the document. The overview and introduction should be written in a clear, concise, and engaging manner. It should provide a brief history of the project, the goals and objectives, and the scope of the work. It should also identify the key stakeholders and the roles of the team members. The overview and introduction should be written in a way that is easy to read and understand. It should be written in a way that is interesting and engaging. It should be written in a way that is informative and useful. The overview and introduction should be written in a way that is clear and concise. It should be written in a way that is easy to read and understand. It should be written in a way that is interesting and engaging. It should be written in a way that is informative and useful.

energy on the overlap Q , and a shift of the symmetry axis of the parabola to the right with respect to the zero overlap vertical by amounts ranging approximately from 0.1 to 0.2 depending on the atom. The E_2 vs. Q dependence is obviously quadratic (the value of the squared correlation coefficient was found to be $r^2 = 0.9993$). Thus, the total energy is very sensitive to the accuracy of core-valence orthogonality, but a non-zero overlap does not mean necessarily a lower energy expectation value. The question whether calculations with inexactly orthogonal Ψ_{core} and Ψ_{val} are still capable of yielding correct *energy differences* remains open.

6.2.3 Wave function Ψ_3 : The effect of core-valence correlation

Further elevation of the total energy occurs after removing the core-valence correlation terms — the effect which is modeled with the wave function Ψ_3 . Inspection of Figs. 5.1 and 5.2 reveals that a loss in the correlation energy $\Delta E_{32} \equiv E_3 - E_2$ resulting from the transition from Ψ_2 to Ψ_3 is relatively small compared to ΔE_{21} and is fairly constant through the series constituting approximately 0.01 hartree for atoms and 0.03–0.04 hartree for the ions.

It has been pointed out in the literature that “any calculation following core-valence partitioning can never be better than the accuracy with which the interactions between core and valence electrons are treated” [15]. Our result $E_1 < E_2 < E_3$, where respective functions Ψ_1 – Ψ_3 have comparable flexibility, agrees with that conclusion.

On the other hand, it is surprising that Ψ_3 -estimates of ionization potentials are very close to the exact values: in fact, far closer than the IP’s based on Ψ_1 . Formally, the improvement occurs because separating the Jastrow correlation function increases the total energy by a larger amount for the ions than for the neutral atoms. As a result, the difference $IP = E(A^+) - E(A)$ approaches the exact values. A plausible explanation for this is that while the average distances of core electrons from the nucleus are almost the

Let \mathcal{H} be a Hilbert space. A linear operator T on \mathcal{H} is called self-adjoint if $T = T^*$, where T^* is the adjoint of T . If T is self-adjoint, then $\langle T\phi, \psi \rangle = \langle \phi, T\psi \rangle$ for all $\phi, \psi \in \mathcal{H}$. The spectral theorem for self-adjoint operators states that if T is self-adjoint, then there exists a unique spectral measure E_T on the Borel subsets of \mathbb{R} such that $T = \int_{\mathbb{R}} \lambda dE_T(\lambda)$. This theorem is fundamental in the study of quantum mechanics, where self-adjoint operators represent physical observables.

1.1. THE SPECTRAL THEOREM FOR SELF-ADJOINT OPERATORS

Let \mathcal{H} be a Hilbert space and T a self-adjoint operator on \mathcal{H} . The spectral theorem for self-adjoint operators states that there exists a unique spectral measure E_T on the Borel subsets of \mathbb{R} such that $T = \int_{\mathbb{R}} \lambda dE_T(\lambda)$. This theorem is fundamental in the study of quantum mechanics, where self-adjoint operators represent physical observables.

Let \mathcal{H} be a Hilbert space and T a self-adjoint operator on \mathcal{H} . The spectral theorem for self-adjoint operators states that there exists a unique spectral measure E_T on the Borel subsets of \mathbb{R} such that $T = \int_{\mathbb{R}} \lambda dE_T(\lambda)$. This theorem is fundamental in the study of quantum mechanics, where self-adjoint operators represent physical observables.

Let \mathcal{H} be a Hilbert space and T a self-adjoint operator on \mathcal{H} . The spectral theorem for self-adjoint operators states that there exists a unique spectral measure E_T on the Borel subsets of \mathbb{R} such that $T = \int_{\mathbb{R}} \lambda dE_T(\lambda)$. This theorem is fundamental in the study of quantum mechanics, where self-adjoint operators represent physical observables.

same for atoms and ions, the valence electrons in ions are on the average closer to the core than they are in atoms. The stronger Coulombic core-valence interaction in the ions thus increases the total energy of the system by a larger amount than in the atoms.

6.2.4 Wave functions Ψ_4 and Ψ_5 : Improving electron correlation

In wave function Ψ_3 the electron-electron correlation factor $J_c J_v$ includes only interelectronic distances of the types *core-core* and *valence-valence*, but for the sake of comparison with Ψ_1 and Ψ_2 the variational parameter b is constrained to the same value in J_c and J_v . Releasing this constraint we introduced the wave function Ψ_4 . As evident from Table 5.9, this does not lead to a substantial change in the total energy, although new parameters b_c and b_v clearly tend to be different (see Table 5.4). However, these small changes result in systematically better IP's (see Table 5.11), especially for the heavier atoms, for which electron correlation is more important.

The wave function Ψ_5 is already flexible enough (it has 5 to 7 parameters) to perform noticeably better than Ψ_2 – Ψ_4 in terms of the total energy and even outdo Ψ_1 for Be and B, thus recovering the increase of energy due to the loss of core-valence antisymmetry.

IP's based on Ψ_5 turn out to be worse than those based on Ψ_4 . The question why re-introducing the core-valence correlation in the Jastrow function has such an effect on the IP's is the central part of the following section.

6.3 Comparative Performance of the Wave Functions

Calculations with the whole set of wave functions Ψ_1 – Ψ_5 provide sufficient material for contributive speculation. First we turn our attention to the concept of a 'constant (frozen) core', which is believed to be not only a reasonable approximation but also the basis for a number of partitioning techniques.

That the core characteristics do not change considerably with the valence environment is confirmed by the observation that in most cases the core energies and electron-nuclear distances \bar{r}_c for the neutral atom and its positive ion differ by less than 0.01 hartree and 0.001 bohr, respectively, the numbers being even lower in the case of Ψ_3 and Ψ_4 . (For the reasons outlined above, the Be atom is an exception).

Furthermore, since the ensembles used in calculations with Ψ_2 – Ψ_5 had the same size, the standard errors allow us to compare the energy variance. Naturally, the variance in the case of complete wave function Ψ_1 is the lowest. For the partitioned wave functions, the result is that the variance of the *total* energy increases in the order

$$\Psi_1 < \Psi_2 \approx \Psi_5 < \Psi_3 \approx \Psi_4,$$

whereas for the variance of E_{core} and constancy of the *core* energy the order is

$$\Psi_4 \approx \Psi_3 < \Psi_5 < \Psi_2,$$

which is exactly the order of decreasing accuracy of ionization potentials! This implies that the most adequate description of the core, associated with the lowest variance, corresponds to the ‘most partitioned’ wave function Ψ_4 . Thus the approximate constancy of the core is not only a physically meaningful notion, it is a condition under which valence-electron-only calculations should succeed.

We argue that the constancy of the core is affected by core-valence correlation terms in the Jastrow function in that removal of these terms leads to a more thorough separation of Ψ_{core} and Ψ_{val} , resulting in more accurate estimates of the properties of valence electrons. Indeed, this idea is supported by a repetitive pattern in the observations: the pair Ψ_5 – Ψ_4 , where Ψ_4 does not include core-valence electron correlation terms yet performs much better on IP’s, is analogous to the pair Ψ_2 – Ψ_3 , where core-valence uncorrelated Ψ_3 gives considerably more accurate estimates of ionization potentials.

When there is a perceptible change in the energy of the core from neutral atom to the ion (as in the cases of Ψ_2 and Ψ_5), the IP determined as a difference of the valence energies is almost without exception worse than that based on the total energies (Tables 5.11 and 5.12). Naturally, for Ψ_3 and Ψ_4 , which provide essentially constant cores, there is almost no difference between I^{tot} and I^{val} .

Assuming that in systems described with partitioned wave functions, removal of one valence electron is followed by a certain restructuring of the core, one might expect that the change in the core would affect the valence energy such that I^{val} is closer to the exact values than I^{tot} . The fact that we do not observe this effect suggests once again that the constancy of the atomic core is indeed a real feature of partitioned systems.

Accuracy of ionization potentials found from the total energies can be regarded as a measure of quality of a wave functions Ψ_i . Quantitatively, we can compare the sums of absolute deviations of the ionization potentials found with Ψ_i from the exact values. We define this quantity $\sigma(I_{\Psi_i})$ as follows

$$\sigma(I_{\Psi_i}) = \sum_{Z=5}^{10} |I_{\Psi_i}(Z) - I_{\text{exact}}(Z)|, \quad (6.1)$$

with Li and Be excluded for the reasons explained above. The values of $\sigma(I_{\Psi_i})$ for Ψ_1 – Ψ_5 and the wave function of Schmidt and Moskowitz are presented in Table 6.2¹.

Wave function	Ψ_1	Ψ_2	Ψ_3	Ψ_4	Ψ_5	Ψ_{SM}
$\sigma(I_{\Psi_i})$	0.1024(12)	0.2236(17)	0.0457(23)	0.0273(23)	0.1034(17)	0.0216(21)

Table 6.2: Accuracy of the ionization potentials estimated with various wave functions as a sum of absolute deviations from the exact values. Ψ_{SM} is the wave function of Schmidt and Moskowitz [37].

The benefits of the partitioning scheme represented by wave function Ψ_4 becomes

¹Propagation of error in a quantity z defined by the expression $z = \sum_i |x_i \pm \Delta x_i|$ is estimated as $\Delta z = \sqrt{\sum_i (\Delta x_i)^2}$.

evident from comparison of I_{Ψ_4} with the literature values based on sophisticated modern all-electron *ab initio* calculations. Exact (non-relativistic, Born–Oppenheimer) IP values are given in Table 5.11. In Table 6.3 we cite selected reference estimates of the ionization potentials, viz. those based on Hartree–Fock calculations, VMC calculations by Alexander and Coldwell, Schmidt and Moskowitz, CI-SD, and CCSD(T) calculations. Graphical representation of comparative accuracy of the best IP's obtained in this (those with Ψ_4) and the literature values are presented in Fig. 6.1.

Atom	I_{Ψ_4}	I_{HF}^a	I_{VMC}^b	I_{VMC}^c	$I_{\text{CI-SD}}^d$	$I_{\text{CCSD(T)}}^e$	I_{exptl}^f
Li	0.1872(1)	0.19632	0.1971(2)	0.1936(6)	0.1963	0.1974	0.19814
Be	0.3311(2)	0.29563	0.320(2)	0.3141(8)	0.3415	0.3417	0.34260
B	0.3056(4)	0.29149	-	0.307(1)	0.3006	0.3026	0.30494
C	0.4179(6)	0.39639	0.420(2)	0.415(1)	0.4100	0.4120	0.41380
N	0.5362(8)	0.51293	0.541(3)	0.5319(6)	0.5311	0.5329	0.53412
O	0.4972(9)	0.43677	0.491(3)	0.4898(6)	0.4898	0.4942	0.50045
F	0.633(1)	0.57760	0.654(4)	0.639(1)	0.6296	0.6347	0.64027
Ne	0.785(1)	0.72928	0.800(4)	0.7977(6)	0.7826	-	0.79248

^a Reference [33]

^d Reference [38]

^b Alexander and Coldwell [35]

^e Reference [39]

^c Moskowitz and Schmidt [37]

^f Reference [40]

Table 6.3: Ionization potentials (a.u.) by various methods.

Comparison shows that the IP's obtained with wave function Ψ_4 are competitive with the best VMC calculations, CI-SD, and even CCSD(T) (see Fig. 6.1) both in terms of accuracy and precision.

It should be mentioned that the cases of Li and Be atoms are special. For the lithium cation, all the partitioned wave functions are identical to $\Psi_1(\text{Li}^+)$, whereas the atomic functions are different. It is therefore inconsistent to compare IP's for Li computed with the partitioned and non-partitioned wave functions, although formally the former IP's

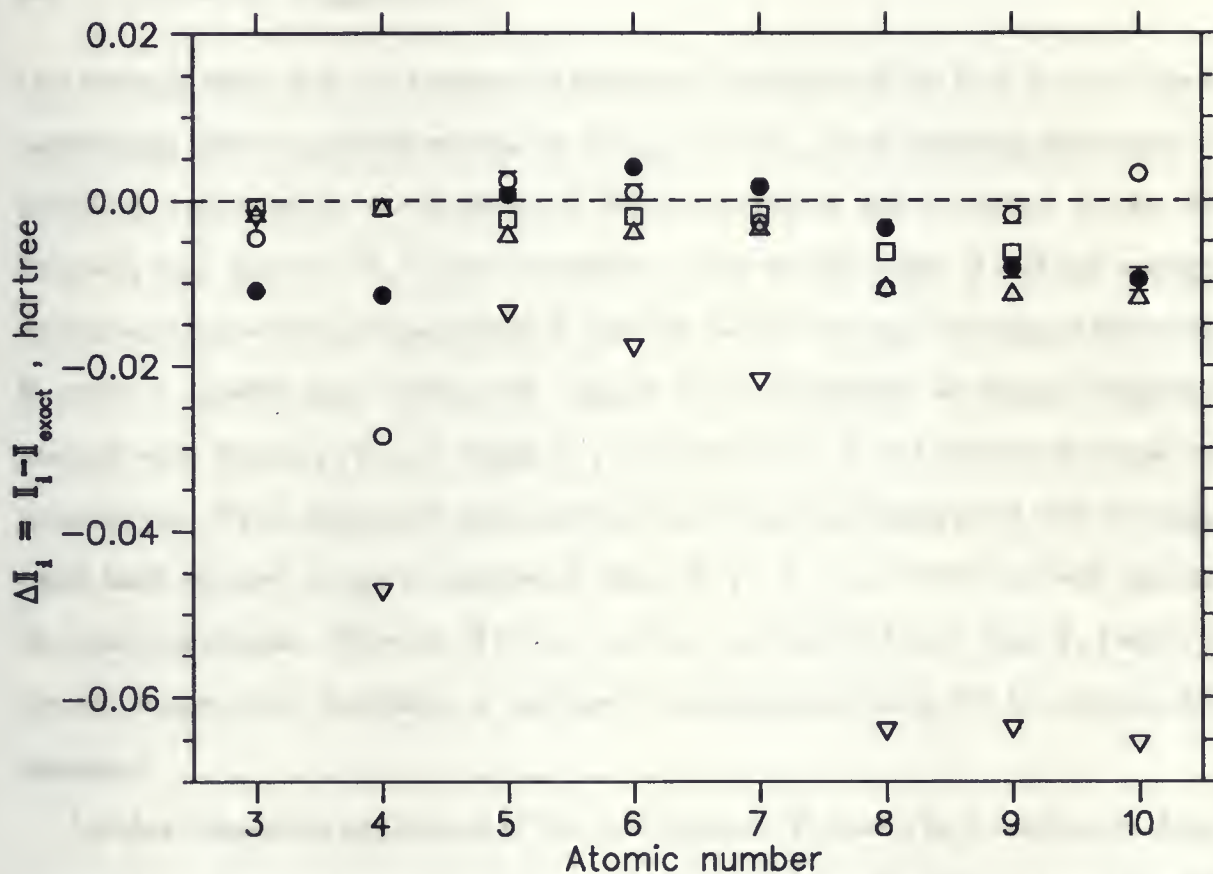


Figure 6.1: Comparison of the accuracy of ionization potentials computed using partitioned wave function Ψ_4 with the IP's from conventional methods. \bullet : ΔI based on Ψ_4 , \circ : best available VMC calculations [37] (Schmidt and Moskowitz), \square : CCSD(T) [39], \triangle : CI-SD calculations [38], ∇ : ΔI based on SCF values [33].



Figure 1. Frequency dependence of the static dielectric function $\epsilon_s(\omega)$ for the CaTiO_3 perovskite. The data were obtained from the experimental data of $\epsilon_s(\omega)$ and ϵ_∞ reported by CaTiO_3 [10]. The solid line is the calculated curve of $\epsilon_s(\omega)$ from the experimental data of $\epsilon_s(\omega)$ and ϵ_∞ reported by CaTiO_3 [10].

are defined. In the case of beryllium, the reason is the above-mentioned inadequacy of a single-determinantal wave function.

6.4 Comments, Suggestions

Our findings show that the accuracy of ionization potentials is the best in cases where partitioning allows maximum separation of Ψ_{core} and Ψ_{val} , while retaining their internal flexibility, evidenced by the accuracy of IP's increasing in the succession Ψ_2 – Ψ_3 – Ψ_4 . However, wave function Ψ_4 is *not* the ultimate point in this series: it still has a single electron-nuclear variational parameter v_s , both for the $1s^2$ -core and $2s^2$ -valence electrons. In order to provide more evidence in support of our hypothesis we suggest exploring another wave function (Ψ_6), in which v_s parameters for core and valence electrons are independent. We do not expect rather unrealistically that Ψ_6 , constructed with the same small basis set and primitive Jastrow as those in Ψ_1 – Ψ_4 , will outdo the best modern *ab initio* calculations. However, if it does perform perceptibly better than Ψ_4 (which is already competitive) credibility of our most important conclusion will be considerably enhanced.

Another interesting application of the wave function Ψ_4 would be a calculation of the negative ions. One can assume that Ψ_4 should be much better for this purpose than Ψ_1 as the case is with the ionization potentials. However, to obtain competitive results it may be necessary to extend the basis set and/or the correlation function.

6.5 Conclusions

We have shown that all-electron partitioning of a complete wave function into core and valence parts in orbital space results in noticeable deterioration in the values of total energies.

The largest error of the partitioning is a loss of antisymmetry of the wave function with respect to interchange of core and valence electrons. Its absolute value increases rapidly with the number of electrons, but relative to the total energy remains virtually constant at the level of about 2 per cent.

The error introduced by neglect of the core-valence correlation is comparatively large for the smaller atoms but definitely smaller than the loss of antisymmetry error for the heavier ones. Its absolute value appears to be almost constant through the first row.

Release of the core-valence orthogonality condition may lead to an increase or decrease in the total energy within a range of small overlaps. Beyond that range the valence electrons collapse into core orbitals.

Provided the core-valence orthogonality is maintained, partitioned wave functions may perform very well on energy differences such as ionization potentials. The decisive factors are: (i) maximum separation (independence) of core and valence shells, accompanied by (ii) high internal flexibility of Ψ_{core} and Ψ_{val} . In those cases, constancy of the atomic core is a good approximation at least with respect to the core energy and the average distance of core electrons from the nucleus.

The first thing I noticed when I stepped out of the plane was the air. It was thick and heavy, like a blanket. The sun was shining brightly, but it felt like it was trying to burn me. I had heard that the weather was bad, but I didn't expect it to be this hot.

I had heard that the weather was bad, but I didn't expect it to be this hot. The sun was shining brightly, but it felt like it was trying to burn me. I had heard that the weather was bad, but I didn't expect it to be this hot. The sun was shining brightly, but it felt like it was trying to burn me.

The sun was shining brightly, but it felt like it was trying to burn me. I had heard that the weather was bad, but I didn't expect it to be this hot. The sun was shining brightly, but it felt like it was trying to burn me.

I had heard that the weather was bad, but I didn't expect it to be this hot. The sun was shining brightly, but it felt like it was trying to burn me. I had heard that the weather was bad, but I didn't expect it to be this hot. The sun was shining brightly, but it felt like it was trying to burn me.

The sun was shining brightly, but it felt like it was trying to burn me. I had heard that the weather was bad, but I didn't expect it to be this hot. The sun was shining brightly, but it felt like it was trying to burn me. I had heard that the weather was bad, but I didn't expect it to be this hot. The sun was shining brightly, but it felt like it was trying to burn me.

Appendix A

The Wave Function as a Product of Slater Determinants

In this appendix we show that a wave function Ψ_D written in the general case as the full unnormalized, unrestricted, open-shell Slater determinant of n spin-orbitals

$$\Psi_D = | \chi_1(1) \chi_2(2) \dots \chi_{n^\uparrow}(n^\uparrow) \bar{\chi}'_1(n^\uparrow+1) \bar{\chi}'_2(n^\uparrow+2) \dots \bar{\chi}'_{n^\downarrow}(n^\uparrow+n^\downarrow) |, \quad (\text{A.1})$$

where $n^\uparrow + n^\downarrow = n$, gives the same variational energy as the wave function $\psi_D^{\uparrow\downarrow}$ written as the (unnormalized) product of two separate Slater determinants of *spatial* orbitals for n^\uparrow spin-up and n^\downarrow spin-down electrons

$$\begin{aligned} \psi_D^{\uparrow\downarrow} &= \psi_D^\uparrow \psi_D^\downarrow \\ &= | \phi_1(1) \phi_2(2) \dots \phi_{n^\uparrow}(n^\uparrow) | | \phi'_1(n^\uparrow+1) \phi'_2(n^\uparrow+2) \dots \phi'_{n^\downarrow}(n^\uparrow+n^\downarrow) |. \end{aligned} \quad (\text{A.2})$$

The spin-orbitals are space-spin orbital products, as usual

$$\begin{aligned} \chi_j(i) &= \phi_j(i) \alpha(i), \\ \bar{\chi}'_j(i) &= \phi'_j(i) \beta(i), \end{aligned} \quad (\text{A.3})$$

with $\phi_j(i)$ is not necessarily equal to $\phi'_j(i)$.

First we expand Ψ_D using the definition of a determinant

$$\Psi_D = \sum_i^{n!} (-1)^{p_i} \hat{P}_i^n \left\{ \chi_1(1) \chi_2(2) \dots \chi_{n^\uparrow}(n^\uparrow) \bar{\chi}'_1(n^\uparrow+1) \bar{\chi}'_2(n^\uparrow+2) \dots \bar{\chi}'_{n^\downarrow}(n) \right\}, \quad (\text{A.4})$$

where \hat{P}_i^n is an operator generating the i -th permutation of the electron labels 1, 2, ..., n and p_i is the number of transpositions required to obtain this permutation from the natural order (1, 2, ..., n).

##

By virtue of (A.3), Eq. (A.4) is equivalent to the following form

$$\begin{aligned} \Psi_D = & \sum_i^{n!} [(-1)^{p_i} \hat{P}_i^n \{ \phi_1(1) \phi_2(2) \dots \phi_{n^\uparrow}(n^\uparrow) \phi'_1(n^\uparrow+1) \phi'_2(n^\uparrow+2) \dots \phi'_{n^\downarrow}(n) \} \\ & \times \hat{P}_i^n \{ \alpha(1) \alpha(2) \dots \alpha(n^\uparrow) \beta(n^\uparrow+1) \beta(n^\uparrow+2) \dots \beta(n) \}]. \end{aligned} \quad (\text{A.5})$$

An immediate observation is that not all $n!$ permutations \hat{P}_i^n of electron labels in the product of spin functions are different. Indeed, any interchange of labels of two electrons with like spins leaves the product of spin functions unchanged, although it produces a new permutation of spatial orbitals. Each of the n^\uparrow spin-up electrons can be assigned any label ranging from 1 to n . A complete set of labels for the spin-up electrons uniquely determines the assignment of labels to the n^\downarrow spin-down ones. Thus the number of *distinct* products of spin functions α and β is equal to the number of combinations

$$C_n^{n^\uparrow} = C_n^{n^\downarrow} = \frac{n!}{(n^\uparrow)! (n - n^\uparrow)!} = \frac{n!}{(n^\uparrow)! (n^\downarrow)!}. \quad (\text{A.6})$$

Factoring out the products of spin-functions we obtain the sum of $C_n^{n^\uparrow}$ terms

$$\begin{aligned} \Psi_D = & (-1)^0 [\alpha(1) \alpha(2) \dots \alpha(n^\uparrow) \beta(n^\uparrow+1) \beta(n^\uparrow+2) \dots \beta(n)] \\ & \times \sum_i^{(n^\uparrow)!} (-1)^{p_i} \hat{P}_i^{n^\uparrow} \{ \phi_1(1) \phi_2(2) \dots \phi_{n^\uparrow}(n^\uparrow) \} \\ & \times \sum_j^{(n^\downarrow)!} (-1)^{p_j} \hat{P}_j^{n^\downarrow} \{ \phi'_1(n^\uparrow+1) \phi'_2(n^\uparrow+2) \dots \phi'_{n^\downarrow}(n) \} \\ & + (-1)^1 [\alpha(n^\uparrow+1) \alpha(2) \dots \alpha(n^\uparrow) \beta(1) \beta(n^\uparrow+2) \dots \beta(n)] \\ & \times \sum_i^{(n^\uparrow)!} (-1)^{p_i} \hat{P}_i^{n^\uparrow} \{ \phi_1(n^\uparrow+1) \phi_2(2) \dots \phi_{n^\uparrow}(n^\uparrow) \} \\ & \times \sum_j^{(n^\downarrow)!} (-1)^{p_j} \hat{P}_j^{n^\downarrow} \{ \phi'_1(1) \phi'_2(n^\uparrow+2) \dots \phi'_{n^\downarrow}(n) \} \\ & + \dots, \end{aligned} \quad (\text{A.7})$$

where the sign $(-1)^{p_k}$ is determined by evenness of the permutation of electron labels in the product of spin functions.

Now the linear combinations of permutations of the products of spatial orbitals appearing in (A.7) are Slater determinants for the respective electrons. Denoting the determinants in the k -th term by D_k^\uparrow and D_k^\downarrow and the respective spin permutation by $(-1)^{p_k} \sigma_k^n$, we introduce the following shorthand for (A.7)

$$\Psi_D = \sum_k^{C_n^\uparrow} (-1)^{p_k} \sigma_k^n D_k^\uparrow D_k^\downarrow. \quad (\text{A.8})$$

Comparing (A.2) with (A.7) we note that D^\uparrow and D^\downarrow in the first term of expansion (A.8) are identical to the Slater determinants appearing in (A.2),

$$\begin{aligned} D_1^\uparrow &= \sum_i^{(n^\uparrow)!} (-1)^{p_i} \hat{P}_i^{n^\uparrow} \{ \phi_1(1) \phi_2(2) \dots \phi_{n^\uparrow}(n^\uparrow) \} = \psi_D^\uparrow, \\ D_1^\downarrow &= \sum_j^{(n^\downarrow)!} (-1)^{p_j} \hat{P}_j^{n^\downarrow} \{ \phi'_1(n^\uparrow+1) \phi'_2(n^\uparrow+2) \dots \phi'_{n^\downarrow}(n) \} = \psi_D^\downarrow. \end{aligned} \quad (\text{A.9})$$

Thus all possible permutations of $\psi_D^{\uparrow\downarrow} = \psi_D^\uparrow \psi_D^\downarrow$ are present in the spatial part of the full wave function Ψ_D .

Now consider the expressions for the expectation value of energy with $\psi_D^{\uparrow\downarrow}$ (A.2) and Ψ_D (A.8). The former is

$$E[\psi_D^{\uparrow\downarrow}] = \frac{\langle \psi_D^{\uparrow\downarrow} | \hat{H} | \psi_D^{\uparrow\downarrow} \rangle}{\langle \psi_D^{\uparrow\downarrow} | \psi_D^{\uparrow\downarrow} \rangle} = \frac{\langle D_1^\uparrow D_1^\downarrow | \hat{H} | D_1^\uparrow D_1^\downarrow \rangle}{\langle D_1^\uparrow D_1^\downarrow | D_1^\uparrow D_1^\downarrow \rangle} = \frac{N^2 E}{N^2} = E, \quad (\text{A.10})$$

where N^2 is a certain factor arising because $\psi_D^{\uparrow\downarrow}$ is not normalized.

When deriving the expression for the latter, $E[\Psi_D]$, we keep in mind that (i) the terms in the sum (A.8) differ only by electron labels which are dummy variables in integration; (ii) the spin parts of wave function Ψ_D are not affected by \hat{H} , and (iii) the spin functions are orthonormal:

$$\langle \sigma_k^n | \sigma_l^n \rangle = \begin{cases} 1 & \text{if } k = l \\ 0 & \text{if } k \neq l. \end{cases} \quad (\text{A.11})$$

The consequence is

$$\begin{aligned}
 \langle (-1)^{p_k} \sigma_k^n D_k^\uparrow D_k^\downarrow | \hat{H} | (-1)^{p_l} \sigma_l^n D_l^\uparrow D_l^\downarrow \rangle &= (-1)^{p_k+p_l} \langle \sigma_k^n | \sigma_l^n \rangle \langle D_k^\uparrow D_k^\downarrow | \hat{H} | D_l^\uparrow D_l^\downarrow \rangle \\
 &= \begin{cases} \langle D_k^\uparrow D_k^\downarrow | \hat{H} | D_l^\uparrow D_l^\downarrow \rangle & \text{if } k = l \\ 0 & \text{if } k \neq l \end{cases} \\
 \langle (-1)^{p_k} \sigma_k^n D_k^\uparrow D_k^\downarrow | (-1)^{p_l} \sigma_l^n D_l^\uparrow D_l^\downarrow \rangle &= (-1)^{p_k+p_l} \langle \sigma_k^n | \sigma_l^n \rangle \langle D_k^\uparrow D_k^\downarrow | D_l^\uparrow D_l^\downarrow \rangle \\
 &= \begin{cases} \langle D_k^\uparrow D_k^\downarrow | D_l^\uparrow D_l^\downarrow \rangle & \text{if } k = l \\ 0 & \text{if } k \neq l \end{cases}
 \end{aligned}$$

Since all spatial terms in (A.7) differ only by labeling the n electrons,

$$\begin{aligned}
 \langle D_k^\uparrow D_k^\downarrow | \hat{H} | D_k^\uparrow D_k^\downarrow \rangle &= \langle D_l^\uparrow D_l^\downarrow | \hat{H} | D_l^\uparrow D_l^\downarrow \rangle = N^2 E, \\
 \langle D_k^\uparrow D_k^\downarrow | D_k^\uparrow D_k^\downarrow \rangle &= \langle D_l^\uparrow D_l^\downarrow | D_l^\uparrow D_l^\downarrow \rangle = N^2,
 \end{aligned}$$

we obtain

$$E[\Psi_D] = \frac{\langle \Psi_D | \hat{H} | \Psi_D \rangle}{\langle \Psi_D | \Psi_D \rangle} = \frac{\sum_k^{C_n^{\uparrow\downarrow}} \langle D_k^\uparrow D_k^\downarrow | \hat{H} | D_k^\uparrow D_k^\downarrow \rangle}{\sum_k^{C_n^{\uparrow\downarrow}} \langle D_k^\uparrow D_k^\downarrow | D_k^\uparrow D_k^\downarrow \rangle} = \frac{C_n^{\uparrow\downarrow} N^2 E}{C_n^{\uparrow\downarrow} N^2} = E \quad (\text{A.12})$$

Thus

$$E[\psi_D^{\uparrow\downarrow}] = E[\Psi_D] = E. \quad (\text{A.13})$$

Unlike the expectation values $E[\psi_D^{\uparrow\downarrow}]$ and $E[\Psi_D]$, the local energies $E_L(\Psi_D)$ and $E_L(\psi_D^{\uparrow\downarrow})$ as well as probability distributions from which they are sampled will be, of course, different.

Appendix B

Cusp Conditions

The cusp conditions should be imposed on wave functions in order to eliminate singularities in the local energy and thereby control the variance. Two types of pairs of charged particles are possible: electron-nuclear and electron-electron pairs. Correspondingly, we consider *electron-nuclear* and *electron-electron* cusp conditions.

B.1 Electron-nuclear cusp conditions

B.1.1 General electron-nuclear cusp conditions

Consider a many-electron system described with a wave function ψ . The total Hamiltonian operator can be written as the sum of one-electron Hamiltonians

$$\hat{H} = \sum_i^n \hat{H}_i = \sum_i^n \left[-\frac{1}{2} \nabla_i^2 - \frac{Z}{r_i} + \frac{1}{2} \sum_{j \neq i}^n \frac{1}{r_{ij}} \right]. \quad (\text{B.1})$$

To treat the electron-nuclear interaction singularities, we need not consider the interelectronic interaction terms. Ignoring these, the contribution to the local energy from electron i is

$$-\frac{1}{2} \frac{\nabla_i^2 \psi}{\psi} - \frac{Z}{r_i}. \quad (\text{B.2})$$

When electron i approaches the nucleus ($r_i \rightarrow 0$) there arises a singularity in the potential energy term ($-Z/r_i$). This singularity is cancelled out if the kinetic energy term gives in the limit $r_i \rightarrow 0$ an equal term with the opposite sign ($+Z/r_i$). The requirement that the

Problem 2

Part (a)

The first condition is that the number of variables is even. The second condition is that the number of variables is greater than or equal to the number of equations. The third condition is that the number of variables is greater than or equal to the number of equations.

(b) The first condition is that the number of variables is even.

(c) The first condition is that the number of variables is even.

The first condition is that the number of variables is even. The second condition is that the number of variables is greater than or equal to the number of equations. The third condition is that the number of variables is greater than or equal to the number of equations.

$$(d) \quad \frac{1}{2} \left(\frac{3}{2} + \frac{7}{2} \right) = \frac{5}{2} \quad \frac{1}{2} \left(\frac{3}{2} + \frac{7}{2} \right) = \frac{5}{2}$$

The first condition is that the number of variables is even. The second condition is that the number of variables is greater than or equal to the number of equations. The third condition is that the number of variables is greater than or equal to the number of equations.

$$(e) \quad \frac{1}{2} \left(\frac{3}{2} + \frac{7}{2} \right) = \frac{5}{2} \quad \frac{1}{2} \left(\frac{3}{2} + \frac{7}{2} \right) = \frac{5}{2}$$

The first condition is that the number of variables is even. The second condition is that the number of variables is greater than or equal to the number of equations. The third condition is that the number of variables is greater than or equal to the number of equations.

The first condition is that the number of variables is even. The second condition is that the number of variables is greater than or equal to the number of equations. The third condition is that the number of variables is greater than or equal to the number of equations.

wave function ψ exhibit such behavior near the nucleus imposes the following restriction:

$$\lim_{r_i \rightarrow 0} \frac{\nabla_i^2 \psi}{\psi} = -\frac{2Z}{r_i}. \quad (\text{B.3})$$

This is called the *general electron-nuclear cusp condition*.

It turns out that the general cusp condition imposed on the wave function can be split into cusp conditions for individual atomic orbitals.

Consider first an uncorrelated wave function written as a product of Slater determinants of spatial orbitals $\psi = \psi_D^{\uparrow\downarrow} \equiv \psi_D^{\uparrow} \psi_D^{\downarrow}$. Without reference to the spin orientation

$$\psi_D = | \phi_1(r_1) \phi_2(r_2) \cdots \phi_n(r_n) |, \quad (\text{B.4})$$

where the first index represents an orbital, the second a particle.

Expansion of ψ_D in terms of cofactors of the elements of the i -th column gives

$$\psi_D = \sum_j^n \phi_j(r_i) A_{ji}. \quad (\text{B.5})$$

Cofactors A_{ji} do not depend on the coordinates of the i -th electron, so that the contribution from the i -th electron to the kinetic energy term is

$$-\frac{1}{2} \frac{\nabla_i^2 \psi}{\psi} = -\frac{1}{2} \frac{\nabla_i^2 \psi_D}{\psi_D} = -\frac{1}{2} \frac{\sum_j^n [\nabla_i^2 \phi_j(r_i)] A_{ji}}{\sum_j^n \phi_j(r_i) A_{ji}}. \quad (\text{B.6})$$

Now, if each orbital individually satisfies the cusp condition

$$\lim_{r_i \rightarrow 0} \frac{\nabla_i^2 \phi_j(r_i)}{\phi_j(r_i)} = -\frac{2Z}{r_i}, \quad (\text{B.7})$$

then

$$\lim_{r_i \rightarrow 0} \frac{\nabla_i^2 \psi_D}{\psi_D} = \frac{\sum_j^n [-2Z/r_i] \phi_j(r_i) A_{ji}}{\sum_j^n \phi_j(r_i) A_{ji}} = -\frac{2Z}{r_i}. \quad (\text{B.8})$$

Thus for ψ_D to satisfy Eq. (B.3), each orbital must individually satisfy Eq. (B.7).

Now consider a correlated wave function of the form

$$\psi = \psi_D^{\uparrow\downarrow} J(r_i, r_j, r_{ij}). \quad (\text{B.9})$$

is continuous at $t = 0$ and $\lim_{t \rightarrow 0^+} f(t) = f(0)$. The Laplace transform of $f(t)$ is

$$(2.10) \quad \mathcal{L}\{f(t)\} = \int_0^\infty e^{-st} f(t) dt$$

provided the integral converges. The Laplace transform of $f(t)$ is denoted by $F(s)$.

Let $f(t)$ be a function defined for $t \geq 0$. The Laplace transform of $f(t)$ is denoted by $F(s)$.

Let $f(t)$ be a function defined for $t \geq 0$. The Laplace transform of $f(t)$ is denoted by $F(s)$.

Let $f(t)$ be a function defined for $t \geq 0$. The Laplace transform of $f(t)$ is denoted by $F(s)$.

Let $f(t)$ be a function defined for $t \geq 0$. The Laplace transform of $f(t)$ is denoted by $F(s)$.

$$(2.11) \quad \mathcal{L}\{f(t)\} = \int_0^\infty e^{-st} f(t) dt$$

Let $f(t)$ be a function defined for $t \geq 0$. The Laplace transform of $f(t)$ is denoted by $F(s)$.

Let $f(t)$ be a function defined for $t \geq 0$. The Laplace transform of $f(t)$ is denoted by $F(s)$.

$$(2.12) \quad \mathcal{L}\{f(t)\} = \int_0^\infty e^{-st} f(t) dt$$

Let $f(t)$ be a function defined for $t \geq 0$. The Laplace transform of $f(t)$ is denoted by $F(s)$.

Let $f(t)$ be a function defined for $t \geq 0$. The Laplace transform of $f(t)$ is denoted by $F(s)$.

$$(2.13) \quad \mathcal{L}\{f(t)\} = \int_0^\infty e^{-st} f(t) dt$$

Let $f(t)$ be a function defined for $t \geq 0$. The Laplace transform of $f(t)$ is denoted by $F(s)$.

$$(2.14) \quad \mathcal{L}\{f(t)\} = \int_0^\infty e^{-st} f(t) dt$$

Let $f(t)$ be a function defined for $t \geq 0$. The Laplace transform of $f(t)$ is denoted by $F(s)$.

$$(2.15) \quad \mathcal{L}\{f(t)\} = \int_0^\infty e^{-st} f(t) dt$$

Let $f(t)$ be a function defined for $t \geq 0$. The Laplace transform of $f(t)$ is denoted by $F(s)$.

$$(2.16) \quad \mathcal{L}\{f(t)\} = \int_0^\infty e^{-st} f(t) dt$$

The problem here is whether the inclusion of J affects condition (B.7).

One can incorporate the electron-electron correlation factor into determinants by modifying the orbitals constituting the determinants as follows

$$\tilde{\phi}(r_i) = \phi(r_i) J_i = \phi(r_i) \exp \left[\sum_{j \neq i}^n f(r_i, r_j, r_{ij}) \right]. \quad (\text{B.10})$$

This leads to

$$\lim_{r_i \rightarrow 0} \frac{\nabla_i^2 \tilde{\phi}(r_i)}{\tilde{\phi}(r_i)} = \lim_{r_i \rightarrow 0} \left[\frac{\nabla_i^2 \phi(r_i)}{\phi(r_i)} + 2 \frac{\nabla_i \phi(r_i)}{\phi(r_i)} \frac{\nabla_i J_i}{J_i} + \frac{\nabla_i^2 J_i}{J_i} \right]. \quad (\text{B.11})$$

The first term has already been discussed.

The second term

$$\lim_{r_i \rightarrow 0} \frac{\nabla_i \phi(r_i)}{\phi(r_i)} \frac{\nabla_i J_i}{J_i}$$

contains no divergences (it is a scalar product of two vectors of *finite* length).

For the third term, introducing the shorthand $f_{ij} = f(r_i, r_j, r_{ij})$, we obtain

$$\begin{aligned} \frac{\nabla_i^2 J_i}{J_i} &= \frac{1}{J_i} \nabla_i \cdot \nabla_i J_i \\ &= \frac{1}{J_i} \nabla_i \cdot \sum_{j \neq i}^n \left[\frac{\partial f_{ij}}{\partial r_i} \frac{\mathbf{r}_i}{r_i} + \frac{\partial f_{ij}}{\partial r_{ij}} \frac{\mathbf{r}_{ij}}{r_{ij}} \right] \\ &= \left(\sum_{j \neq i}^n \left[\frac{\partial f_{ij}}{\partial r_i} \frac{\mathbf{r}_i}{r_i} + \frac{\partial f_{ij}}{\partial r_{ij}} \frac{\mathbf{r}_{ij}}{r_{ij}} \right] \right)^2 \end{aligned} \quad (\text{B.12})$$

$$+ \sum_{j \neq i}^n \left[\frac{\partial^2 f_{ij}}{\partial r_i^2} + 2 \frac{\partial^2 f_{ij}}{\partial r_i \partial r_{ij}} \frac{\mathbf{r}_i \cdot \mathbf{r}_{ij}}{r_i r_{ij}} + \frac{\partial^2 f_{ij}}{\partial r_{ij}^2} + \frac{\partial f_{ij}}{\partial r_i} \frac{2}{r_i} + \frac{\partial f_{ij}}{\partial r_{ij}} \frac{2}{r_{ij}} \right] \quad (\text{B.13})$$

The only term diverging in the limit $r_i \rightarrow 0$ is

$$\frac{\partial f_{ij}}{\partial r_i} \frac{2}{r_i}. \quad (\text{B.14})$$

If one wants to use an electron-electron correlation function which does not affect the individual orbital cusp conditions, $f(r_i, r_j, r_{ij})$ must satisfy

$$\lim_{r_i \rightarrow 0} \frac{\partial f_{ij}}{\partial r_i} \frac{2}{r_i} = 0. \quad (\text{B.15})$$

It is straightforward to verify that J as given by (2.4) obeys (B.15).

B.1.2 Specific cusp conditions imposed on the atomic orbitals

Applying formulas given in Appendix D one obtains the following relationships

$$\begin{aligned}
 \lim_{r \rightarrow 0} \frac{\nabla_i^2 \phi_{1s}}{\phi_{1s}} &= -\frac{2}{r}(\zeta_1 + w_{1s}) \\
 \lim_{r \rightarrow 0} \frac{\nabla_i^2 \phi_{2s}}{\phi_{2s}} &= -\frac{2}{r}(\zeta_2 + w_{2s} - c) \\
 \lim_{r \rightarrow 0} \frac{\nabla_i^2 \phi_{2p(q_\alpha)}}{\phi_{2p(q_\alpha)}} &= -\frac{4}{r}(\zeta_2 + w_{2p})
 \end{aligned} \tag{B.16}$$

Using (B.7) the individual orbital cusp conditions are immediately found to be¹

Orbital	Cusp condition
ϕ_{1s}	$w_{1s} = Z - \zeta_1$
ϕ_{2s}	$w_{2s} = Z - \zeta_2 + c = Z - \zeta_1, \quad c = \zeta_2 - \zeta_1$
$\phi_{2p(q_\alpha)}$	$w_{2p} = Z/2 - \zeta_2$

(B.17)

The orbitals ϕ_{2s}^\perp (2.10) and ϕ_{2s}' (2.14) are both linear combinations of ϕ_{2s} and ϕ_{1s} . It follows from (B.7) that the cusp conditions for ϕ_{2s}^\perp and ϕ_{2s}' are combinations of cusp conditions (B.17) for the constituting orbitals.

B.2 Electron-electron cusp conditions

Electron-electron cusp conditions are necessary to eliminate singularities of the local energy when two electrons i and j approach each other, i.e. $\mathbf{r}_{ij} \rightarrow 0$ ($\mathbf{r}_{ij} \equiv \mathbf{r}_j - \mathbf{r}_i$).

In a wave function of the form

$$\psi = \psi_D^{\uparrow\downarrow} J, \tag{B.18}$$

¹In the case of ϕ_{2s} , there is an infinite number of ways to select two related parameters w_{2s} and c , so that (B.16) is obeyed. The specific choice here is $w_{2s} = w_{1s} = Z - \zeta_1$, which gives $c = \zeta_2 - \zeta_1$.

where $\psi_D^{\uparrow\downarrow}$ is the determinantal part (product of determinants), the interelectronic distance appears only in the correlation function, which is in the general case as follows

$$J = \exp \left[\sum_{i=1}^{n-1} \sum_{j=i+1}^n f(r_i, r_j, r_{ij}) \right]. \quad (\text{B.19})$$

Consider contributions to the local energy from electron i

$$E_i = -\frac{1}{2} \frac{\nabla_i^2 \psi}{\psi} - \frac{Z}{r_i} + \frac{1}{2} \sum_{j=1}^n \frac{1}{r_{ij}} \quad (\text{B.20})$$

Substitution of $\psi = \psi_D^{\uparrow\downarrow} J$ into (B.20) gives

$$\begin{aligned} E_i &= T_i + V_i = -\frac{1}{2} \frac{\nabla_i^2 \psi_D^{\uparrow\downarrow}}{\psi_D^{\uparrow\downarrow}} - \frac{\nabla_i \psi_D^{\uparrow\downarrow}}{\psi_D^{\uparrow\downarrow}} \frac{\nabla_i J}{J} - \frac{1}{2} \frac{\nabla_i^2 J}{J} - \frac{Z}{r_i} + \frac{1}{2} \sum_{j=1}^n \frac{1}{r_{ij}} \\ &= -\frac{1}{2} \frac{\nabla_i^2 \psi_D^{\uparrow\downarrow}}{\psi_D^{\uparrow\downarrow}} - \sum_{j \neq i}^n \frac{\nabla_i \psi_D^{\uparrow\downarrow}}{\psi_D^{\uparrow\downarrow}} \left(\frac{\partial f_{ij}}{\partial r_i} \frac{\mathbf{r}_i}{r_i} + \frac{\partial f_{ij}}{\partial r_{ij}} \frac{\mathbf{r}_{ij}}{r_{ij}} \right) - \frac{1}{2} \left(\frac{\partial f_{ij}}{\partial r_i} \frac{\mathbf{r}_i}{r_i} + \frac{\partial f_{ij}}{\partial r_{ij}} \frac{\mathbf{r}_{ij}}{r_{ij}} \right)^2 \\ &\quad - \frac{1}{2} \sum_{j \neq i}^n \left(\frac{\partial^2 f_{ij}}{\partial r_i^2} + 2 \frac{\partial^2 f_{ij}}{\partial r_i \partial r_{ij}} \frac{\mathbf{r}_i \cdot \mathbf{r}_{ij}}{r_i r_{ij}} + \frac{\partial^2 f_{ij}}{\partial r_{ij}^2} + \frac{\partial f_{ij}}{\partial r_i} \frac{2}{r_i} + \frac{\partial f_{ij}}{\partial r_{ij}} \frac{2}{r_{ij}} \right) - \frac{Z}{r_i} + \frac{1}{2} \sum_{j=1}^n \frac{1}{r_{ij}}. \end{aligned} \quad (\text{B.21})$$

If electrons i and j approaching each other belong to *different* determinants then $\lim_{r_{ij} \rightarrow 0} \psi_D^{\uparrow\downarrow} \neq 0$, and the only divergent term in the kinetic energy expression is

$$\frac{\partial f_{ij}}{\partial r_{ij}} \frac{1}{r_{ij}}.$$

Since it must cancel the respective term in the potential energy

$$-\frac{1}{2} \frac{1}{r_{ij}}, \quad (\text{B.22})$$

we obtain the following condition

$$\lim_{r_{ij} \rightarrow 0} \frac{\partial f_{ij}}{\partial r_{ij}} = \frac{1}{2}. \quad (\text{B.23})$$

This is the electron-electron cusp condition for two electrons belonging to different determinants. In the case of two-determinant non-partitioned wave functions this means that the two electrons have opposite spins.

If colliding electrons i and j belong to the *same* determinant then $\lim_{r_{ij} \rightarrow 0} \psi_D^{\uparrow\downarrow} = 0$, so that we need to consider the following diverging terms in the kinetic energy

$$\lim_{r_{ij} \rightarrow 0} \left[-\frac{\nabla_i \psi_D^{\uparrow\downarrow}}{\psi_D^{\uparrow\downarrow}} \frac{\partial f_{ij}}{\partial r_{ij}} \frac{\mathbf{r}_{ij}}{r_{ij}} - \frac{\partial f_{ij}}{\partial r_{ij}} \frac{1}{r_{ij}} \right]. \quad (\text{B.24})$$

Expanding $\psi_D^{\uparrow\downarrow}$ in the vicinity of $\mathbf{r}_i = \mathbf{r}_j$

$$\begin{aligned} \psi_D^{\uparrow\downarrow}(\mathbf{r}_i, \mathbf{r}_j, \dots) &= \psi_D^{\uparrow\downarrow}(\mathbf{r}_i, \mathbf{r}_i + \mathbf{r}_{ij}, \dots) \\ &= \psi_D^{\uparrow\downarrow}(\mathbf{r}_i, \mathbf{r}_i = \mathbf{r}_j, \dots) + \mathbf{r}_{ij} \cdot \nabla_i \psi_D^{\uparrow\downarrow}(\mathbf{r}_i, \mathbf{r}_j = \mathbf{r}_i, \dots) + \dots \\ &\approx \mathbf{r}_{ij} \cdot \nabla_i \psi_D^{\uparrow\downarrow} \end{aligned} \quad (\text{B.25})$$

Thus

$$\lim_{r_{ij} \rightarrow 0} \frac{\nabla_i \psi_D^{\uparrow\downarrow}}{\psi_D^{\uparrow\downarrow}} \frac{\partial f_{ij}}{\partial r_{ij}} \frac{\mathbf{r}_{ij}}{r_{ij}} = \lim_{r_{ij} \rightarrow 0} \frac{1}{\mathbf{r}_{ij}} \frac{\partial f_{ij}}{\partial r_{ij}} \frac{\mathbf{r}_{ij}}{r_{ij}} = \lim_{r_{ij} \rightarrow 0} \frac{\partial f_{ij}}{\partial r_{ij}} \frac{1}{r_{ij}}. \quad (\text{B.26})$$

The sum of diverging terms (B.26) in the kinetic energy expression

$$-2 \frac{\partial f_{ij}}{\partial r_{ij}} \frac{1}{r_{ij}} \quad (\text{B.27})$$

will be cancelled by (B.22) if

$$\lim_{r_{ij} \rightarrow 0} \frac{\partial f_{ij}}{\partial r_{ij}} = \frac{1}{4} \quad (\text{B.28})$$

for all pairs of electrons belonging to the same determinant.

In the case of the Jastrow correlation function (2.4),

$$f_{ij} = \frac{a_{ij} r_{ij}}{1 + b r_{ij}}, \quad (\text{B.29})$$

so that the electron-electron cusp conditions are

$$\lim_{r_{ij} \rightarrow 0} \frac{\partial f_{ij}}{\partial r_{ij}} = a_{ij} = \begin{cases} \frac{1}{4} & \text{if electrons } i \text{ and } j \text{ belong to the same determinant,} \\ \frac{1}{2} & \text{if electrons } i \text{ and } j \text{ belong to different determinants.} \end{cases} \quad (\text{B.30})$$

Appendix C

Simplex Optimization

The simplex technique belongs to the group of *direct search methods*. These methods rely only on evaluating $f(\mathbf{x})$ at a sequence of points $\mathbf{x}_0, \mathbf{x}_1, \mathbf{x}_2, \dots$ and comparing these values, in order to reach the optimal point \mathbf{x}^* .

The principal advantage of the direct search methods is that they do not require evaluation of derivatives of $f(\mathbf{x})$, which usually presents a problem.

A *simplex* in n -dimensional space consists of $(n+1)$ points \mathbf{x}_i ($i = 0, 1, \dots, n$) which do not lie on a hyperplane (i.e. the vectors $\mathbf{r}_i \equiv \mathbf{x}_i - \mathbf{x}_0$, $i = 1, \dots, n$, are linearly independent), and all their interconnecting line segments, polygonal faces, etc. The points are called *vertices* of the simplex.

Let \mathbf{x}_0 be an initial estimate of \mathbf{x}^* . The algorithm for the search of \mathbf{x}^* with modifications due to Langfelder [16] is as follows.

1. Generate the vertices of an initial simplex in n -dimensional space $\mathbf{x}_1, \mathbf{x}_2, \dots, \mathbf{x}_n$

$$\mathbf{x}_i = \mathbf{x}_0 + h_i \mathbf{e}_i, \quad i = 1, \dots, n \quad (\text{C.1})$$

where \mathbf{e}_i are the unit coordinate vectors and h_i are 'dimensions' of the simplex.

2. Evaluate $f(\mathbf{x}_i)$ at the vertices \mathbf{x}_i ($i = 1, 2, \dots, n$).
3. Determine the 'worst' vertex \mathbf{x}_p (the one with the highest function) and evaluate $f_p = f(\mathbf{x}_p)$.
4. Find the 'center of mass' (centroid) of the remaining vertices

$$\mathbf{X} = \frac{1}{n} (\mathbf{x}_0 + \mathbf{x}_1 + \dots + \mathbf{x}_{p-1} + \mathbf{x}_{p+1} + \dots + \mathbf{x}_n).$$

CHAPTER 1

THE FUNDAMENTALS

The first part of the book is devoted to the study of the basic concepts of the theory of functions of a real variable. It begins with a discussion of the real number system and the properties of the real numbers.

The next part of the book is devoted to the study of the properties of the real numbers.

The third part of the book is devoted to the study of the properties of the real numbers. It begins with a discussion of the real number system and the properties of the real numbers.

The fourth part of the book is devoted to the study of the properties of the real numbers. It begins with a discussion of the real number system and the properties of the real numbers.

The fifth part of the book is devoted to the study of the properties of the real numbers. It begins with a discussion of the real number system and the properties of the real numbers.

The sixth part of the book is devoted to the study of the properties of the real numbers. It begins with a discussion of the real number system and the properties of the real numbers.

The seventh part of the book is devoted to the study of the properties of the real numbers. It begins with a discussion of the real number system and the properties of the real numbers.

The eighth part of the book is devoted to the study of the properties of the real numbers. It begins with a discussion of the real number system and the properties of the real numbers.

The ninth part of the book is devoted to the study of the properties of the real numbers. It begins with a discussion of the real number system and the properties of the real numbers.

The tenth part of the book is devoted to the study of the properties of the real numbers. It begins with a discussion of the real number system and the properties of the real numbers.

The eleventh part of the book is devoted to the study of the properties of the real numbers. It begins with a discussion of the real number system and the properties of the real numbers.

The twelfth part of the book is devoted to the study of the properties of the real numbers. It begins with a discussion of the real number system and the properties of the real numbers.

The thirteenth part of the book is devoted to the study of the properties of the real numbers. It begins with a discussion of the real number system and the properties of the real numbers.

5. *Reflection.* Reflect the vertex x_p about the centroid X as $x' = X - (x_p - X)$ (Fig. 1) and evaluate $f(x')$.

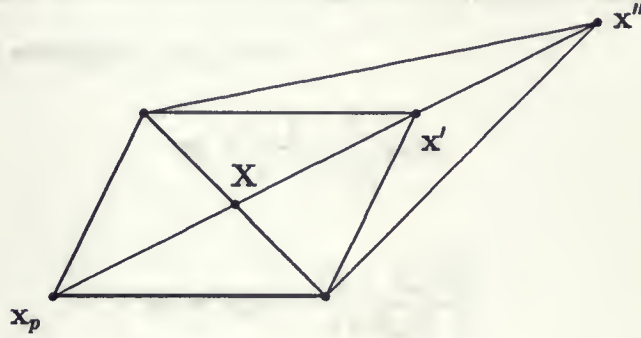


Figure 1. Reflection and expansion of a vertex x_p ($n=2$).

6. *Expansion.* If $f(x') < f_p$, replace x_p by x' and try to expand the simplex (Fig. 1) introducing a new vertex $x'' = X - (x' - X)$. Evaluate $f(x'')$.
- (a) If $f(x'') < f(x')$, replace x_p by x'' and return to step (3).
 - (b) If $f(x'') > f(x')$, return to step (3).
7. *Contraction.* If $f(x') > f_p$, contract the simplex (Fig. 2), i.e. find the vertex $x'' = X + \frac{1}{2}(x_p - X)$.

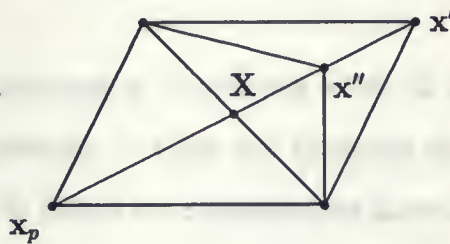


Figure 2. Contraction of the simplex ($n=2$).

- (a) If $f(x'') < f_p$, replace x_p by x'' and return to step (3).
- (b) If $f(x'') > f_p$, restart or enlarge the simplex.

9. *Restart.* The simplex is restarted until it gets locked within two consecutive trials.

First determine the new estimate \mathbf{x}'_0 of \mathbf{x}^* by choosing \mathbf{x}'_0

- (i) as the current best vertex (when the ensemble is relatively small), or
- (ii) as the weighted average of all points

$$\mathbf{x}'_0 = \frac{1}{n+1} \sum_{i=0}^n \mathbf{x}_i w_i,$$

where

$$w_i = \exp \left[-\frac{(f_i - f_m)^2}{(\Delta f_m)^2} \right],$$

where f_m is the lowest function value and Δf_m is its error (if the ensemble is large enough to ensure small statistical errors).

Then generate the next simplex

$$\mathbf{x}_i = \mathbf{x}'_0 + (-1)^q k h_i \mathbf{e}_i, \quad i = 1, \dots, n \quad (\text{C.2})$$

where q is the number of the consecutive restart, and k is a size control factor.

Return to step (2).

10. *Enlargement.* The ensemble is enlarged if the simplex cannot move within three consecutive trials. Increase the number of configurations and/or blocks, and return to step (2).

11. *Termination.* The algorithm is terminated when all the vertices of a simplex are within a specified precision *or* when the ensemble reaches the maximum allowed size and the simplex is locked for 3 consecutive moves.

When the expanding or restarting simplex attempts to cross the specified boundaries, the move is truncated.

Appendix D

Compendium of Formulas

D.1 Numerical evaluation of the integral $\langle \phi_{1s} | \phi_{2s} \rangle$.

Since the orbital functions

$$\begin{aligned}\phi_{1s} &= e^{-\zeta_1 r} e^{-\frac{w_s r}{1+v_s r}}, \\ \phi_{2s} &= (1+cr) e^{-\zeta_2 r} e^{-\frac{w_s r}{1+v_s r}}\end{aligned}\quad (\text{D.1})$$

are not analytically integrable, a numerical procedure has to be employed in order to evaluate the following integrals

$$\langle \phi_{1s} | \phi_{1s} \rangle = 4\pi \int_0^\infty r^2 e^{-2\zeta_1 r} e^{-2\frac{w_s r}{1+v_s r}} dr, \quad (\text{D.2})$$

$$\langle \phi_{2s} | \phi_{2s} \rangle = 4\pi \int_0^\infty r^2 (1+cr)^2 e^{-2\zeta_2 r} e^{-2\frac{w_s r}{1+v_s r}} dr, \quad (\text{D.3})$$

$$\langle \phi_{1s} | \phi_{2s} \rangle = 4\pi \int_0^\infty r^2 (1+cr) e^{-(\zeta_1+\zeta_2)r} e^{-2\frac{w_s r}{1+v_s r}} dr. \quad (\text{D.4})$$

Integration is performed with high accuracy, 15-point quadrature formulas using unevenly spaced abscissae¹

$$\int_0^\infty e^{-x} f(x) dx = \sum_{i=1}^{15} A_i f(x_i). \quad (\text{D.5})$$

The obvious transformations of variables involve $x = 2\zeta_1 r$ for (D.2), $x = 2\zeta_2 r$ for (D.3) and $x = (\zeta_1 + \zeta_2)r$ for (D.4).

¹The 12-decimal-digit values of abscissae x_i and weights A_i were taken from: V. I. Krylov. *Priblizhennoe vychislenie integralov*, Moskva, 1967.

D.2 Derivatives of the atomic orbitals and correlation functions

Given below are the first and second derivatives of the atomic orbitals and correlation functions. Although some expressions are straightforward, we list them for completeness and convenience, so that they can be readily used to follow derivation of the cusp conditions (see Appendix B). Atomic orbitals ϕ are viewed here as a product of the ‘pure’ orbital φ and electron-nuclear correlation factor: $\phi = \varphi J^{en}$. Symbols q_α and q_β are generalizations for x , y , and z ($\alpha, \beta = 1, 2, 3$, respectively).

C.2.1 Derivatives of the ‘pure’ atomic orbitals

$$\begin{aligned}\varphi_{1s} &= e^{-\zeta_1 r} \\ \frac{\partial}{\partial q} \varphi_{1s} &= -\zeta_1 \frac{q}{r} e^{-\zeta_1 r} \\ \nabla^2 \varphi_{1s} &= \zeta_1 \left(\zeta_1 - \frac{2}{r} \right) e^{-\zeta_1 r}\end{aligned}\tag{D.6}$$

$$\begin{aligned}\varphi_{2s} &= (1 + cr) e^{-\zeta_2 r} \\ \frac{\partial}{\partial q} \varphi_{2s} &= q \left[\frac{c - \zeta_2}{r} - c \zeta_2 \right] e^{-\zeta_2 r} \\ \nabla^2 \varphi_{2s} &= \left[\zeta_2^2 (1 + cr) - 4c \zeta_2 + \frac{2(c - \zeta_2)}{r} \right] e^{-\zeta_2 r} \\ \phi'_{2s} &= N_{2s} \phi_{2s} - k N_{1s} \phi_{1s}\end{aligned}\tag{D.7}$$

$$\begin{aligned}\varphi_{2p(q_\alpha)} &= q_\alpha e^{-\zeta_2 r} \\ \frac{\partial}{\partial q_\beta} \varphi_{2p(q_\alpha)} &= \begin{cases} \left(1 - \zeta_2 \frac{q_\alpha^2}{r} \right) e^{-\zeta_2 r}, & \text{if } \alpha = \beta \\ -\zeta_2 \frac{q_\alpha q_\beta}{r} e^{-\zeta_2 r}, & \text{if } \alpha \neq \beta \end{cases} \\ \nabla^2 \varphi_{2p(q_\alpha)} &= \zeta_2 q_\alpha \left(\zeta_2 - \frac{4}{\zeta_2} \right) e^{-\zeta_2 r}\end{aligned}\tag{D.8}$$

Lemma 1.1. Let f be a function on \mathbb{R}^n with compact support. Then

if f is in $L^p(\mathbb{R}^n)$ for some $p > 1$, then f is in $L^q(\mathbb{R}^n)$ for all $q < p$. Moreover, if f is in $L^p(\mathbb{R}^n)$ for some $p > 1$, then f is in $L^q(\mathbb{R}^n)$ for all $q < p$. Finally, if f is in $L^p(\mathbb{R}^n)$ for some $p > 1$, then f is in $L^q(\mathbb{R}^n)$ for all $q < p$. Proof. Let f be a function on \mathbb{R}^n with compact support. Then f is in $L^p(\mathbb{R}^n)$ for some $p > 1$. Let $q < p$. Then f is in $L^q(\mathbb{R}^n)$ for all $q < p$. Finally, if f is in $L^p(\mathbb{R}^n)$ for some $p > 1$, then f is in $L^q(\mathbb{R}^n)$ for all $q < p$. \square

Lemma 1.2. Let f be a function on \mathbb{R}^n with compact support. Then

if f is in $L^p(\mathbb{R}^n)$ for some $p > 1$, then f is in $L^q(\mathbb{R}^n)$ for all $q < p$.

$$\begin{aligned} (1.1) \quad & \|f\|_q \leq \|f\|_p \\ & \|f\|_q \leq \|f\|_p \\ & \|f\|_q \leq \|f\|_p \end{aligned}$$

$$\begin{aligned} (1.2) \quad & \|f\|_q \leq \|f\|_p \\ & \|f\|_q \leq \|f\|_p \\ & \|f\|_q \leq \|f\|_p \end{aligned}$$

$$\begin{aligned} (1.3) \quad & \|f\|_q \leq \|f\|_p \\ & \|f\|_q \leq \|f\|_p \\ & \|f\|_q \leq \|f\|_p \end{aligned}$$

C.2.2 Derivatives of the electron-nuclear correlation function

$$\begin{aligned}
 J_i^{en} &= \exp\left(-\frac{wr_i}{1+vr_i}\right) \\
 \frac{\partial J_i^{en}}{\partial x_i} &= -J_i^{en} \frac{x_i}{r_i(1+vr_i)^2} \\
 \nabla_i^2 J_i^{en} &= J_i^{en} w \frac{wr_i - 2(1+vr_i)}{r_i(1+vr_i)^4}
 \end{aligned} \tag{D.9}$$

C.2.3 Derivatives of the electron-electron correlation function

$$\begin{aligned}
 J &= \exp\left(\sum_{i=1}^{n-1} \sum_{j=i+1}^n \frac{ar_{ij}}{1+br_{ij}}\right) \\
 \frac{\partial J}{\partial x_i} &= J \sum_{j \neq i}^n \frac{a(x_i - x_j)}{r_{ij}(1+br_{ij})^2} \\
 \nabla_i^2 J &= \frac{1}{J} \left[\left(\frac{\partial J}{\partial x_i}\right)^2 + \left(\frac{\partial J}{\partial y_i}\right)^2 + \left(\frac{\partial J}{\partial z_i}\right)^2 \right] + J \sum_{j \neq i}^n \frac{2a}{r_{ij}(1+br_{ij})^3}
 \end{aligned} \tag{D.10}$$

D.3 The local energy

The local energy at the point \mathbf{R} is defined as

$$E_L = \frac{\hat{H}\Psi(\mathbf{R})}{\Psi(\mathbf{R})}, \tag{D.11}$$

with the electronic Hamiltonian

$$\hat{H} = -\frac{1}{2} \sum_{i=1}^n \nabla_i^2 + U(\mathbf{R}), \tag{D.12}$$

where the potential energy operator

$$U(\mathbf{R}) = -\sum_{i=1}^n \frac{Z}{r_i} + \sum_{i=1}^{n-1} \sum_{j=i+1}^n \frac{1}{r_{ij}}. \tag{D.13}$$

Now J depends on coordinates of all n electrons, whereas Slater determinants are functions of only certain electrons depending on their spin and assignment to the core or valence shell. This is stressed in the notation used in the formulas. The explicit forms of wave functions Ψ are given below.

10.1.1. (a) Find the Laplace transform of the function $f(t)$ defined by

$$f(t) = \begin{cases} 0 & \text{if } t < 0 \\ t & \text{if } 0 \leq t < 1 \\ 1 & \text{if } 1 \leq t < 2 \\ 0 & \text{if } t \geq 2 \end{cases}$$

(b) Find the Laplace transform of the function $f(t)$ defined by

$$f(t) = \begin{cases} 0 & \text{if } t < 0 \\ t & \text{if } 0 \leq t < 1 \\ 1 & \text{if } 1 \leq t < 2 \\ 0 & \text{if } t \geq 2 \end{cases}$$

$$f(t) = \begin{cases} 0 & \text{if } t < 0 \\ t & \text{if } 0 \leq t < 1 \\ 1 & \text{if } 1 \leq t < 2 \\ 0 & \text{if } t \geq 2 \end{cases}$$

(c) Find the Laplace transform of the function

$f(t) = \begin{cases} 0 & \text{if } t < 0 \\ t & \text{if } 0 \leq t < 1 \\ 1 & \text{if } 1 \leq t < 2 \\ 0 & \text{if } t \geq 2 \end{cases}$

$$f(t) = \begin{cases} 0 & \text{if } t < 0 \\ t & \text{if } 0 \leq t < 1 \\ 1 & \text{if } 1 \leq t < 2 \\ 0 & \text{if } t \geq 2 \end{cases}$$

(d) Find the Laplace transform of the function

$$f(t) = \begin{cases} 0 & \text{if } t < 0 \\ t & \text{if } 0 \leq t < 1 \\ 1 & \text{if } 1 \leq t < 2 \\ 0 & \text{if } t \geq 2 \end{cases}$$

(e) Find the Laplace transform of the function

$$f(t) = \begin{cases} 0 & \text{if } t < 0 \\ t & \text{if } 0 \leq t < 1 \\ 1 & \text{if } 1 \leq t < 2 \\ 0 & \text{if } t \geq 2 \end{cases}$$

(f) Find the Laplace transform of the function $f(t)$ defined by $f(t) = \begin{cases} 0 & \text{if } t < 0 \\ t & \text{if } 0 \leq t < 1 \\ 1 & \text{if } 1 \leq t < 2 \\ 0 & \text{if } t \geq 2 \end{cases}$

(g) Find the Laplace transform of the function

C.3.1 The local energy with Ψ_1

Wave function Ψ_1 has the form

$$\Psi_1 = \psi_D^\dagger \psi_D^\dagger J. \quad (\text{D.14})$$

Thus, the local energy is

$$\begin{aligned} E_L = & -\frac{1}{2} \left(\sum_i^{n^\dagger} \frac{\nabla_i^2 \psi_D^\dagger}{\psi_D^\dagger} + \sum_i^{n^\dagger} \frac{\nabla_i^2 \psi_D^\dagger}{\psi_D^\dagger} + \sum_i^n \frac{\nabla_i^2 J}{J} \right) \\ & - \sum_i^{n^\dagger} \frac{\nabla_i \psi_D^\dagger}{\psi_D^\dagger} \frac{\nabla_i J}{J} - \sum_i^{n^\dagger} \frac{\nabla_i \psi_D^\dagger}{\psi_D^\dagger} \frac{\nabla_i J}{J} + U. \end{aligned} \quad (\text{D.15})$$

C.3.2 The local energy with Ψ_2

Wave function Ψ_2 has the form

$$\Psi_2 = \psi_{D_c}^\dagger \psi_{D_c}^\dagger \psi_{D_v}^\dagger \psi_{D_v}^\dagger J. \quad (\text{D.16})$$

$$\begin{aligned} E_L = & -\frac{1}{2} \left(\sum_i^{n_c^\dagger} \frac{\nabla_i^2 \psi_{D_c}^\dagger}{\psi_{D_c}^\dagger} + \sum_i^{n_c^\dagger} \frac{\nabla_i^2 \psi_{D_c}^\dagger}{\psi_{D_c}^\dagger} + \sum_i^{n_v^\dagger} \frac{\nabla_i^2 \psi_{D_v}^\dagger}{\psi_{D_v}^\dagger} + \sum_i^{n_v^\dagger} \frac{\nabla_i^2 \psi_{D_v}^\dagger}{\psi_{D_v}^\dagger} + \sum_i^n \frac{\nabla_i^2 J}{J} \right) \\ & - \sum_i^{n_c^\dagger} \frac{\nabla_i \psi_{D_c}^\dagger}{\psi_{D_c}^\dagger} \frac{\nabla_i J}{J} - \sum_i^{n_c^\dagger} \frac{\nabla_i \psi_{D_c}^\dagger}{\psi_{D_c}^\dagger} \frac{\nabla_i J}{J} - \sum_i^{n_v^\dagger} \frac{\nabla_i \psi_{D_v}^\dagger}{\psi_{D_v}^\dagger} \frac{\nabla_i J}{J} - \sum_i^{n_v^\dagger} \frac{\nabla_i \psi_{D_v}^\dagger}{\psi_{D_v}^\dagger} \frac{\nabla_i J}{J} + U. \end{aligned} \quad (\text{D.17})$$

C.3.3 The local energy with Ψ_3 and Ψ_4

Wave functions Ψ_3 ($b_c = b_v$) and Ψ_4 ($b_c \neq b_v$) have the form

$$\Psi_3 = \psi_{D_c}^\dagger \psi_{D_c}^\dagger \psi_{D_v}^\dagger \psi_{D_v}^\dagger J_c J_v, \quad (\text{D.18})$$

$$\Psi_4 = \psi_{D_c}^\dagger \psi_{D_c}^\dagger \psi_{D_v}^\dagger \psi_{D_v}^\dagger J_c J'_v.$$

$$\begin{aligned} E_L = & -\frac{1}{2} \left(\sum_i^{n_c^\dagger} \frac{\nabla_i^2 \psi_{D_c}^\dagger}{\psi_{D_c}^\dagger} + \sum_i^{n_c^\dagger} \frac{\nabla_i^2 \psi_{D_c}^\dagger}{\psi_{D_c}^\dagger} + \sum_i^{n_v^\dagger} \frac{\nabla_i^2 \psi_{D_v}^\dagger}{\psi_{D_v}^\dagger} + \sum_i^{n_v^\dagger} \frac{\nabla_i^2 \psi_{D_v}^\dagger}{\psi_{D_v}^\dagger} + \sum_i^{n_c} \frac{\nabla_i^2 J_c}{J_c} + \sum_i^{n_v} \frac{\nabla_i^2 J_v}{J_v} \right) \\ & - \sum_i^{n_c^\dagger} \frac{\nabla_i \psi_{D_c}^\dagger}{\psi_{D_c}^\dagger} \frac{\nabla_i J_c}{J_c} - \sum_i^{n_c^\dagger} \frac{\nabla_i \psi_{D_c}^\dagger}{\psi_{D_c}^\dagger} \frac{\nabla_i J_c}{J_c} - \sum_i^{n_v^\dagger} \frac{\nabla_i \psi_{D_v}^\dagger}{\psi_{D_v}^\dagger} \frac{\nabla_i J_v}{J_v} - \sum_i^{n_v^\dagger} \frac{\nabla_i \psi_{D_v}^\dagger}{\psi_{D_v}^\dagger} \frac{\nabla_i J_v}{J_v} + U. \end{aligned} \quad (\text{D.19})$$

C.3.4 The local energy with Ψ_5

Wave function Ψ_5 ($b_c \neq b_v \neq b_{cv}$) has the form

$$\Psi_5 = \psi_{D_c}^\dagger \psi_{D_c}^\dagger \psi_{D_v}^\dagger \psi_{D_v}^\dagger J_c J_v J_{cv}, \quad (\text{D.20})$$

but it is more convenient to regard it as having one all-electron Jastrow correlation function pairing all electrons,

$$\Psi_5 = \psi_{D_c}^\dagger \psi_{D_c}^\dagger \psi_{D_v}^\dagger \psi_{D_v}^\dagger J, \quad (\text{D.21})$$

so that the local energy is given by

$$\begin{aligned} E_L = & -\frac{1}{2} \left(\sum_i^{n_c^\dagger} \frac{\nabla_i^2 \psi_{D_c}^\dagger}{\psi_{D_c}^\dagger} + \sum_i^{n_c^\dagger} \frac{\nabla_i^2 \psi_{D_c}^\dagger}{\psi_{D_c}^\dagger} + \sum_i^{n_v^\dagger} \frac{\nabla_i^2 \psi_{D_v}^\dagger}{\psi_{D_v}^\dagger} + \sum_i^{n_v^\dagger} \frac{\nabla_i^2 \psi_{D_v}^\dagger}{\psi_{D_v}^\dagger} + \sum_i^n \frac{\nabla_i^2 J}{J} \right) \\ & - \sum_i^{n_c^\dagger} \frac{\nabla_i \psi_{D_c}^\dagger}{\psi_{D_c}^\dagger} \frac{\nabla_i J}{J} - \sum_i^{n_c^\dagger} \frac{\nabla_i \psi_{D_c}^\dagger}{\psi_{D_c}^\dagger} \frac{\nabla_i J}{J} - \sum_i^{n_v^\dagger} \frac{\nabla_i \psi_{D_v}^\dagger}{\psi_{D_v}^\dagger} \frac{\nabla_i J}{J} - \sum_i^{n_v^\dagger} \frac{\nabla_i \psi_{D_v}^\dagger}{\psi_{D_v}^\dagger} \frac{\nabla_i J}{J} + U. \end{aligned} \quad (\text{D.22})$$

Bibliography

- [1] B. L. Hammond, P. J. Reynolds and W. A. Lester, Jr. Valence quantum Monte Carlo with *ab initio* effective core potential. *J. Chem. Phys.*, **87**, 1130 (1987).
- [2] P. Politzer and R. G. Parr. Separation of core and valence regions in atoms. *J. Chem. Phys.*, **64**, 4634 (1976).
- [3] P. Politzer. Electrostatic potential – electronic density relationships in atoms. *J. Chem. Phys.*, **72**, 3027 (1980).
- [4] N. Desmarais and S. Fliszár. Core and valence electrons in atoms and ions: Configuration interaction calculations. *Theor. Chim. Acta*, **94**, 187, (1996).
- [5] S. Fliszár, N. Desmarais, and G. Dancausse. Valence and core energies of atoms in Hartree-Fock theory. *Can. J. Chem.*, **70**, 537 (1992).
- [6] P. A. Christiansen, Y. S. Lee, and K. S. Pitzer. Improved *ab initio* effective core potentials for molecular calculations. *J. Chem. Phys.*, **71**, 4445 (1979).
- [7] L. F. Pacios and P. A. Christiansen. *Ab initio* relativistic effective potentials with spin-orbit operators. I. Li through Ar. *J. Chem. Phys.*, **82**, 2665 (1985).
- [8] S. Fahy, X. W. Wang, and S. G. Louie. Variational Monte Carlo nonlocal pseudopotential approach to solids: Formulation and application to diamond, graphite, and silicon. *Phys. Rev. B*, **42**, 3503 (1990).
- [9] P. Schwerdtfeger, T. Fischer, M. Dolg, G. Igel-Mann, A. Nicklaß and H. Stoll. The accuracy of pseudopotential approximation. I. An analysis of the spectroscopic constants for the electronic ground states of InCl and InCl₃ using various three valence electron pseudopotentials for indium. *J. Chem. Phys.*, **105**, 2050 (1995).
- [10] W. Müller, J. Flesch, and W. Meyer. Treatment of intershell correlation effects in *ab initio* calculations by use of core polarization potentials. Method and application to alkali and alkaline earth atoms. *J. Chem. Phys.*, **80**, 3297 (1980).
- [11] Y. Sakai and S. Huzinaga. The use of model potentials on molecular calculations. *J. Chem. Phys.*, **76**, 2537 (1981).
- [12] B. L. Hammond, P. J. Reynolds and W. A. Lester, Jr. Damped-core quantum Monte Carlo: Effective treatment for large- \tilde{Z} systems. *Phys. Rev. Lett.* **61**, 2312 (1988).

- [13] S. C. Leasure, T. P. Martin and G. G. Balint-Kurti. *Ab initio* valence-electron-only molecular electronic structure calculations: Theory and test applications. *J. Chem. Phys.*, **80**, 1186 (1984).
- [14] G. G. Balint-Kurti, S. C. Leasure, and T. P. Martin. An *ab initio* method for performing valence-electron-only calculations. *Chem. Phys. Lett.*, **81**, 297 (1981).
- [15] E. L. Shirley and R. M. Martin. Many-body core-valence partitioning. *Phys. Rev. B*, **47**, 15413 (1993).
- [16] P. Langfelder. Calculation of non-differential properties for atomic ground states. *Master of Science Thesis*, Brock University, 1997.
- [17] A. Banerjee. Construction of orthogonal subspaces. *Int. J. Quantum Chem.*, **29**, 747 (1991).
- [18] I. N. Levine. *Quantum Chemistry*, 4th ed., Englewood Cliffs, New Jersey, 1991.
- [19] B. L. Hammond, W. A. Lester, Jr. and P. J. Reynolds. *Monte Carlo Methods in Ab Initio Quantum Chemistry*. World Scientific, 1994.
- [20] D. M. Ceperley, L. Mitas. Quantum Monte Carlo Methods in Chemistry. in *Advances in Chemical Physics*, **43**, 1, John Wiley & Sons, 1996.
- [21] J. B. Anderson. Fixed-Node Quantum Monte Carlo. *Int. Rev. Quantum Chem.* **14**, 85 (1995).
- [22] N. Metropolis, A. W. Rosenbluth, M. N. Rosenbluth, A. H. Teller, and E. Teller. Equations of state calculations by fast computing machines. *J. Chem. Phys.*, **21**, 1087 (1953).
- [23] M. H. Kalos. *Monte Carlo Methods*, v. 1, John Wiley & Sons, New York, 1986.
- [24] C. Chatfield. *The Analysis of Time Series: An Introduction*, 4th ed., Chapman and Hall, London, 1989, pp. 18–20.
- [25] C. J. Umrigar. Accelerated Metropolis method. *Phys. Rev. Lett.*, **71**, 408 (1993).
- [26] R. Y. Rubinstein. *Simulation and the Monte Carlo Method*. John Wiley & Sons, 1981.
- [27] A. Doboš. Private communication.
- [28] D. Ceperley, G. V. Chester, and M. H. Kalos. Monte Carlo simulation of a many-fermion study. *Phys. Rev. B*, **16**, 3081 (1977).

- [29] S. M. Rothstein. Valence energy in variational Monte Carlo: CuH dissociation energy. *Int. J. Quantum Chem.*, **60**, 803 (1996).
- [30] P.-O. Löwdin. Virial theorem and scaling problem. *J. Mol. Spect.* **3**, 46, (1959).
- [31] R. T. Brown. Virial theorem, the variational principle, and nonlinear parameters in quantum mechanics. *J. Chem. Phys.*, **48**, 4698 (1967).
- [32] W. G. Cochran. *Sampling techniques*, p. 30, John Wiley & Sons, New York, 1964.
- [33] E. R. Davidson, S. A. Hagstrom, S. J. Chakravorty, V. M. Umar, and C. F. Fischer. Ground-state correlation energies for two- to ten-electron atomic ions. *Phys. Rev. A*, **44**, 7071, (1991).
- [34] S. J. Chakravorty, S. R. Gwaltney, E. R. Davidson, F. A. Parpia, and C. F. Fischer. Ground-state correlation energies for atomic ions with 3 to 18 electrons. *Phys. Rev. A*, **47**, 3649, (1993).
- [35] S. A. Alexander and R. L. Coldwell. Calculating atomic properties using variational Monte Carlo *J. Chem. Phys.*, **103**, 2572 (1995).
- [36] K. E. Schmidt and J. W. Moskowitz. Correlated Monte Carlo wave functions for the atoms He through Ne. *J. Chem. Phys.*, **93**, 4172 (1990).
- [37] J. W. Moskowitz and K. E. Schmidt. Correlated Monte Carlo wave functions for some cations and anions of the first row atoms. *J. Chem. Phys.*, **97**, 3382 (1992).
- [38] P.-O. Widmark, P.-A. Malmqvist, B. O. Roos. Density matrix averaged atomic natural orbital (ANO) basis set for correlated molecular wave functions. *Theor. Chim. Acta*, **77**, 291 (1990).
- [39] M. Urban, R. J. Bartlett, and S. A. Alexander. Basis set quantum chemistry and quantum Monte Carlo: Selected atomic and molecular results. *Int. J. Quantum Chem.*, **26**, 271 (1992).
- [40] *CRC Handbook of Chemistry and Physics*, 75th ed., CRC Press, Boca Raton, 1994.

- [1] J. J. J. J., *Journal of the American Mathematical Society*, 1995, 8(1), 1-10.
- [2] J. J. J. J., *Journal of the American Mathematical Society*, 1996, 9(1), 1-10.
- [3] J. J. J. J., *Journal of the American Mathematical Society*, 1997, 10(1), 1-10.
- [4] J. J. J. J., *Journal of the American Mathematical Society*, 1998, 11(1), 1-10.
- [5] J. J. J. J., *Journal of the American Mathematical Society*, 1999, 12(1), 1-10.
- [6] J. J. J. J., *Journal of the American Mathematical Society*, 2000, 13(1), 1-10.
- [7] J. J. J. J., *Journal of the American Mathematical Society*, 2001, 14(1), 1-10.
- [8] J. J. J. J., *Journal of the American Mathematical Society*, 2002, 15(1), 1-10.
- [9] J. J. J. J., *Journal of the American Mathematical Society*, 2003, 16(1), 1-10.
- [10] J. J. J. J., *Journal of the American Mathematical Society*, 2004, 17(1), 1-10.
- [11] J. J. J. J., *Journal of the American Mathematical Society*, 2005, 18(1), 1-10.
- [12] J. J. J. J., *Journal of the American Mathematical Society*, 2006, 19(1), 1-10.
- [13] J. J. J. J., *Journal of the American Mathematical Society*, 2007, 20(1), 1-10.
- [14] J. J. J. J., *Journal of the American Mathematical Society*, 2008, 21(1), 1-10.
- [15] J. J. J. J., *Journal of the American Mathematical Society*, 2009, 22(1), 1-10.
- [16] J. J. J. J., *Journal of the American Mathematical Society*, 2010, 23(1), 1-10.
- [17] J. J. J. J., *Journal of the American Mathematical Society*, 2011, 24(1), 1-10.
- [18] J. J. J. J., *Journal of the American Mathematical Society*, 2012, 25(1), 1-10.
- [19] J. J. J. J., *Journal of the American Mathematical Society*, 2013, 26(1), 1-10.
- [20] J. J. J. J., *Journal of the American Mathematical Society*, 2014, 27(1), 1-10.
- [21] J. J. J. J., *Journal of the American Mathematical Society*, 2015, 28(1), 1-10.
- [22] J. J. J. J., *Journal of the American Mathematical Society*, 2016, 29(1), 1-10.
- [23] J. J. J. J., *Journal of the American Mathematical Society*, 2017, 30(1), 1-10.
- [24] J. J. J. J., *Journal of the American Mathematical Society*, 2018, 31(1), 1-10.
- [25] J. J. J. J., *Journal of the American Mathematical Society*, 2019, 32(1), 1-10.
- [26] J. J. J. J., *Journal of the American Mathematical Society*, 2020, 33(1), 1-10.
- [27] J. J. J. J., *Journal of the American Mathematical Society*, 2021, 34(1), 1-10.
- [28] J. J. J. J., *Journal of the American Mathematical Society*, 2022, 35(1), 1-10.
- [29] J. J. J. J., *Journal of the American Mathematical Society*, 2023, 36(1), 1-10.
- [30] J. J. J. J., *Journal of the American Mathematical Society*, 2024, 37(1), 1-10.





